



PETERSBURG NUCLEAR PHYSICS INSTITUTE NAMED BY B.P. KONSTANTINOV
OF NATIONAL RESEARCH CENTER "KURCHATOV INSTITUTE"

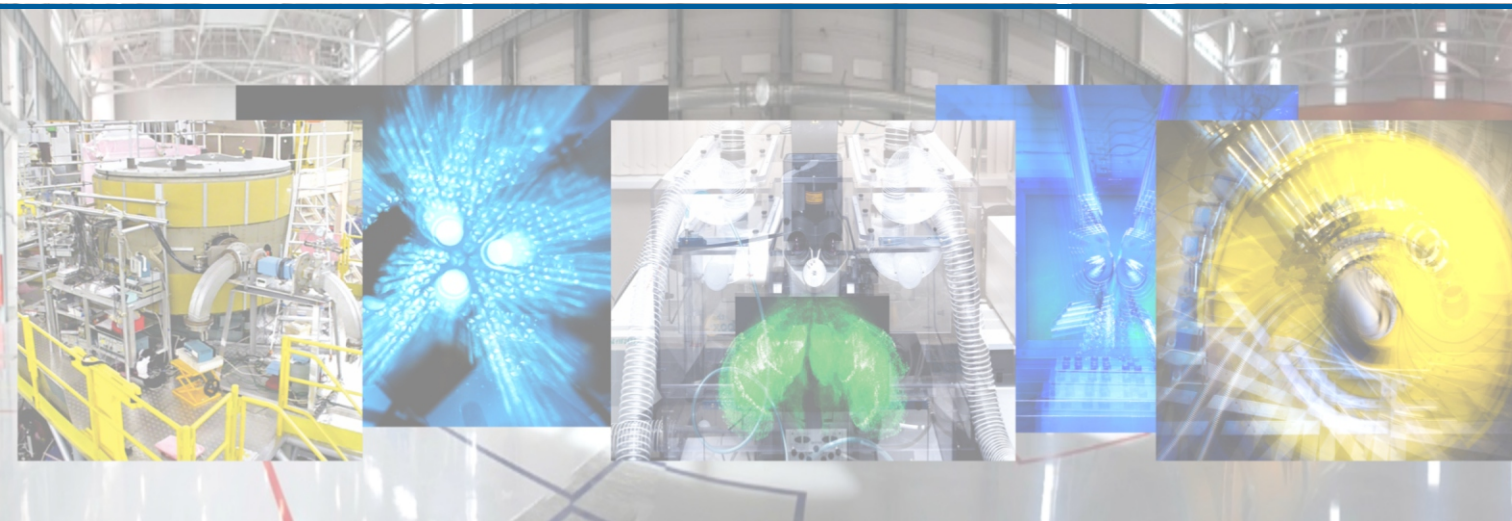


PNPI Scientific Highlights

2021



PETERSBURG NUCLEAR PHYSICS INSTITUTE NAMED BY B.P. KONSTANTINOV
OF NATIONAL RESEARCH CENTER “KURCHATOV INSTITUTE”



PNPI Scientific Highlights 2021

Gatchina • 2022

Chief-editors:

V.V. Voronin
S.V. Sarantseva
S.I. Vorobyov

Proofreaders:

E.Yu. Orobets
N.V. Silinskaya
A.I. Zaitseva (translation)

Editors:

D.N. Aristov	V.V. Sarantsev
S.I. Vorobyov	M.V. Suyasova
N.N. Gubanova	A.V. Titov
A.L. Konevega	O.L. Fedin
A.I. Kurbakov	S.R. Friedmann
R.A. Niyazov	K.A. Shabalin

Technical editing and design:

T.A. Parfeeva

Layout composition:

E.V. Veselovskaya
N.O. Pavlova

Executive in charge

S.I. Vorobyov

PNPI Scientific Highlights 2021. – Gatchina, Leningradskaya obl.:
NRC “Kurchatov Institute” – PNPI Publishing, 2022. – 132 pages.

The publication is a compilation of abstracts of the most significant results of scientific research at NRC “Kurchatov Institute” – PNPI in 2021. In addition to an abstract, each scientific result in the volume features references to the full articles of leading domestic and foreign publications, where the study is described in detail and where one can get acquainted with its full content.

Table of Contents

- 7** Preface
- 11** Research Divisions
- 29** Theoretical and Mathematical Physics
- 43** Research Based on the Use of Neutrons, Photons and Muons
- 53** Research Based on the Use of Protons and Ions. Neutrino Physics
- 71** Biological Research
- 87** Nuclear Medicine (Isotope Production, Beam Therapy,
Bio- and Nanotechnologies for Medical Purposes)
- 91** Nuclear Reactor and Accelerator Physics
- 97** Applied Research and Developments
- 109** Basic Installations
- 115** Scientific and Organizational Activities



Dear colleagues, dear friends!

NRC “Kurchatov Institute” – PNPI, which in 2021 was celebrating its 50-year anniversary of becoming an independent research institution, is a multispecialized multidisciplinary research center which forms part of National Research Center “Kurchatov Institute” from the very beginning of its formation.

According to the RF Presidential Edict No. 356 of 25.07.2019 “On Measures to Promote Synchrotron and Neutron Studies and Research Infrastructure in the Russian Federation” as well as in the framework of the national project “Science and Universities” and Federal scientific-technical program for the development of synchrotron and neutron studies and research infrastructure in the Russian Federation for the period 2019–2027, NRC “Kurchatov Institute” – PNPI successfully implements various projects at the PIK Neutron Research Facility, which is a unique scientific “megascience” project.

An anniversary year for NRC “Kurchatov Institute” – PNPI has become a major landmark for the whole Russian science community. On 8 February, 2021, during a meeting of the Presidential Council for Science and Higher Education chaired by the President of the Russian Federation, Vladimir Putin ordered the energy launch of the PIK reactor and trial experiments at five research stations which had already been commissioned.

Longstanding traditions, unique scientific, technological and human resources are all indicative of the professionalism, energy and passion for work of the powerhouse that is Kurchatov Institute!

Today NRC “Kurchatov Institute” is one of the largest and internationally recognized Russia’s research centers conducting fundamental and applied research in various fields.

Let the work of high-end professionals contribute to the prosperity and development of the Russian state and the national science in the future!



President of NRC “Kurchatov Institute” Mikhail V. Kovalchuk

ЮРИЙ АЛЕКСАНДРОВИЧ
КОНСТАНТИНОВА



Preface

Petersburg Nuclear Physics Institute named by B.P. Konstantinov of NRC "Kurchatov Institute" (hereinafter – the Institute), which in 2021 celebrated its 50-year anniversary of becoming an independent research institution, is a multidisciplinary research center that conducts fundamental and applied research in the field of particle and high-energy physics, nuclear physics, condensed matter physics, molecular and radiation biophysics.

The scientific achievements of Institute's researchers have been awarded the Lenin and State prizes, the prizes of the Government of the Russian Federation and the Academic prizes. Three employees were elected full members and eight employees – the corresponding members of the Russian Academy of Sciences (RAS). In 2021 the Institute employed 2 070 workers including 507 researchers, 76 Doctors of Sciences and 256 Candidates of Sciences. At the moment, one employee is the corresponding member of RAS.

The Institute consists of five research divisions sharing a common infrastructure:

- Theoretical Physics Division,
- Neutron Research Division,
- High Energy Physics Division,
- Molecular and Radiation Biophysics Division,
- Advanced Development Division.

The long-term and short-term research program of the Institute can be found in two documents, which are the Program of Activity of NRC "Kurchatov Institute" and the Institute's Program of Research and Development (R&D) in accordance with the State assignment.

Just like other institutes within the National Research Center "Kurchatov Institute", the Institute takes an active part in various international projects and collaborates with the largest international research centers within its main research areas.

The Institute operates and builds basic facilities for physical research. The WWR-M research

reactor built in 1959 was temporarily shut down since 31 December 2015. For a long time, it was used to conduct fundamental and applied research in the field of nuclear physics, condensed matter physics, radiation materials science, radiation biology, the production of radionuclides for medical and technical use. In 2021, the proton synchrocyclotron SC-1000 constructed in 1970 operated only for the total of 1 657 h due to the global pandemic of coronavirus disease (COVID-19). The creation of the ophthalmological beam line with the design of proton beam output energy from 40 up to 80 MeV at the isochronous cyclotron C-80 was continued. The beam line will be used for the future oncological ophthalmological center for proton radiation therapy; simulation and optimization of the beam line of variable output energy proton beams at C-80 for testing the electronic component base was carried out; activities within the scope of Kurchatov Genomic Center were performed.

In 2021, works on the implementation of investment projects on modernization and renovation of engineering facilities of PIK neutron facility continued. Undoubtedly, this year was an important stage towards the creation of the PIK neutron facility. One of the most significant events of the year of Russian science is the energy launch of the PIK reactor and trial experiments at five experimental stations in the hall of horizontal experimental channels. These stations were commissioned in 2020 in line with the RF Presidential Edict No. 356 of 25.06.2019. They are: polarized neutron reflectometer (NERO-2), test neutron reflectometer (TNR), test neutron spectrometer (T-Spectrum), texture diffractometer (TEX-3), polarized neutron diffractometer (PND), which provide the implementation of a basic set of neutron techniques: diffractometry, reflectometry and spectrometry.

Although 2021 passed in the mode of restrictions on mass events, it was still full of events



in scientific and social life, both in-person and virtual ones. The Institute hosted 14 socially significant events (meetings, conferences and schools). The most remarkable of them are: the Workshop “Neutron Diffraction – 2021”, the VII International Conference and XIV School for Young Scientists and Specialists in the Topical Subject “Interaction of Hydrogen Isotopes with Structural Materials”, the First Summer School of the Council of Young Scientists and Specialists of NRC “Kurchatov Institute” – PNPI, the VI International Workshop “Dzyaloshinskii-Moriya Interaction and Exotic Spin Structures” (DMI-2021), the V All-Russian Conference “Fundamental Glycobiology”, the VIII All-Russian Youth Science Forum “Open Science 2021”, the VI Youth School of the PIK Reactor (Professionalism. Intellect. Career. PIK-2021), etc.

In 2021, the first graduation from the Institute's aspirantura (doctoral) program took place after the Institute had obtained its educational license. Seven graduation diplomas of aspirantura (doctoral) program were issued, which certify the successful completion of the third level of higher education in four fields of science: “Genetics”, “Nuclear and Particle Physics”, “Condensed Matter Physics” and “Biophysics”.

In 2021, 10 students entered the full-time doctoral course: 3 students in the training field 06.06.01 “Life Sciences” (subfield 03.02.07 “Genetics”) and 7 students in the training field 03.06.01 “Physics and Astronomy” (sub-

fields – 01.04.02 “Theoretical Physics”, 01.04.07 “Condensed Matter Physics”, 01.04.16 “Nuclear and Particle Physics”, 03.01.02 “Biophysics”).

In 2021, more than 170 students of Russia's universities conducted academic and research work, did practical training, prepared final qualification works for Bachelor's and Specialist's degree and Master theses in the laboratories of the Institute.

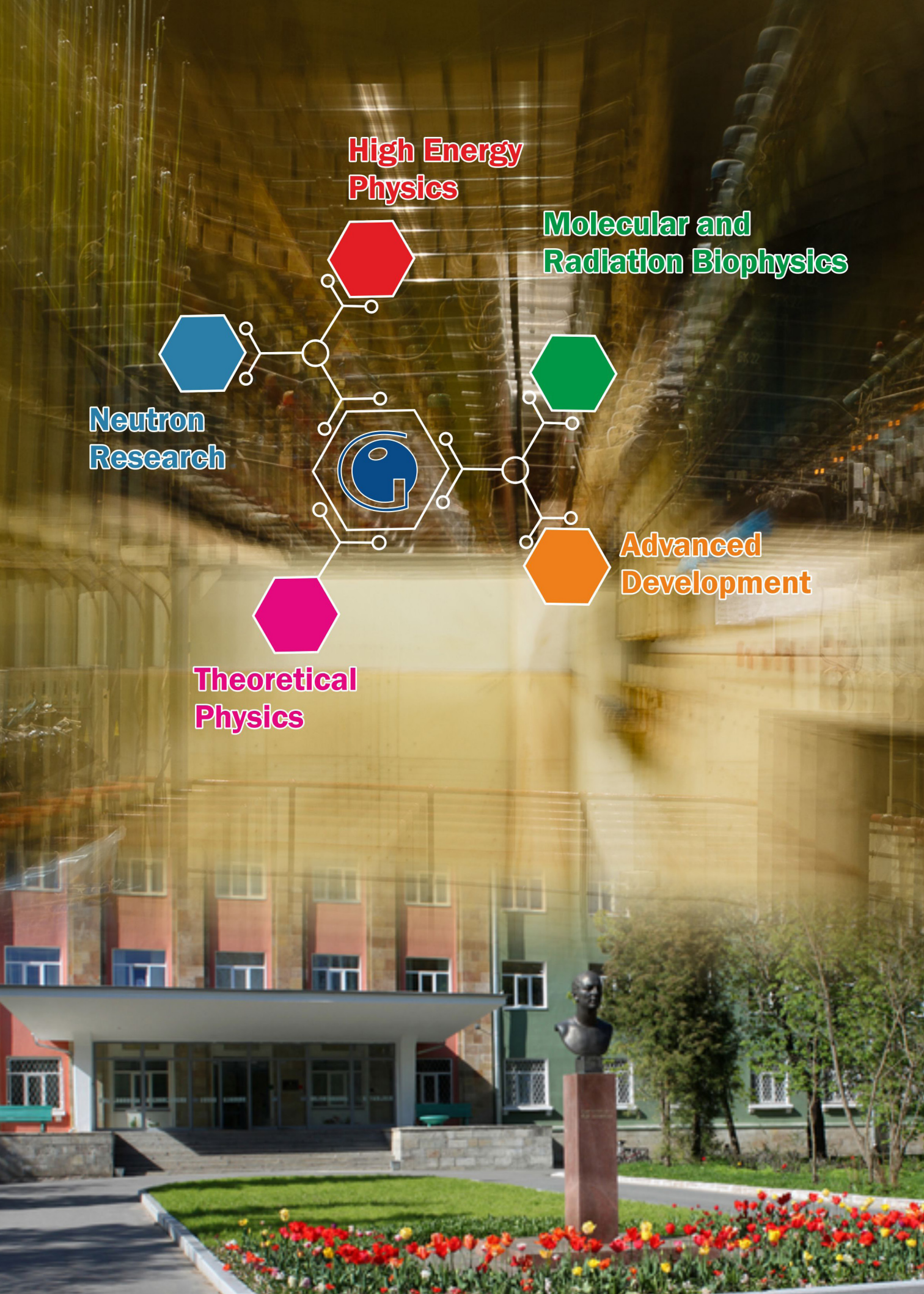
This publication is a collection of brief descriptions of the most significant and important research results of NRC “Kurchatov Institute” – PNPI obtained in 2021. This description is preceded by reviews of the heads of Institute's scientific divisions. The structure of divisions is also provided. It is followed by the abstracts of papers, the presentation of which was discussed and recommended by the scientific councils of the divisions. In addition to the abstract, each research result contains references to articles in leading Russian and foreign journals, describing the work in detail and where its full content can be found.

The results of the work of the Institute's researchers were published in 650 articles, including 446 research papers in peer-reviewed journals indexed by Web of Science and Scopus databases, and around 420 reports were presented at more than 150 international and Russian conferences.

The final section contains general information about the NRC “Kurchatov Institute” – PNPI.



Director of NRC “Kurchatov Institute” – PNPI
Sergey E. Gorchakov



**High Energy
Physics**

**Molecular and
Radiation Biophysics**

**Neutron
Research**

**Advanced
Development**

**Theoretical
Physics**

Research Divisions

- 12** Theoretical Physics Division
- 14** Neutron Research Division
- 18** High Energy Physics Division
- 21** Molecular and Radiation Biophysics Division
- 25** Advanced Development Division

Theoretical Physics Division

Theoretical Physics Division (TPD), headed by Dr. D.N. Aristov, consists of 7 departments:

- Theory of Electroweak Interactions (headed by Dr. V.Yu. Petrov);
- Theory of Strong Interactions (headed by Dr. V.Yu. Petrov);
- Quantum Field Theory (headed by Dr. V.A. Kudryavtsev);
- High Energy Physics (headed by Dr. V.Yu. Petrov);
- Condensed Matter Theory (headed by Dr. D.N. Aristov);
- Nuclei Theory (headed by Dr. M.G. Ryskin);
- Theory of Atoms (headed by Dr. A.I. Mikhailov)

and the Group of Physics of Nuclear Reactors (headed by Dr. M.S. Onegin).

TPD employs 50 research staff members (18 Doctors of Sciences and 22 Candidates of Sciences).



Dr. D.N. Aristov,
head of TPD

Research of TPD covers a great majority of areas of modern theoretical physics – from elementary particle physics and quantum field theory to physics of nuclear reactors.

High energy scattering is a traditional topic for TPD. For years, the research of TPD staff members has defined the world standard in this field. In 2021, a review was published on the generalized parton distribution (GPD) approach, which is a further development of the method for baryon-to-meson transition distribution amplitudes (TDA). The new GPD method allows us to account for a class of hard exclusive reactions for which a description in terms of collinear quantum chromodynamics (QCD) factorization is possible. An experiment at JLab Hall C has been proposed and agreed upon in 2023 to test the predictions of the new method.

The hypothesis of the so-called AdS/CFT duality (anti-de Sitter/conformal field theory) has attracted much attention from theorists and TPD is one

of the world leaders in this area. Duality means that a nontrivial field theory ($N = 4$ supersymmetric Yang–Mills theory) in $d = 4$ is equivalent to some string theory in anti-de Sitter space and both theories are exactly solvable. In fact, the duality is expressed in the connection of the anomalous dimensions of operators in supersymmetric theory with the string spectrum in the anti-de Sitter space. In the 2021 papers of TPD staff, the nonplanar contribution to the anomalous dimension of twist-2 operators has been calculated for the first time, which will allow us to check the hypothesis beyond the leading order.

Earlier it was shown that a soliton non-Abelian vortex tube (string) in the $N = 2$ supersymmetric QCD behaves as a critical superstring. Moreover, the closed superstring states appearing in four dimensions are identified with hadrons of such supersymmetric QCD. In the papers of 2021, a soliton gauge-string duality with AdS/ CFT correspondence is verified for this string. By calculating the correlation functions of the normalizable vertex operators on the $SL(2, \mathbb{R})/U(1)$ cigar, it was demonstrated that in channels with $SL(2, \mathbb{R})$ spin $j < -1/2$ this correspondence works, but in a channel with spin $j = -1/2$ the duality is lost. The theoretical analysis will continue.

Among TPD works in the field of condensed state theory one can mention a series of papers devoted to the development of the microscopic

theory of Raman scattering on disordered arrays of nanoparticles of non-polar crystals. The developed approach makes it possible not only to describe the position and shape of the Raman peak, but also to derive, with great accuracy, a number of important powder parameters from this description. The method has been successfully tested by analyzing a large set of experimental data.

Quantum interferometers using the Aharonov-Bohm effect are actively used for accurate measurements of the magnetic field. Recently, due to technological advances, the possibility of using topological materials in interferometers has been actively discussed. In the works of TPD staff it was

shown that electrons passing through such interferometers acquire spin polarization, the magnitude of which can be controlled by magnetic flux. The possibility of using such interferometers for quantum computing was also investigated.

In 2021, the research staff of TPD published 53 research papers in peer-reviewed journals indexed by Web of Science and Scopus databases, presented 26 papers at international and Russian conferences. Eight courses of lectures were delivered at Saint Petersburg University and Alferov Saint Petersburg National Research Academic University of RAS. One postgraduate student of the Institute has been recruited to work in TPD.

Neutron Research Division

Neutron Research Division (NRD), headed by Dr. A.I. Kurbakov, consists of 4 departments.

Neutron Physics Department (headed by Corresponding Member of RAS Prof. A.P. Serebrov) consists of 4 laboratories:

- Neutron Physics Laboratory (headed by Corresponding Member of RAS Prof. A.P. Serebrov);
- X- and γ -Ray Spectroscopy Laboratory (headed by Prof. V.V. Fedorov);
- Nuclear Spectroscopy Laboratory (headed by Dr. I.A. Mitropolsky);
- Molecular and Atomic Beams Laboratory (headed by Dr. V.F. Ezhov)

and 2 groups:

- Weak Interaction Research Group (headed by Dr. A.N. Pirozhkov);
- Nuclear Fission Physics Group (headed by A.M. Gagarsky).

Condensed Matter Research Department (headed by Dr. I.A. Zobkalo) consists of 4 laboratories:

- Disordered State Physics Laboratory (headed by Dr. V.V. Runov);
- Crystal Physics Laboratory (headed by Dr. Yu.P. Chernenkov);
- Material Research Laboratory (headed by Dr. A.I. Kurbakov);
- Neutron Physical and Chemical Research Laboratory (headed by Dr. V.T. Lebedev)

and Condensed Matter Electrodynamics Group (headed by Dr. O.V. Gerashchenko).

Semiconductor Nuclear Detectors Department (headed by Dr. A.V. Derbin).

Operation of Neutron Stations at the PIK Reactor Department (headed by Dr. V.V. Tarnavich).

NRD employs 104 research staff members (12 Doctors of Sciences and 52 Candidates of Sciences).



**Dr. A.I. Kurbakov,
head of NRD**

The main directions of NRD scientific activity are fundamental studies in the field of nuclear and elementary particles, and condensed matter physics.

The neutron is a very convenient research tool because it is involved in all types of interactions currently known. The purpose of the research carried out in NRD is the development and widespread introduction of methods and technical resources primarily using neutron radiation to study the composition, structure and fundamental properties of matter, predict, create and analyze the properties of new materials, and new physical phenomena inside, develop domestic unique experimental facilities and analytical techniques for neutron research.

NRD is the main executor at NRC "Kurchatov Institute" – PNPI of the thematic area No. 7 "Research in the Field of Neutron Physics" of the Program of Activities of the NRC "Kurchatov Institute". The employees of the division participate as performers in the implementation of some other areas of this Program.

The priority task at the moment is the development and creation of unique physical instruments for the PIK reactor facility.

With the active participation of many NRD employees, five research experimental stations were mounted on neutron beams and commissioned in the hall of horizontal experimental channels of the PIK reactor. These are the polarized neutron reflectometer (NERO-2), the test neutron reflectometer (TNR), the test neutron spectrometer (T-Spectrum), the texture neutron diffractometer (TEX-3) and the polarized neutron diffractometer (PND). The experimental stations commissioned provide the implementation of a basic set of neutron techniques: diffractometry, reflectometry and spectrometry.

Scientists and engineers of NRD are now developing new physical instruments for PIK facility and have already started to create their units. These are condensed matter physics instruments: powder diffractometers D1 and D3; single-crystal diffractometers DC-1 and DIPOL; neutron inelastic scattering spectrometers IN1, IN2, IN3 and IN4; small-angle scattering diffractometers Tenzor, Membrana, SANS-2 and SESANS. In nuclear physics, this is a source of ultracold neutrons (UCN), which will house a gravitational trap (GTRAP) and a magnetic trap (MTRAP) to measure the neutron lifetime, an EDM spectrometer (*n*EDM), neutron β -decay installation, neutron EDM by crystal diffraction method (DEDM); "Neutrino" installation; fission fragment multiplicity study facility (FISCO); nuclear radiation spectrometer (PROGRAS); neutron radiation analysis (INAA), neutron radiography facility.

2021 was a successful year as far as the scientific results are concerned. At the competition for the best scientific works of NRC "Kurchatov Institute" – PNPI, research teams, in which the main performers were NRD scientists, received one first, one second and two third awards. Year 2021 has become the most fruitful over recent years in terms of the number of dissertation defenses. NRD employees defended two doctor's degree dissertations – V.G. Zinoviev and N.K. Pleshakov (presently an employee of the Engineering Center "Neutron Technologies"), and six candidate's degree dissertations – V.A. Lyamkin, A.V. Chechkin, M.Kh. Yuzuyuk, V.A. Matveev, P.I. Konik and S.S. Lisin.

The European Physical Society has awarded the prestigious "Giuseppe and Vanna Cocconi Prize 2021" to the scientific Collaboration Borexino for outstanding contributions to particle astrophysics and cosmology, namely, for the pioneering observation of solar neutrinos from the *pp*-chain and the CNO-cycle. Among 95 laureates there are several NRD employees: A.V. Derbin, V.N. Muratova, D.A. Semenov, E.V. Unzhakov, I.S. Drachnev, N.V. Niyazova, I.S. Lomskaya.

DAAD (German Academic Exchange Service) scholarships were awarded to eight young NRD employees.

In 2021, NRD scientists published 69 papers in Web of Science journals and 1 monography

by V.V. Fedorov "History and Development of Physical Ideas about the Structure of the Surrounding World". The history of the evolution of ideas about the structure of matter from ancient times to the present day is outlined. The book deals with problems solved in neutron physics, high-energy physics, nuclear and thermonuclear energy.

In 2021, NRD was able to plan and hold six scientific schools and conferences, which can be considered as a great achievement in our current difficult situation.

During 2021, NRD employees carried out investigations within the framework of 6 RSF and 10 RFBR projects, in which NRD scientists were the leaders.

In the field of research of the fundamental properties of matter new important results have been obtained in 2021. The search for reactor anti-neutrinos oscillations in the neutrino laboratory at the SM-3 reactor (Dimitrovgrad) makes it possible to determine the parameters of neutrino oscillations into a sterile state by the method of relative measurements. The results obtained to date are confirmed in comparison with the results of other experiments. In particular, a joint analysis of the "Neutrino-4" and BEST experiments data suggests the reliability of detecting the effect of neutrino oscillations to a sterile state at the level of 4.9σ . Achieving accuracy within one experiment up to the level of 5σ will allow us to speak about the discovery of physics beyond the Standard Model (Neutron Physics Laboratory headed by Prof. A.P. Serebrov).

In NRC "Kurchatov Institute" – PNPI, we continued to measure the β -spectra of ^{144}Ce – ^{144}Pr and ^{210}Bi nuclei with β -spectrometers based on Si(Li)-detectors. The β -spectrum of ^{144}Pr was analyzed to search for a massive neutrino in the range 0.01–2.6 MeV. The results of measurements of the β -spectrum of ^{210}Bi using the β -spectrometer created according to the "target-detector" scheme were used by the Borexino Collaboration to isolate the signal from CNO-neutrino. Measurements with the Borexino detector were completed. Analysis of the complete data set has begun to obtain new results on solar neutrinos, rare processes and correlations with transient sources. An ana-

ysis of the correlations of events in the Borexino detector with fast radio bursts was carried out. New restrictions on the neutrino fluence of all flares associated with fast radio bursts have been established. The search for temporal correlations of Borexino detector signals and gravitational waves detected by the LIGO, VIRGO, KAGRA detectors is continued. Continued work in the DarkSide and DEAP Collaborations focused on the search for dark matter particles. New data were obtained on the use of SiPM for reading a scintillation signal, on the separation of Ar isotopes, and on the sensitivity of the Ar detector to supernova neutrinos. The results of the experiment on the search for resonant absorption of solar axions by ^{83}Kr nuclei conducted at the Baksan Neutrino Observatory of the Institute for Nuclear Research of RAS were processed, which made it possible to establish new restrictions on the coupling constants and the hadronic axion mass (Semiconductor Nuclear Detectors Department headed by Dr. A.V. Derbin).

The measurements of the $^{236}\text{U}(n, f)$ fission cross section completely cover the energy range of 1–20 MeV (reactor spectrum), which is in demand in today's nuclear technologies and technologies of the near future, as well as the most difficult region of 20–300 MeV, which is critically important from an experimental point of view for the development of promising ADS-technologies (Nuclear Fission Physics Group headed by A.M. Gagarsky).

A study of possible systematic effects in the measurement of the neutron lifetime by the method of magnetic storage of UCN was carried out. It is shown that magnetic storage of UCN has a huge advantage over material traps. The presence of a magnetic shutter in the magnetic trap on the exit neutron guide, which is transparent to depolarized neutrons, makes it possible to carry out experiments on measuring the neutron lifetime with registration of all possible UCN losses during their storage in the trap (in on-line mode). This unique opportunity distinguishes these experiments from experiments with UCN storage in material traps and allows to fundamentally exclude the main systematic effects caused by neutron losses during their storage (Molecular and Atomic Beams Laboratory headed by Dr. V.F. Ezhov).

In the field of condensed matter physics, the following most important results were obtained using various neutron scattering methods. According to the study of critical fluctuations in $\text{Mn}_{1-x}\text{Fe}_x\text{Si}/\text{Ge}$, a fundamental conclusion was made for the physics of magnetism in helimagnets that two interactions, ferromagnetic exchange and the Dzyaloshinskii–Moriya interaction, turn out to be independent and their magnitude can be controlled separately by changing the concentration of chemical elements in quasibinary compounds $\text{Mn}_{1-x}\text{Fe}_x\text{Si}$ and $\text{Mn}_{1-x}\text{Fe}_x\text{Ge}$ (Disordered State Physics Laboratory headed by Dr. V.V. Runov, research by Dr. S.V. Grigoriev).

A comparative analysis of the ground magnetic state in $\text{A}_3\text{M}_2\text{SbO}_6$ layered oxides with a honeycomb superstructure made it possible to describe the mechanisms of the formation of magnetic properties and the origin of various magnetic phase transitions in 2D layered and frustrated compounds. The qualitative and quantitative results of the work can be used to theoretically substantiate the general mechanisms and principles of the magnetic order formation in systems with reduced dimensionality and strong frustration of exchange interactions, as well as to search for new systems of low-dimensional magnets with unique quantum ground states such as a spin liquid (Material Research Laboratory headed by Dr. A.I. Kurbakov).

Studies of phase transitions and magnetic structure in rare-earth multiferroics-ferroborates revealed a crucial role for single-ion anisotropy. The combined use of neutron scattering and high-resolution optical spectroscopy turned out to be very productive and makes it possible to solve a complex fundamental problem – the origin of electric polarization in multiferroics-ferroborates (Crystal Physics Laboratory headed by Dr. Yu.P. Chernenkov, research by Dr. I.V. Golosovsky).

The multiferroic $\text{Nd}_{0.8}\text{Tb}_{0.2}\text{Mn}_2\text{O}_5$ was studied using polarized neutron diffraction. It is shown that such a system has the ability to generate several magnetic phases with resembling incommensurate wave vectors. At low temperatures, magnetic ordering has a structure in the form of an elliptical spiral. Ellipticity parameters are determined. The distinction in the population of chiral domains can be changed by applying an external electric

field of several kilovolt per centimeter, which indicates a strong magnetoelectric coupling (Crystal Physics Laboratory headed by Dr. Yu.P. Chernenkov, research by Dr. I.A. Zobkalo).

Using the small angle polarized neutron scattering (SAPNS) method, it was possible, for the first time, to estimate the scale of magnetic correlations in materials based on reduced graphene oxide (rGO). The result obtained is unique, since such information cannot be obtained by other methods. The experiments showed the presence of small-angle magnetic-nuclear interference scattering for both native rGO and a composite based on it in magnetic fields of the order of 1 T, which unambiguously indicates the presence of magnetized regions on a scale of 1 000 Å in the materials under study (Disordered State Physics Laboratory headed by Dr. V.V. Runov).

Using a set of research techniques, the structure and catalytic properties of thin silica films doped with Pt and Pd nanoparticles synthesized using the sol-gel method were determined. It has been established that bimetallic Pt-Pd nanoparticles 6–15 nm in size exhibit catalytic activity, and Pd nanoparticles with a size of about 6 nm react to the presence of hydrogen by changing the photoresponse (research by NRD Scientific Secretary Dr. N.N. Gubanova).

Self-consistent theoretical calculations of the electronic spectrum $E\sigma(k)$ of ferromagnetic films of cobalt and its silicide under graphene grown on silicon carbide, graphene-Co-SiC and graphene-Si-Co-SiC were performed within the framework of the spin density functional theory (SDFT). It is shown that ferromagnetic films are localized between the buffer layer and the substrate. Geometrical optimization of both systems was carried out, the densities of electronic states were calculated, and the distribution of magnetic moments was found. The maximum value of the number of monolayers of iron and cobalt films on hexagonal boron nitride *h*-BN, which have perpendicular magnetic anisotropy was obtained (Condensed Matter Electrodynamics Group headed by Dr. O.V. Geraschenko, research by Dr. S.M. Dunaevsky).

In 2021, the research staff of NRD published 69 research papers in peer-reviewed journals indexed by Web of Science and Scopus databases (including 53 papers published in foreign editions), obtained 1 patent and 1 certificate of state registration of specialized programs; 2 Doctor of Sciences dissertations and 6 Candidate of Sciences dissertations were defended.

High Energy Physics Division

High Energy Physics Division (HEPD), science headed by Corresponding Member of RAS

Prof. A.A. Vorobyov, headed by Prof. O.L. Fedin, consists of 10 laboratories:

- Elementary Particle Physics Laboratory (headed by Prof. G.D. Alkhazov);
 - Relativistic Nuclear Physics Laboratory (headed by Dr. Yu.G. Ryabov);
 - Short-Lived Nuclei Laboratory (headed by Dr. V.N. Panteleev);
 - Meson Physics Laboratory (headed by Dr. S.I. Vorobyov);
 - Few Body System Laboratory (acting head – O.V. Miklukho);
 - Crystal Optics of Charged Particles Laboratory (headed by Dr. Yu.M. Ivanov);
 - Hadron Physics Laboratory (headed by Dr. O.L. Fedin);
 - Physics of Exotic Nuclei Laboratory (headed by Prof. Yu.N. Novikov);
 - Baryonic Physics Laboratory (headed by Dr. A.A. Dzyuba);
 - Cryogenic and Superconductive Techniques Laboratory (headed by Dr. A.A. Vasilyev)
- and 4 technical departments:**
- Radio Electronics Department (headed by Dr. V.L. Golovtsov);
 - Tracking Detector Department (headed by Prof. A.G. Krivshich);
 - Computing Systems Department (headed by A.E. Shevel);
 - Muon Chambers Department (headed by V.S. Kozlov).

HEPD employs 115 research staff members (14 Doctors of Sciences and 56 Candidates of Sciences).



Prof. A.A. Vorobyov,
Corresponding Member
of RAS,
science head of HEPD



Prof. O.L. Fedin,
head of HEPD

HEPD activity is mainly aimed at the experimental research in the field of elementary particle physics and nuclear physics. In addition, the development of innovative methods for obtaining radioisotopes for medical applications and studies of magnetic properties of materials with the use of the μ SR-method are being performed. As in previous years, research works were conducted at facilities of NRC “Kurchatov Institute” – PNPI and at accelerators of the world’s leading nuclear centers.

In 2021, the following experiments were carried out.

1. At the synchrocyclotron of NRC “Kurchatov Institute” – PNPI:
 - Production and studies of short-lived nuclei with the isotope mass separator on-line facility IRIS;
 - Studies of polarization effects in proton quasi-elastic scattering off nuclei;
 - Studies of magnetic properties of materials with μ SR-method.
2. In the European Center for Nuclear Research (CERN):
 - Participation in CMS, ATLAS, LHCb and ALICE experiments at the Large Hadron Collider (LHC);

– Production and studies of short-lived nuclei with the isotope mass separator on-line facility ISOLDE;

– Studies of possibilities to use crystal collimation of the LHC beams (experiment UA9).

3. At the electron accelerator at the Bonn University (Germany) – study of nucleon structure by γ - p -scattering.

4. At the meson factory at the Paul Scherrer Institute (Switzerland) – search for muonic catalysis of the nuclear fusion reaction $d^3\text{He}$.

5. At the Max Planck Institute for Nuclear Physics (Heidelberg, Germany):

– Ultraprecise measurement of the mass difference of $^{187}\text{Re} - ^{187}\text{Os}$, which is necessary to determine the effective mass of antineutrinos.

– Search for muonic catalysis of the nuclear fusion reaction $d^3\text{He}$.

The experiment MuSun (high precision studies of muon capture on deuteron) has been completed at the Paul Scherrer Institute meson factory (Switzerland), the data analysis is ongoing.

New HEPD projects include preparations of the following experiments:

– “Proton” for measurements of the proton charge radius in elastic electron-proton scattering at the electron accelerator MAMI (Mainz, Germany);

– AMBER/NA66 for measurements of the proton charge radius in elastic muon-proton scattering on the SPS beam at CERN;

– R3B, MATS, PANDA and CBM at the accelerator complex FAIR (Helmholtz Center for Heavy Ion Research, Germany);

– SHiP for search of new particles from hidden sector at CERN;

– MPD at the NICA collider which is under construction in Dubna,

as well as the following projects:

– IRINA for production and studies of short-lived nuclei at the PIK high flux neutron reactor;

– PITRAP for precision mass measurements of short-lived nuclei at the PIK high flux neutron reactor;

– RIC-80 for production of radioisotopes for medical applications.

One of the main activities of HEPD is the participation in fundamental research at unique accelerator facilities in world scientific centers, such

as the LHC at the CERN and at the new generation accelerator research complex at the European Facility for Antiproton and Ion Research (FAIR).

At the CERN HEPD participated in the LHC experiments CMS, ATLAS, LHCb and ALICE from the initial stages of design and construction of these detectors with a significant intellectual and instrumental contribution to the various subsystems of the detectors. After the LHC start-up, HEPD physicists and engineers, along with other participants of the experiments, have shared responsibilities in maintenance and operation of these detectors and have taken part in the analysis of the experimental data. The analysis of the experimental data collected in Run 2 (2015–2018) continues to yield a great amount of new results.

The most significant of them, obtained in 2021 with the participation of staff of the Division, is the detection of the decay of the Higgs boson into muons in the CMS experiment, the first direct observation of the quantum chromodynamic “dead cone” effect in hard proton-proton interactions in the ALICE experiment. This effect was predicted by the theorists of our Institute in 1991 (Yu.L. Dokshitser, S.I. Troyan, V.A. Khose), however until recently, its observation in many experiments was difficult. Our physicists continue to study rare decays of beauty particles in the LHCb experiment. To date, in the LHCb experiment 55 new hadronic states have been discovered, among which there are candidates for pento- and tetraquark states. ATLAS experiment continues to search for dark matter particles with our participation, which will establish new, more stringent restrictions on the cross section for the production of such particles.

In 2021, the major activities of HEPD groups participating in the LHC experiments were focused on the preparation of the CMS, ATLAS, LHCb and ALICE detectors to operation at Run 3 after their modernization to be able operate after increasing LHC collider luminosity.

The study of the properties of quark gluon plasma (QGP) is the one of the fundamental research directions in HEPD which started in the 1980s in the PHENIX experiment (Brookhaven National Laboratory, USA) and continued in the ALICE experiment (CERN). After the launch of FAIR accelerator facility, the study of QGP will be carried out

in the CBM experiment. In relation to the construction of NICA collider in Dubna (nuclotron-based ion collider facility) which is designed to conduct studies of nuclear matter in ion-ion collisions, the Division has cooperated on the creation of a multipurpose MPD detector and the development of the physics program of the experiment. HEPD is also involved in the design development of the concept and physics research program for the se-

cond SPD detector at the NICA collider, to study collisions of polarized particle and the spin structure of the nucleon.

In 2021, the research staff of HEPD published 180 research papers in peer-reviewed journals indexed by Web of Science and Scopus databases, presented 43 research reports at international and Russian events.

Molecular and Radiation Biophysics Division

Molecular and Radiation Biophysics Division (MRBD), headed by Dr. A.L. Konevega, consists of 13 laboratories:

- Biophysics of Macromolecules (headed by Dr. V.V. Isaev-Ivanov);
- Genetics of Eukaryotes (headed by Dr. V.G. Korolev);
- Protein Biosynthesis (headed by Dr. A.L. Konevega);
- Molecular Genetics (headed by Dr. V.N. Verbenko);
- Biopolymers (headed by Dr. A.L. Timkovsky);
- Human Molecular Genetics (headed by Dr. S.N. Pchelina);
- Enzymology (headed by Dr. A.A. Kulminskaya);
- Experimental and Applied Genetics (headed by Dr. S.V. Sarantseva);
- Medical Biophysics (headed by Prof. Dr. L.A. Noskin);
- Medical and Bioorganic Chemistry (headed by Dr. F.M. Ibatullin);
- Proteomics (headed by Dr. S.N. Naryzhny);
- Cryoastrobiology (headed by Dr. S.A. Bulat);
- Molecular and Cellular Biophysics (headed by Dr. G.N. Rychkov)

and 3 centers:

- Center for Preclinical and Clinical Research (headed by Dr. A.P. Trashkov);
- Resource Center (headed by Dr. N.A. Verlov);
- Kurchatov Genome Center (headed by Dr. A.A. Kulminskaya)

and Engineering Support Department (acting principal engineer – P.A. Sotnikov).

MRBD employs 133 research staff members (13 Doctors of Sciences and 52 Candidates of Sciences).



Dr. A.L. Konevega,
head of MRBD

The main areas of activity of MRBD are research in molecular biology and biochemistry, structural biophysics, molecular and medical genetics.

Recent years have been marked by the rapid emergence of a new science – proteomics – on the arena of scientific research. The scientific community is particularly interested in what this science is based on and how its methods work. Finding, identifying, separating, quantifying and qualitatively analyzing protein molecules that play a role in the functioning of the body are the main tasks of pro-

teomics. The human proteome consists of a diverse and heterogeneous series of gene products/proteoforms/protein species. The work of S.N. Naryzhny (Proteomics Laboratory) is devoted to searching among this variety of proteomic forms characteristic of various diseases, in particular, glioblastoma multiforme (GMF). The work shows the possibility of using haptoglobin proteoforms as a potential plasma biomarker specific for GMF on the basis of the performed analysis.

At MRBD, interlaboratory work has been underway for several years to study extracellular vesicles (EVs, exosomes), which play an important role in many biological processes. For example, EVs are involved in important processes in the development of GMF, including malignant transformation and invasion. In addition, exosomes, secreted by many cells, are natural particles capable of carrying large amounts of nucleic acids and proteins while maintaining their stability. However, the efficiency and

strategy of EV-based therapies depend on the distribution of these particles in the body tissues. A study conducted by T.A. Shtam (Protein Biosynthesis Laboratory) and colleagues showed that EVs isolated from grapefruit are effective in the delivery of exogenous proteins, in particular bovine serum albumin (BSA) and heat shock protein (HSP70). In addition, the biodistribution of EVs in various body tissues was assessed using the radioactive tag ^{125}I .

Another important observation is made in the work of S.N. Pchelina (Human Molecular Genetics Laboratory), where mutations in the *GBA1* gene leading to Gaucher disease (HD), which in turn is a high risk factor for Parkinson's disease (PD), are studied. The *GBA1* gene encodes an important lysosomal enzyme, glucocerebrosidase (GCase). Mutations disrupt the 3D structure of GCase and its transport into the lysosome, which leads to a decrease in the activity of the enzyme in the lysosome. The commonality of the pathogenesis of these diseases makes the development of strategies aimed both at treating GD and PD associated with mutations in the *GBA1* gene (GBA-BP) promising. A.E. Kopytova together with G.N. Rychkov (Laboratory of Molecular and Cellular Biophysics) proposed a possible mechanism of action of ambroxol and a method of searching for promising pharmacological chaperones. In addition, it is shown that primary macrophage culture is a suitable model for testing the effectiveness of drugs that affect the activity of Gcase and ambroxol effectively restores the activity and concentration of GCase protein, as well as increases its transport into lysosomes.

The Division was not left out of the research of the currently relevant disease – coronavirus infection (COVID-19), caused by severe acute respiratory syndrome coronavirus-2 (SARS-CoV-2) of the coronavirus family HCoV. T.S. Usenko (Human Molecular Genetics Laboratory), for the first time analyzed the transcriptome in COVID-19 patients at the time of admission to the intensive care unit to assess the outcome of the disease in the acute period (30 days). Using bioinformatic methods, a list of over 300 differentially expressed genes (DEGs) was identified and, in particular, the low-density lipoprotein receptor activation pathway was highlighted.

For the first time we have shown a decrease in the expression level of *STAB1*, *PPARG*, *CD36*, *ITGAV* and *ANXA2* genes, whose products are involved in cholesterol metabolism, in survivors compared to those who died. And this confirms the important role of changes in cholesterol metabolism in determining the outcome of coronavirus infection.

In another study by E.V. Semenova (Center for Preclinical and Clinical Research) we performed long-term observation of the behavior of humoral immune response to SARS-CoV-2 virus infection and quantitative assessment of anti-SARS-CoV-2 immunoglobulin levels in blood of healthy donors living under conditions of coronavirus pandemic and patients who had COVID-19. The dynamics of anti-SARS-CoV-2 IgG is consistent with the notion of "classical" humoral immunity in viral infection. At the same time, the IgA immunoglobulin behavior during SARS-CoV-2 infection was found to differ from the IgA behavior for previous generations of coronaviruses. It is possible that SARS-CoV-2-specific IgAs play an independent role in providing protective immunity during minor viral loads. However, elevated IgA levels are not an absolute defense against COVID-19 disease.

Research in microbiology and biotechnology is traditional for MRBD. The work of the staff of the Enzymology Laboratory investigated the antibacterial properties of fucoidans from the brown algae *Fucus vesiculosus* of the Barents Sea. Natural fucoidans are a polydisperse mixture of compounds whose composition may vary greatly depending on the species, the algae habitat, and methods of isolation. Comparison of the action of two fractions of sulfated polysaccharides with different degrees of purification on microorganisms *Escherichia coli*, *Bacillus licheniformis*, *Staphylococcus epidermidis* and *Staphylococcus aureus* showed a significant bacteriostatic effect of fucoidans on *E. coli* cells and no morphological changes. And the effect on *S. epidermidis* and *S. aureus* was a significant reduction in size. In general, the coarse fraction of fucoidans showed greater inhibitory activity against microbes compared to the purified fraction.

Works devoted to the repair (reparation) of various genetic DNA lesions hold a special place in MRBD research. These works, traditional for MRBD, were performed on unicellular microorganisms –

Saccharomyces cerevisiae yeast. In eukaryotes, tolerance to DNA damage is determined by two repair pathways, homologous recombination repair and the pathway controlled by the RAD6-epistatic gene group. Proliferating cell nuclear antigen (PCNA) monoubiquitination mediates an error-prone pathway, whereas polyubiquitination stimulates an error-free pathway. The error-free pathway includes components of recombination repair; however, the factors that act on this pathway remain largely unknown. E.A. Alekseeva (Eukaryote Genetics Laboratory) analyzed the functions of the Hsm3 protein in the NuB4 complex in the yeast *S. cerevisiae*. A new member of the error-free DNA damage tolerance pathway, a product of the *HIM* gene, was identified earlier, and the mechanism of the error-free DNA damage bypass pathway in the *him1* mutant acts through recruitment of the highly erroneous Pol η polymerase to perform reparative DNA synthesis during genome postreplicative repair. In the yeast nucleus, the NuB4 nuclear complex consists of three proteins: Hat1, Hat2 and Hif1, and physically interacts with Hsm3p. Genetic analysis of the properties of three mutants *hsm3Δ*, *hif1Δ* and *hat1Δ* provided evidence that a significant increase in dNTP levels suppresses *hsm3*- and *hif1*-dependent mutagenesis. Moreover, *hsm3Δ* and *hif1Δ* mutations significantly reduce the efficiency of induction of RNR (ribonucleotide reductase) gene expression after UV irradiation. This decrease in expression is the reason for the switch of precision polymerases to the highly erroneous polymerase Pol η during reparative DNA synthesis. Thus, Pol η is responsible for *hsm3*- and *hif1*-dependent mutagenesis and the Hsm3 protein, like the Hif1 protein, can be a functional subunit of the NuB4 complex and participate in chromatin assembly during the repair process.

Interrelation of the nervous system, its physiology and functioning are under the control of various genes; model organisms, in particular *Drosophila melanogaster*, are used to study various aspects of nervous system functioning. In the work of E.V. Ryabova and P.A. Melentev (Laboratory of Experimental and Applied Genetics) we studied the functioning of glial cells under conditions of swiss cheese gene knockdown in surface glia (blood-brain barrier) as well as in cortex glia of central nervous sys-

tem and enveloping glia of peripheral nervous system. These types of glial cells provide homeostasis in the nervous tissue, protecting it from external influences. The work shows that swiss cheese gene knockdown in the superficial glia causes morphological and functional changes in the subperineurial glia, and in the wrapping glia – morphological changes in the structures formed by these cells. In addition, we described changes in the transcriptome when the expression of the swiss cheese gene was suppressed in these types of glia, and we also found an increase in the level of reactive oxygen species. The changes detected were accompanied by a decrease in locomotor activity of the flies. The results indicate a significant role of the swiss cheese gene in several types of glial cells to provide protection of the nervous system from oxidative stress and to control the locomotor activity of individuals. In the next part of the study, by suppressing the expression of the swiss cheese gene in the neurons of *D. melanogaster* adults, neurodegeneration in the brain was induced. This caused a decrease in their lifespan, as well as a decrease in locomotor activity and memory impairment. At the same time, the level of reactive oxygen species increased in the brain, lipid droplets accumulated, and the number of mitochondria decreased. These results suggest that oxidative stress and altered lipid metabolism develop in neurons in response to dysfunction of the swiss cheese gene product, and that the pathological process in a number of neurodegenerative diseases, such as hereditary spastic paraplegia, involves disturbances of mitochondria, lipid droplets and the endoplasmic reticulum.

The work of the Protein Biosynthesis Laboratory deserves special attention. The study of the fundamental features of the protein-synthesizing system (ribosome) is a complex and urgent task. The emergence and spread of antibiotic resistance in bacteria is one of the most serious problems in medicine, since known and long used antibiotics lose their effectiveness over time. One approach to solving the problem of resistance is a thorough study of antibacterial drugs and the mechanisms of resistance to them. In the work of E.V. Polesskova and coauthors, an *in vitro* translation system was created, which consists of elements of the protein

synthesis system from *E. coli* with replacement of one of the elongation factors with a heterologous protein from the thermophilic microorganism *Thermus thermophilus*. In the presence of the thermophilic factor EF-Tu in the system, the rates of binding and decoding reactions in the A site decreased by an order of magnitude, whereas the presence of the thermophilic factor EF-G did not affect the kinetic parameters of factor-dependent translocation and inhibition. This observation means that the translocation process is largely determined by the interaction between tRNA and ribosome and can be efficiently catalyzed by thermophilic EF-G. E.M. Maksimova and colleagues carried out a thorough study of antibacterial drugs and mechanisms of resistance to them. In this work kinetic and thermodynamic study of the effect of amicoumacin A on the main steps of polypeptide synthesis was carried out. It was shown that antibiotic amicoumacin A binds near the E site codon and stabilizes mRNA and decreases the rate of formation of a functional 70S initiator complex, promotes formation of erroneous 30S initiator complexes, and decreases the rate of peptidyl-tRNA movement from A site to P site and decreases the number of ribosomes able to synthesize polypeptides. Thus, it stops bacterial growth by inhibiting the ribosome during translation.

D.M. Baitin and I.V. Bakhlanova (Laboratory of Molecular Genetics) also devoted their work to the problem of emergence and evolution of bacterial resistance. This ability of bacteria is based on genetic variability followed by selection of resistant variants. In the presence of a complex system of evolutionary adaptation regulation in which

the pathway of horizontal transfer of resistance genes is not the only one, bacterial cells adapt to the action of antibiotics by activating the mechanism of cellular SOS-response and associated induced mutagenesis. And to suppress the evolutionary pathways of resistance emergence, universal targets in the form of proteins critical for bacterial metabolism and inhibitors to them are searched for. Protein RecA is functionally involved in chromosomal transformation, conjugation and mutagenesis induction and thus represents an ideal target for the search of compounds blocking its activity. The structure and function of RecA retain the highest conservativity among bacteria, including pathogenic ones. This article is devoted to comparison of various strategies of search for inhibitory compounds and substantiates the advantage and universality of the strategy of creation of peptide inhibitors, which are functional fragments of intermolecular interface. Such peptides contain only natural amino acids, which are highly specific for their targets and therefore do not have a wide range of side effects and are nontoxic for humans.

In 2021, the research staff of MRBD published more than 120 research papers in peer-reviewed journals indexed by Web of Science and Scopus databases, 48 of them were published in foreign journals. The employees of the department made more than 62 reports at conferences. There is an active training of scientific staff, 26 doctoral students studying in the aspirantura (doctoral) course in NRC "Kurchatov Institute" – PNPI and 8 members of the Division supervise the work of doctoral students from other institutions.

Advanced Development Division

Advanced Development Division (ADD), headed by Dr. A.V. Titov, consists of 3 laboratories:

- Chemistry and Spectroscopy of Carbon Materials (acting head – Dr. M.V. Suyasova);
- Holographic Information and Measurement Systems (headed by Dr. B.G. Turukhano);
- Quantum Chemistry (headed by Dr. A.V. Titov)

and 3 departments:

- Accelerator Department (headed by Dr. E.M. Ivanov), which includes Laboratory of Physics and Technology of Accelerators (headed by Dr. S.A. Artamonov);
- Applied Nuclear Physics Department (headed by Dr. V.A. Solovey), which includes Laboratory of Radiation Physics (headed by Dr. A.S. Vorobyev);
- Information Technology and Automation Department (headed by S.B. Oleshko), which includes Laboratory of Information and Computing Systems (headed by S.B. Oleshko).

ADD employs of 51 research staff members (7 Doctors of Sciences and 27 Candidates of Sciences).



Dr. A.V. Titov,
head of ADD

The basic accelerator facilities of the Institute are concentrated in the Accelerator Department (AD) of ADD. First of all, it is a unique synchrocyclotron with an energy of 1 000 MeV, SC-1000, with a current of 1 μ A of the output beam. SC-1000 is used to conduct a wide range of scientific and applied studies in various fields – from nuclear physics to medicine.

Its main distinguishing features are:

- Highly efficient output system (30%), the efficiency of which is five times higher than that of a standard regenerative system;
- The system of time stretching of the derived proton beam, which makes it possible to increase the time filling coefficient of the beam from 2 to 85%.

For a number of physical and applied studies, proton beams of other energies are required. For this purpose, proton beams of variable energy from 60 to 1 000 MeV were created at the SC-1000 of NRC “Kurchatov Institute” – PNPI by the staff

of AD. The diameter of the obtained beams is $\sim 30\text{--}80$ mm, $\Delta p/p$ is in the range of 1.3–14%, and the intensity varies in the range of $10^7\text{--}10^{12}$ s $^{-1}$.

In addition to the main proton beam, there is a second one of “low” intensity, about 1% of the main beam, which is extracted from the synchrocyclotron chamber simultaneously with the main beam. The beam can be used for both physical and applied purposes, in particular, for the proton radiation therapy, which can significantly reduce the costs of irradiation of patients.

For scientific research, there are secondary beams of π^\pm and μ^\pm mesons obtained on the external meson-forming target. In the accelerator chamber, neutrons with energies from 0.01 eV to 950 MeV are generated as a result of a single-turn discharge of a proton beam onto an internal neutron-forming lead target.

The improvement of space and aviation technology is largely associated with the use of micro- and nanoelectronics elements. One of the main conditions for their successful use is their long-term robust performance in the radiation fields of outer space and the upper atmosphere. Currently, the regulations of Russia and the standards of the leading countries of the world include mandatory tests of radiation resistance of modern electronic equipment used in aviation and space technology, relating to the effects of various types of

radiation. A specialized center for proton radiation testing with an energy of 60–1 000 MeV, including two test benches with beam diagnostic systems, modern dosimetry devices, an automated results processing system and a modern infrastructure for users, became operational at the synchrocyclotron of NRC “Kurchatov Institute” – PNPI in 2015.

The international regulatory document JEDEC STANDARD prescribes testing of electronic components and radio products in neutron fluxes with a spectrum that is similar to that of atmospheric neutrons. In 2015, the Nuclear Fission Physics Group of NRD and AD of ADD completed the creation of such a neutron source at the GNEIS neutron source of the SC-1000 synchrocyclotron.

The high intensity of the neutron beam allows for an accelerated testing of electronics – 1 h of exposure of the product on the beam is equivalent to 100 years of stay in flight. Thus, since 2015, the universally valid center for radiation-resistance testing of electronic components has been in operation in NRC “Kurchatov Institute” – PNPI, which now is capable of fully testing the electronics on beams of protons with variable energy and on neutron beams with the range repeating that of atmospheric neutrons.

AD of ADD and the D.V. Efremov Scientific Research Institute of Electrophysical Apparatus are joining efforts to launch a multipurpose cyclotron complex based on the built isochronous cyclotron C-80 with a variable proton energy of 40–80 MeV and a current of the output beam up to 100 μ A. The high energy of the accelerated beam combined with the high intensity will allow the production of high-quality radioisotopes and radiopharmaceuticals that are not available for commercial cyclotrons, in particular generator isotopes. Generator isotopes open the way for positron emission tomography in medical centers remote from the cyclotron. The project also provides for the development of a method for creating ultrapure medical isotopes using a magnetic separator. The energy range of the proton beam (60–70 MeV) of the cyclotron C-80 makes it possible to create the only ophthalmological center in Russia today for proton therapy of oncological diseases of the organs of vision. AD of ADD has long been engaged in the development of this project

together with the A.I. Alikhanov Institute of Theoretical and Experimental Physics of NRC “Kurchatov Institute” (NRC “Kurchatov Institute” – ITEP).

When creating equipment for the ophthalmology room and radiation planning, the vast experience accumulated at NRC “Kurchatov Institute” – ITEP will be used, where about 1 400 patients underwent proton therapy sessions until 2010.

The Laboratory of Holographic Information and Measurement Systems (LHIMS) of ADD is one of the world leaders in the field of precision measurements at the nanometer scale. To carry out these studies, the LHIMS has a modern, unique underground vibration-free holographic laboratory. On the basis of this laboratory and unique test benches for the synthesis of linear and radial holographic diffraction gratings, 14 types of nanotechnological equipment and devices can be produced, including: photovoltaic converters of linear and angular displacements, long meters, two-, three-, four- and more coordinate measuring machines, radius meters, plane meters, turntables for measuring with the resolution 10 nm and hundredths of a second. In 2015, for the first time in the world, a linear holographic lattice with a length of 1 300 mm and a resolution of 1 nm was created in the LHIMS. The works of LHIMS were awarded at the exhibition “Army-2015”.

For many years, the Department of Information Technology and Automation (DITA) of ADD has been actively involved in the ATLAS project of the Large Hadron Collider at CERN. Employees of the Laboratory of Information and Computing Systems are engaged in the development and support of various software systems for the detector control system (DCS) and the data acquisition system (DAQ) of the ATLAS experiment. The Department also supports the local computer network of the Institute, various information and computing systems based on Web technologies, as well as information systems to support the administrative and economic activities of the Institute. The design and technology group of the department participated in the work on the Proton program carried out by HEPD to conduct research on the PS1 muon beam (CERN) using the IKAR installation. The task of DITA was to modernize IKAR by creating and embedding segmented anode blocks into

the set-up. The work was completed on time, and the upgraded IKAR installation was installed on the beam and passed the necessary beam tests.

The discovery of the subglacial Lake Vostok in Antarctica was the last major geographical discovery of the XX century. Its research will provide unique data on the origin and evolution of life forms in ecosystems that are characterized by an extremely high degree of oligotrophy, as well as extreme conditions. These include: the expected extremely high oxygen content in the water (50–100-fold increase compared to the usual concentration for terrestrial lakes), high pressure – 350 bar, the inability of the ecosystem to use solar energy due to the extremely thick layer of ice covering the lake. NRC “Kurchatov Institute” – PNPI is the main organization for the study of the water column of the lake. The employees of ADD, MRBD and NRD are actively involved in this program. The Institute faces the most difficult technical task of developing such a technology of penetration into the water column of the lake, in which its contamination with drilling fluid filling the well will be excluded. This task requires the development of unique devices that record hydrophysical, hydrochemical and microbiological parameters online, as well as allowing sterile sampling of water and soil in the volumes necessary for subsequent laboratory analyses.

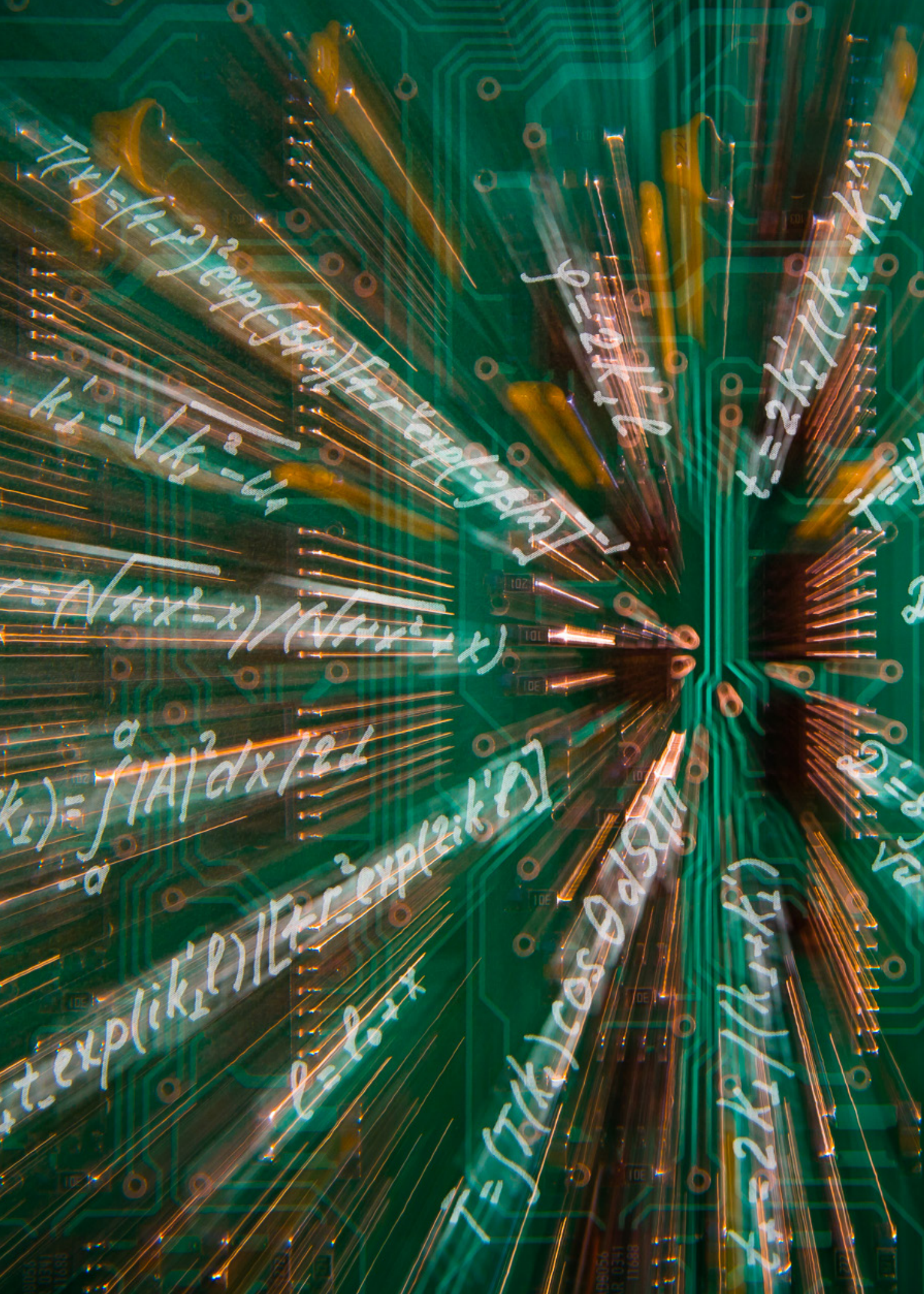
The Applied Nuclear Physics Department has manufactured equipment designed to study the water column of Lake Vostok. Before sending this equipment to Antarctica, it is necessary to conduct deep-water tests. The equipment created was tested in the deep-water areas of Lake Ladoga, and in 2014, 2015 and 2018 – at the Vostok Station. The tests were successful.

The main research trend of the Laboratory of Chemistry and Spectroscopy of Carbon Materials (LCSCM) of ADD is the development of new fullerene and endometallofullerene derivatives, the study of their physical and chemical properties, radiation resistance and self-assembly in aqueous solutions. One of the most important scientific and practical tasks of the LCSCM is the development of new endometallofullerene derivatives which are promising as systems for targeted drug delivery. Commonly used radiopharmaceuticals contain a radioisotope in combination with a chelating agent

that binds the radioactive atom firmly enough and prevents its binding to blood components and other body tissues. However, the stability of such a chelate complex is not absolute and therefore small amounts of toxic radioactive metal can be released into the body. For this purpose, the laboratory studies the radiation resistance of endometallofullerenes and their derivatives under irradiation.

The main direction of the work of the Quantum Chemistry Laboratory of ADD is the development of relativistic methods for calculating the electronic structure of molecules containing heavy atoms. This activity was initiated back in the early 80s of the last century by the need to calculate unusual properties in two-atom molecules with one heavy atom, the knowledge of which is necessary to search for new physics on such molecules beyond the Standard Model. The calculations were based on a two-step method developed by the laboratory, which made it possible to divide the calculation structure of such molecules into two consecutive calculations in the valence region and in the region of the core of a heavy atom. The accuracy achieved in these calculations is currently the world record. The laboratory staff did not limit themselves to calculations of various physicochemical properties of twoatomic molecules with completely filled shells localized in atomic cores and, and have moved on to studies of the electronic structure and properties of substantially more complex chemical compounds. The development of new effective methods, algorithms and software packages for precise modeling of the electronic structure and properties of compounds of heavy elements allowed us to begin a systematic study of the properties of molecules containing lanthanides, actinoids and heavy transition metals and to proceed to calculations in solid-phase systems and to conduct a study of the chemical and spectroscopic properties of compounds of superheavy elements from the “island of stability”.

In 2021, the research staff of ADD published 44 research papers in peer-reviewed journals indexed by Web of Science and Scopus databases, made more than 60 reports at Russian and international scientific conferences and scientific seminars, and also received 5 patents and certificates of invention.



Theoretical and Mathematical Physics

- 30** Quantum chromodynamics instanton production in diffractive processes at the Large Hadron Collider
- 31** Scalar isoscalar mesons and scalar glueball from J/Ψ -meson radiative decays
- 33** Nucleon-to-meson and nucleon-to-photon transition distribution amplitudes
- 34** Calculation and study of the leading non-planar contribution to the anomalous dimension of twist-2 operators in the maximally extended supersymmetric Yang–Mills theory
- 35** Calculation of the $^{179}\text{HfF}^+$ cation for the search for new physics
- 36** Compound-tunable embedding potential – new approach for modeling actinide, lanthanide and transition metal impurities in materials
- 37** Theoretical study of Aharonov–Bohm helical interferometers
- 38** Theory of Raman scattering of light in nanopowders of nonpolar crystals
- 39** Mean-field approach for skyrmion lattices description in centrosymmetric frustrated antiferromagnets
- 40** Generalized relativistic pseudopotentials for light elements
- 41** Critical non-Abelian flux tube and holography for little string theory

Quantum chromodynamics instanton production in diffractive processes at the Large Hadron Collider

M.G. Ryskin¹, V.A. Khoze¹, V.V. Khoze², D.L. Milne²

¹ Theoretical Physics Division of NRC “Kurchatov Institute” – PNPI

² Institute of Particle Physics Phenomenology of Durham University, England

A nontrivial classical solution – instanton in quantum chromodynamics (QCD instanton) was discovered long ago in 1975. Instantons play an important role in QCD vacuum description, in chiral invariance violation, etc. Nevertheless, up to now nobody succeeded to observe the instanton experimentally.

In the experiment, QCD instanton should look like a fireball formed from a large number of particles distributed isotropically. However, events in which several pairs of partons collide simultaneously have a similar structure.

We have proposed to search for the instanton at the Large Hadron Collider (LHC) in diffractive events, where the probability of multiple parton interactions is strongly suppressed. When the leading proton carries away more than 99.5% of the incoming energy, the remaining energy is not sufficient to produce new secondaries in the interaction of another parton pair.

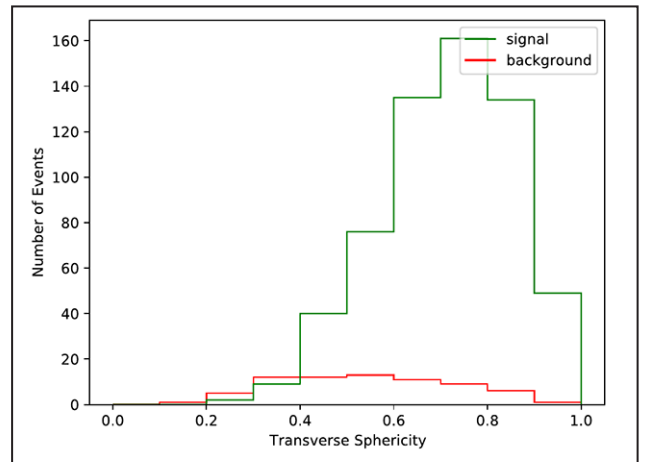
The large size (small mass) instantons are practically invisible. They decay into a few minijets with about 1 GeV energy. Similar minijets are produced in the usual soft interactions. The cross section of heavy instantons drops rapidly with the instanton mass. Therefore, we are looking for the instanton with the mass of 30–50 GeV. In such a case, selecting events with the leading proton and large multiplicity (more than 20 charged particles with a transverse energy of more than 15 GeV within

the pseudorapidity interval from 0 to 2), but without the jets with a large transverse momentum it looks possible to get the signal an order of magnitude larger than that coming from the background (Fig.).

In the case of instanton, the sphericity (S) distribution has a peak at $S \sim 0.7$ –0.8 while a rather flat (with a weak maximum at $S \sim 0.5$) distribution is predicted for the background.

Note that the expected cross section (~ 1 nb) is rather large and can be observed at the LHC.

The cross section of instanton production in processes with a large rapidity gap (including the diffractive events) was calculated for the first time.



Sphericity distribution for the instanton and the background for $L = 1 \text{ pb}^{-1}$

Scalar isoscalar mesons and scalar glueball from J/Ψ -meson radiative decays

A.V. Sarantsev¹, I.I. Denisenko²

¹ Theoretical Physics Division of NRC “Kurchatov Institute” – PNPI

² Joint Institute for Nuclear Research

Radiative decays of J/Ψ -mesons are the most promising source for studying the bound state of two gluons – the glueball. In the radiative decay of the J/Ψ -meson, the c-quark and c-antiquark are annihilated into two gluons with the emission of a photon (Fig. 1). Gluons can couple to resonances, which, in turn, decay into stable mesons. High statistical data on the radiative decays of the J/Ψ -meson into the channels $\gamma\pi\pi$, γKK , $\gamma\eta\eta$, $\gamma\eta\eta'$ were obtained by the BESIII Collaboration. Moreover, the collaboration performed an energy-independent partial wave analysis of the data, which showed that only two partial waves with $JP = 0+$ (scalar states) and $2+$ (tensor states) are born in these channels. The contribution of the scalar wave and the contribution of the dominant multifield $E1$ of the tensor wave to the $J/\Psi \rightarrow \gamma\pi\pi$ and $J/\Psi \rightarrow \gamma KK$ reactions is shown in Fig. 2. As can be seen, the $0+$ wave has a complex structure in the region of masses 1500–2200 MeV, while in the tensor wave, we see the production of the ground states $f_2(1270)$ and $f_2(1525)$ and practically no other structure up to an invariant mass of 2200 MeV.

We have analyzed the scalar wave together with data on J/Ψ -decay into channels $\gamma\eta\eta$, $\gamma\eta\eta'$, $\gamma\phi\phi$, data on pion-pion scattering into channels $\pi\pi$, KK , $\eta\eta$, $\eta\eta'$ and data on proton-antiproton annihilation into three mesons. The analysis was carried out within the framework of the dispersion N/D method, which takes into account the properties of analyticity and unitarity of the scattering amplitude. As a result of the analysis, contributions from 10 scalar resonances (in principle, all 10 are well known) were identified, which can be assigned to two groups according to the quark-antiquark configuration: predominantly singlets and

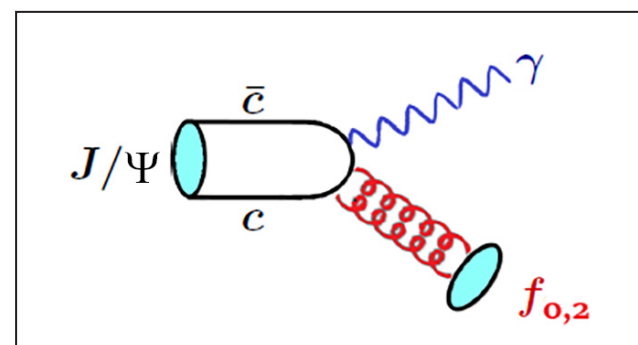


Fig. 1. Radiative decay of the J/Ψ -meson

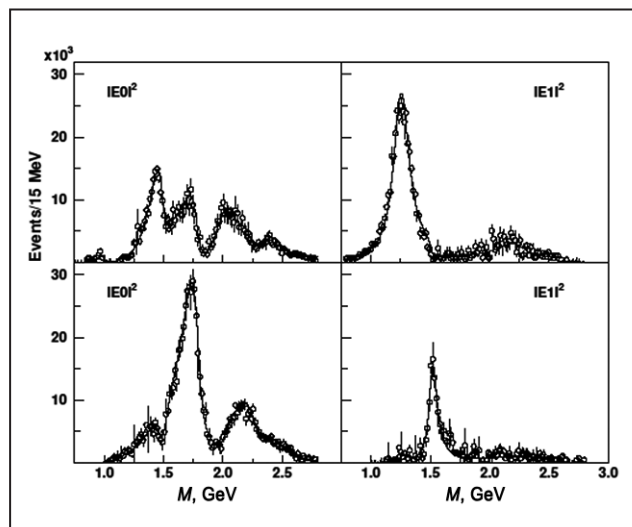


Fig. 2. Contribution of scalar (left column) and dominant tensor wave $E1$ (right column) to $J/\Psi \rightarrow \gamma\pi\pi$ (upper plots) and $J/\Psi \rightarrow \gamma KK$ (lower plots) reaction cross section

predominantly octets. The intensity of the production of these states and decay rates into various final states are given in the Table. The decay rates into the unmeasured final states are calculated for resonances with masses less than 1800 MeV based on the unitarity condition for the obtained

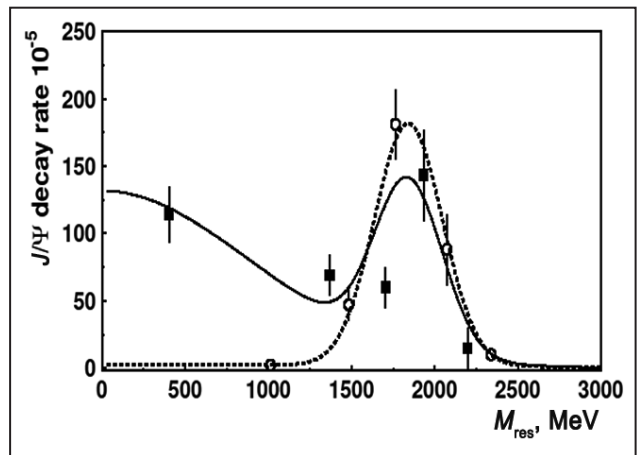
Table. Intensity of decay of resonances into various final states in 10^{-5}

$\text{BR}(J/\Psi \rightarrow \gamma f_0)$	$\gamma\pi\pi$	γKK	$\gamma\eta\eta$	$\gamma\eta\eta'$	$\gamma\omega\phi$	Missing	Total
$f_0(500)$	105 ± 20	5 ± 5	4 ± 3	~ 0	~ 0	~ 0	114 ± 21
$f_0(980)$	1.3 ± 0.2	0.8 ± 0.3	~ 0	~ 0	~ 0	~ 0	2.1 ± 0.4
$f_0(1370)$	38 ± 10	13 ± 4	3.5 ± 1.0	0.9 ± 0.3	~ 0	14 ± 5	69 ± 12
$f_0(1500)$	9.0 ± 1.7	3 ± 1	1.1 ± 0.4	1.2 ± 0.5	~ 0	33 ± 8	47 ± 9
$f_0(1710)$	6 ± 2	23 ± 8	12 ± 4	6.5 ± 2.5	1 ± 1	7 ± 3	56 ± 10
$f_0(1770)$	24 ± 8	60 ± 20	7 ± 1	2.5 ± 1.1	22 ± 4	65 ± 15	181 ± 26
$f_0(2020)$	42 ± 10	55 ± 25	10 ± 10	-	-	38 ± 13	145 ± 32
$f_0(2100)$	20 ± 8	32 ± 20	18 ± 15	-	-	38 ± 13	108 ± 25
$f_0(2200)$	5 ± 2	5 ± 5	0.7 ± 0.4	-	-	38 ± 13	49 ± 17
$f_0(2330)$	4 ± 2	2.5 ± 0.5	1.5 ± 0.4	-	-	-	8 ± 3

amplitudes. Note that the intensity for the decay into the inelastic channels are in a good agreement with the measured intensity of J/Ψ decay into the $\gamma 4\pi$ channel.

For resonances with masses in the region of 2000–2300 MeV, where there are no pion-pion scattering data and it is not possible to restore inelasticity based on the unitarity condition, we simply divided the measured intensity of J/Ψ decay into the $\gamma 4\pi$ channel in this region equally between three states. This hypothesis needs to be tested. The production intensities for the two groups of found resonances are shown as *black squares* (singlets) and *open circles* (octets) in Fig. 3. The plot shows a specific production intensity pattern for resonances with a peak at 1850 MeV and a Gaussian distribution with a width of 350 MeV. The only reasonable explanation for this phenomenon is the creation of a glueball with the mass of 1850 MeV that mixes with nearby quark-antiquark states.

It should be noted that the masses of the states found are in good agreement with the quark model,

**Fig. 3.** Production intensity of octet (open circles) and singlet (full squares) scalar states in radiative decays of J/Ψ

and no additional state beyond this classification has been found. It is possible that the mass and width of the additional state coincided with the characteristics of one of the standard quark-antiquark states and we could not identify it, or the glueball does not form a pole in the scattering plane and is realized only through mixing with other states.

Nucleon-to-meson and nucleon-to-photon transition distribution amplitudes

K.M. Semenov-Tian-Shansky¹, A.A. Shaikhutdinova¹, B. Pire², L. Szymanowski³

¹ Theoretical Physics Division of NRC “Kurchatov Institute” – PNPI

² Ecole Polytechnique, France

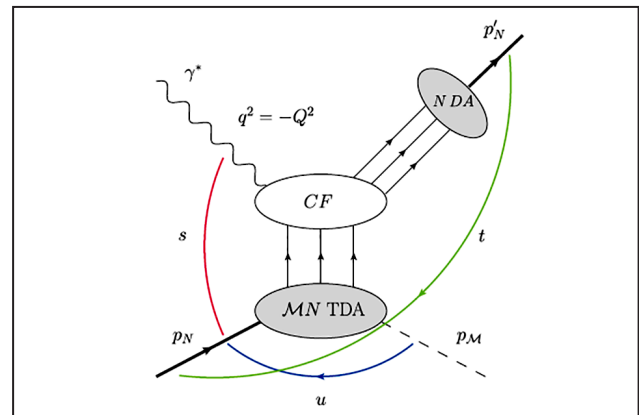
³ National Centre for Nuclear Research, Poland

In the specific kinematics the amplitudes of hard exclusive reactions can be factorized in form of convolutions of hard parts, which allow a description in the framework of perturbative quantum chromodynamics (QCD), and of hardronic matrix elements of non-local QCD operators on the light cone. A generalization of this approach for hard exclusive electroproduction of meson (and photons) off nucleons in the backward direction $e(k) + N(p_N) \rightarrow e(k') + \gamma^*(q) + N(p_N) \rightarrow e(k') + N'(p'_N) + M(p_M)$ in the generalized Bjorken kinematics (large $q^2 = -Q^2$ and $s = (q + p_N)^2$, fixed $x_B = Q^2/(2p_N q)$, small value of $|u| = |(p_N - p_M)| \ll Q^2, W^2$) has led to a necessity to introduce new non-perturbative objects: nucleon-to-meson and nucleon-to-photon matrix elements of three-quark light-cone operators. These quantities were called nucleon-to-meson and nucleon-to-photon transition distribution amplitudes (TDAs). The collinear factorization reaction mechanism for the hard subprocess $\gamma^* N \rightarrow N' M$ involving TDAs is presented in the Figure.

The physical picture contained in nucleon-to-meson (and nucleon-to-photon) TDAs turns to be a further development of that of generalized parton distributions (GPDs) and of baryon distribution amplitudes (DAs), baryon light-cone wave functions. Nucleon-to-meson TDAs describe partonic correlations between states of different baryonic charges. This provides an access to study non-minimal Fock components of hardronic light-cone wave functions. Switching TDAs to the impact parameter space al-

lows one to perform femtophotography of hadrons from a new perspective.

The interest for the description of hard exclusive processes within the collinear factorization framework is boosted by a large number of international experimental projects in this field (JLab@12 GeV, PANDA@GSI-FAIR, JPARC). Special attention should be paid to the preparation of the research program for the EIC and EicC electron-ion colliders planned for construction. Moreover, at the moment the CLAS Collaboration (JLab, Newport News, USA) is preparing a detailed dedicated experiment to study backward electroproduction of pseudoscalar mesons using CEBAF accelerator.



Leading order collinear factorization mechanism for the hard subprocess $\gamma^*(q) + N(p_N) \rightarrow N'(p'_N) + M(p_M)$: MN TDA denotes nucleon-to-meson transition distribution amplitude; N DA stands for nucleon distribution amplitude; CF denotes the hard part (coefficient function)

1. Pire B., Semenov-Tian-Shansky K.M., Szymanowski L. // Phys. Rep. 2021. V. 940. P. 1–121.
2. Ayerbe Gayoso C., ..., Pire B., Semenov-Tian-Shansky K.M., ..., Szymanowski L. et al. // Eur. Phys. J. A. 2021. V. 57. No. 12. P. 342.
3. Pire B., Semenov-Tian-Shansky K.M., ..., Szymanowski L. arXiv:2201.12853 [hep-ph].

Calculation and study of the leading non-planar contribution to the anomalous dimension of twist-2 operators in the maximally extended supersymmetric Yang–Mills theory

V.N. Velizhanin¹, B.A. Kiehl²

¹ Theoretical Physics Division of NRC “Kurchatov Institute” – PNPI

² Institute for Theoretical Physics II, Hamburg University, Germany

The study of the AdS/CFT-correspondence between the maximally extended supersymmetric Yang–Mills theory and superstring theory in anti-de Sitter space is one of the most actual topics in high-energy physics. One of the main objects of research within the framework of the duality between quantum field theory and superstring theory are composite operators and their paired string states, with the results for the dimensions of operators and quantum corrections to them and the results for the energy of the corresponding string states being compared. Over 20 years of studying AdS/CFT-correspondence, the effective methods have been developed that are applied on both sides of the duality and allow obtaining the results for both weak and strong coupling. However, almost all these remarkable results were obtained only in the planar case. Going beyond the planar limit allows us to explore new aspects of the AdS/CFT-correspondence between gauge theory and superstring theory, in which nonplanarity in quantum field theory corresponds to loop corrections in superstring theory.

The non-planar contribution to the anomalous dimension of twist-2 operators in the maximally extended supersymmetric Yang–Mills theory first appears in the fourth order of perturbation the-

ory, and our own computer programs as well as third-party publicly available specialized computer programs were used to compute it by the standard calculation of the corresponding Feynman diagrams. The results of calculations obtained by us for several fixed values of the Lorentz spin of operators were then used to find the leading non-planar contribution to the so-called cusp anomalous dimension and the general form of the leading non-planar contribution to the anomalous dimension of twist-2 operators for an arbitrary Lorentz spin of operators.

The availability of the general result made it possible for the first time to study the analytic properties of the non-planar contribution and obtain completely new information about the corresponding contribution in the Balitsky–Fadin–Kuraev–Lipatov evolution equations and the generalized doubly logarithmic equation, as well as to find non-planar contributions in various limiting cases, in particular, the non-planar contribution to the anomalous dimension of the one-magnon operator in the β -deformed version of the considered model. The results obtained will provide the important test for studying the effects of nonplanarity in the framework of the AdS/CFT-correspondence.

1. Kiehl B.A., Velizhanin V.N. // Phys. Rev. Lett. 2021. V. 126. No. 6. P. 061603.
 2. Kiehl B.A., Velizhanin V.N. // Nucl. Phys. B. 2021. V. 968. P. 115429.

Calculation of the $^{179}\text{HfF}^+$ cation for the search for new physics

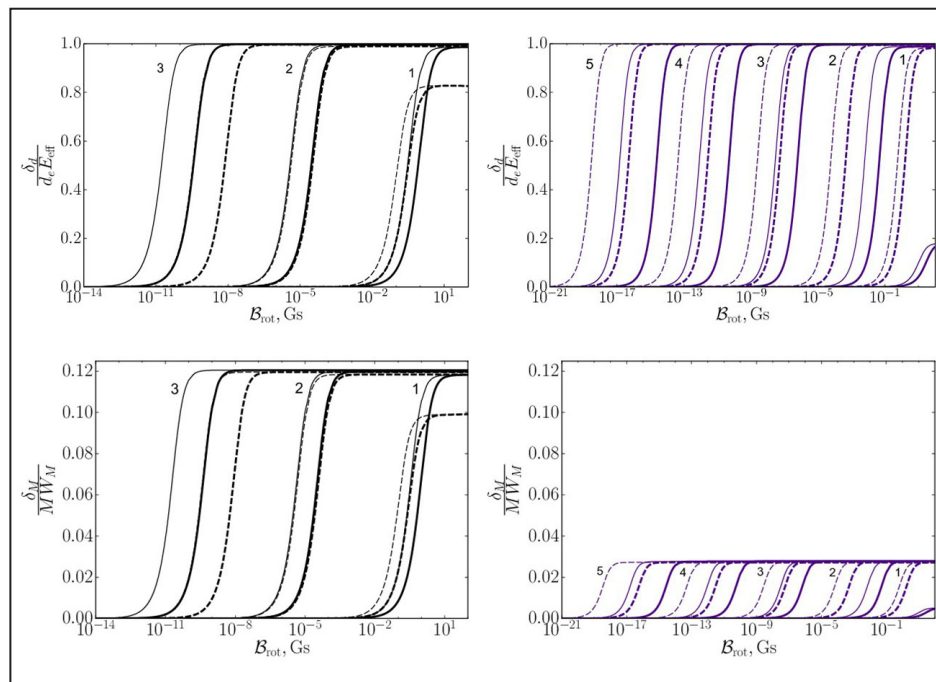
I.P. Kurchavov, A.N. Petrov

Advanced Development Division of NRC “Kurchatov Institute” – PNPI

The nuclear magnetic quadrupole moment (MQM) is the lowest T , P -odd magnetic moment. Measuring the MQM allows setting limits on T , P -odd nuclear forces, neutron electric dipole moment (EDM), quantum chromodynamics vacuum angle θ , chromo-EDM of quarks. A feature of experiments with trapped ions is the use of rotating magnetic and electric fields.

We calculated the energy levels and g -factors as functions of the static electric field. Such calculations are necessary to control and suppress systematic errors in the experiment and to determine the level population scheme. The Figure shows the obtained energies of interaction with the electron EDM and MQM of the ^{179}Hf nucleus as a func-

tion of the rotating magnetic field for the components of the hyperfine structure of the main rotational level $J = 1$ of the electronic state ${}^3\Delta_1$ $^{179}\text{HfF}^+$ that we proposed for the experiment ($F_1 = 7/2$, $F = 3$ and $F_1 = 11/2$, $F = 5$). The total moment of the cation is $\mathbf{F} = \mathbf{F}_1 + \mathbf{l}^2$, where $\mathbf{F}_1 = \mathbf{J} + \mathbf{l}^1$, $\mathbf{l}^1 = 9/2$ and $\mathbf{l}^2 = 1/2$ are the spins of the hafnium and fluorine nuclei. The selected levels have almost the same sensitivity to EDM and about five times different sensitivity to MQM, which will allow distinguishing between the effects of electronic EDM and MQM in the experiment. Following our results, these levels are considered by the E. Cornell group for the preparation of the experiment.



Electric dipole moment (top) and magnetic quadrupole moment (bottom) related splits for $^{179}\text{HfF}^+$ for $F = 7/2$, $F = 3$ (left) and $F = 11/2$, $F = 5$ (right). The numbers on the graph correspond to the projection of \mathbf{F} onto the direction of the rotating field (variable axis). Thin line for $\omega = 150$ kHz, thick line for $\omega = 250$ kHz, where ω is the field rotation frequency. The solid and dashed lines distinguish the components of the Stark doublets. Rotating electric field $\varepsilon_{\text{rot}} = 110$ V/cm

Compound-tunable embedding potential – new approach for modeling actinide, lanthanide and transition metal impurities in materials

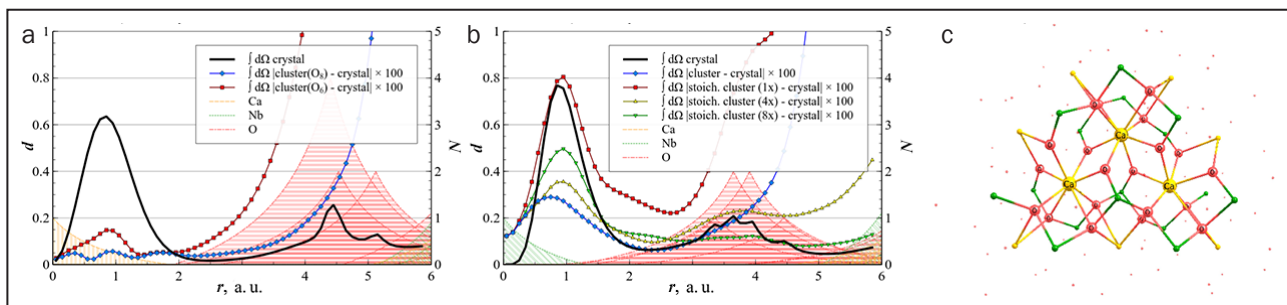
D.A. Maltsev, Yu.V. Lomachuk, V.M. Shakhova, N.S. Mosyagin, L.V. Skripnikov, A.V. Titov
 Advanced Development Division of NRC “Kurchatov Institute” – PNPI

Embedding potential is an important approach to study local properties and processes, and properties of substitute atoms in crystals, as it allows one to significantly improve the computational accuracy, along with making it easier to model charged point defects containing heavy atoms. The compound-tunable embedding potential (CTEP) models the environment of a given crystal fragment as a combination of “pseudoatoms”, described by the effective core potentials tuned for a particular compound, and additional partial charges.

In the present work the impurity Ta and U atoms were studied in a calcium niobate crystal. Structure and electronic density from periodic crystal calculations were reproduced with high precision in cluster calculations for fragments of perfect crystal (Fig. a, b). In these clusters the Nb → Ta and Ca → U substitutions were made with subsequent structural relaxation. Nb and Ta atoms are exceptionally close in terms of structural and chemical properties, so the structural changes were comparable to usual errors of methods involved.

Ca → U substitution, however, is a more complex case: these atoms differ by not only chemical and structural properties (first, ionic radii), but there is also a significant difference in the oxidation state (ionic charge), so that the resulting fragment is charged (+2 for U^{IV} and +4 for U^{VI}). As expected, calculations yielded a considerable structural distortion.

In real crystalline materials, two or more charged defects with opposite charges can be located nearby, so that their charges are locally compensated. The minimal cluster, which includes only the near environment of a central atom, cannot be used to model such groups of defects, however, this task can be solved by building an extended cluster, such as a cluster with three Ca centers (Fig. c). As for the minimal clusters, structure and electronic density were reproduced in cluster calculations with high accuracy. Two substitution types were modeled, taking structural relaxation into account. Additionally, X-ray emission chemical shifts were calculated on Nb and U atoms.



Comparison of electronic density, obtained in periodic-structure and cluster calculations (a, b): total density in crystal (black line) and difference between cluster and crystal, multiplied by 100 (colored lines). Two clusters (with 6 and 8 neighbor O) are compared for Ca center, while for Nb center CTEP is compared to stoichiometric models. Colored peaks qualitatively represent positions of neighbor atoms. Cluster with three Ca centers for modeling two substitution types: first, where two Ca⁺² cations are substituted by the U⁺⁴ cation and a hole (vacancy), and second, where three Ca⁺² cations are substituted by the U⁺⁶ cation and two holes (c)

1. Lomachuk Yu.V., Maltsev D.A., Mosyagin N.S. et al. // Phys. Chem. Chem. Phys. 2021. V. 22. P. 17922.

2. Shakhova V.M., Maltsev D.A., Lomachuk Yu.V. et al. // Phys. Chem. Chem. Phys. 2022. V. 24. P. 19333.

Theoretical study of Aharonov–Bohm helical interferometers

R.A. Niyazov¹, D.N. Aristov¹, V.Yu. Kachorovskii²

¹ Theoretical Physics Division of NRC “Kurchatov Institute” – PNPI

² Ioffe Institute

The discovery of topological materials represents an opportunity to create a new field of nanodevices – topological electronics. Devices based on topological materials will transmit the signal better and will be resistant to defects. They are very attractive for the study of coherent quantum phenomena and the creation of quantum computers.

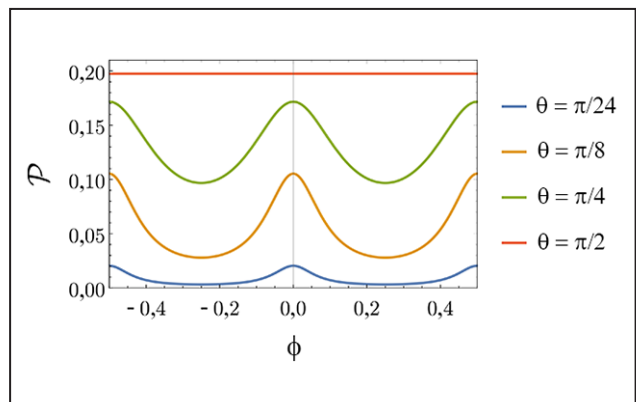
Therefore, in this scientific work, two-dimensional topological insulators were studied. At the edge of such materials, there are one-dimensional conducting states in which the direction of electron momentum is related to its spin projection (helical states). Electrons cannot scatter on non-magnetic impurities in such states due to their topological protection. Therefore, the transmission of electrons occurs without dissipation.

The Aharonov–Bohm interferometer based on helical edge states (HES) of a two-dimensional topological insulator was theoretically investigated. A wide range of temperature variation in the system has been studied. The influence of magnetic impurities on the transmission of electrons has been studied.

It was shown that in the presence of a magnetic impurity, a quantum contribution to the electron transmission coefficients appears. Due to the Aharonov–Bohm effect, it rapidly oscillates with a change in the magnetic flux penetrating the area covered by the HES. Such an extremely sharp de-

pendence of conductance and spin polarization on magnetic flux opens up wide possibilities for applications in the field of controlled spin filtering (Fig.) and sensitive magnetic field detectors.

It has also been demonstrated that a HES-based tunneling interferometer can be described in terms of an ensemble of flux-driven qubits. The number of active qubits involved in charge and spin transfer is determined by the ratio of temperature to the distance between levels. Such an ensemble of qubits can operate effectively at high temperatures and be used for quantum calculations. This opens up wide avenues for high-temperature quantum computing.



Polarization of an electron beam at the output of a helicoidal interferometer with an increase in the strength of scattering by a magnetic impurity

- Niyazov R.A., Aristov D.N., Kachorovskii V.Yu. // Phys. Rev. B. 2021. V. 103. P. 122154.
- Niyazov R.A., Aristov D.N., Kachorovskii V.Yu. // JETP Lett. 2021. V. 113. P. 689.

Theory of Raman scattering of light in nanopowders of nonpolar crystals

O.I. Utesov¹, A.G. Yashenkin¹, S.V. Koniakhin²

¹ Theoretical Physics Division of NRC “Kurchatov Institute” – PNPI

² Alferov Saint Petersburg National Research Academic University of RAS

Physics and physical chemistry of nanoparticles is a rapidly developing area of science with very promising industrial applications. These applications cover the composite materials design, optics, quantum computing, renewable energy, visualization of biological processes, targeted delivery of drugs inside the body, etc. Crystalline nanoparticles including semiconducting and carbon-based ones (such as nanodiamonds) as well as quantum dots play a very important role in these research activities. The attestation and standardization of such particles parameters as their size, shape, phase composition and surface morphology are essential for further utilization in science and technology. Presently, they are performed with the use of quite expensive (and sometimes destructive) methods such as high-resolution transmission microscopy, X-ray powder diffraction, dynamical light scattering, atomic force microscopy, and so on. It would be extremely fruitful to adopt the Raman spectroscopy for these needs, which is a simple and cheap but very powerful optical nondestructive method that allows investigating the elementary excitations in crystals, and, specifically, the phonons.

This year the microscopic theory of Raman spectra of nonpolar crystalline nanoparticles was completed, formulated within two almost equivalent approaches referred to as the atomistic DMM-BPM method and the continuous EKFG method. This theory, which includes also the microscopic quantum description of the optical phonon lines broadening due to their scattering by crystal imperfections, allows interpreting the Raman spectra with

much better accuracy and precision than the previously used phenomenological model of phonon confinement (PCM). This approach make it possible to determine the nanoparticles mean size, the variance of probability function for their size distribution, the nanoparticles shape parameterized by the number of crystallite facets, and the level of crystallite (both surface and bulk) imperfectness exclusively from the Raman spectrum of nanoparticle ensemble (powder or suspension).

The Raman spectrum of a nanopowder is evaluated in four steps.

1. Determination of spectrum and wave functions for optical phonon modes of a nanoparticle performed either within the framework of the atomistic dynamical matrix method or by means of its continuous counterpart in the form of Klein–Fock–Gordon equation under Dirichlet boundary conditions.

2. Calculation of intensity of light scattering by optical phonon modes performed within the framework of the conventional bond polarization model or its continuous version. The important result is the separation of modes onto Raman active and Raman silent ones.

3. Phonon lines broadening. The finite experimental line widths in nanodiamonds were shown to be induced by crystal imperfections, and their empirical inverse dependence on the particle size has been explained theoretically.

4. Accounting for the size distribution of nanoparticles in a powder. A method to significantly accelerate the calculations using the scaling properties of EKFG equation has been proposed.

1. Utesov O.I., Yashenkin A.G., Koniakhin S.V. // J. Phys. Chem. C. 2021. V. 125. No. 33. P. 18444.

2. Yashenkin A.G., Utesov O.I., Koniakhin S.V. // J. Raman Spectrosc. 2021. V. 52. Iss. 11. P. 1847.

Mean-field approach for skyrmion lattices description in centrosymmetric frustrated antiferromagnets

O.I. Utesov

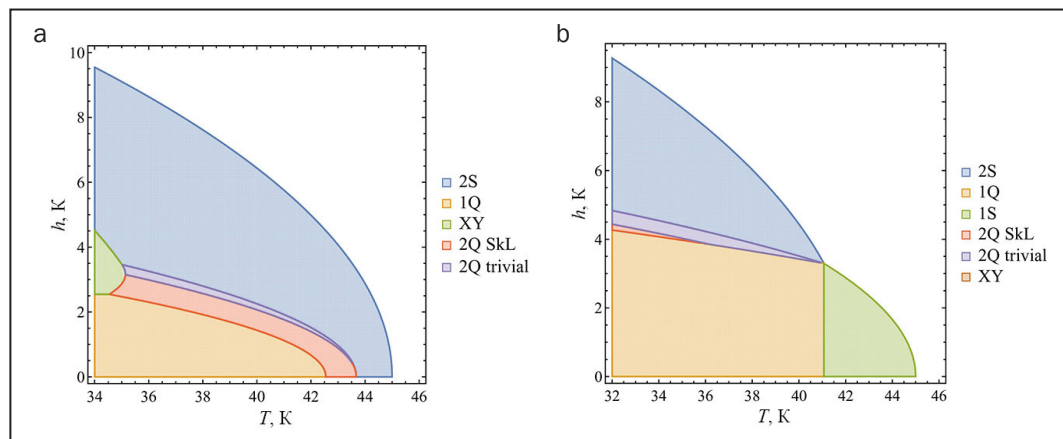
Theoretical Physics Division of NRC “Kurchatov Institute” – PNPI

Skyrmions and their ordered arrays – skyrmion lattices – are among the most extensively studied objects in condensed matter physics. Importantly, this interest is not only caused by a diversity of related physical phenomena, but also by the possibility of practical utilization of these structures. The latter relies on non-trivial topological properties of skyrmions.

It is well-known that topologically non-trivial spin structures can be stabilized in non-centrosymmetric helimagnets with Dzyaloshinskii–Moriya interaction, e. g., MnSi. However, skyrmion lattices can also be stable in centrosymmetric frustrated antiferromagnets of high symmetry. In the case of tetragonal symmetry, besides simple phases modulated in one direction, phases with two modulation vectors are also possible, which was indeed observed experimentally in GdRu_2Si_2 .

In the present research, the mean-field approach for the high-temperature part of the phase diagram of a tetragonal frustrated magnet with dipolar forces was developed. It was shown that in

a model, which takes into account only exchange and magnetodipolar interactions, under temperature lowering a phase with two modulation vectors (superposition of two screw spirals) appears as an intermediate one (the model parameters were estimated for the GdRu_2Si_2 compound). Moreover, from the topological properties point of view, it represents a meron-antimeron lattice with the average topological charge equal to zero. In the external magnetic field, this phase becomes a topologically-nontrivial square skyrmion lattice, which, as shown in the study, is thermodynamically stable in a particular domain of the phase diagram (Fig. a). In the case of additional easy-axis anisotropy of sufficient strength, the phase diagram shown in Figure b was obtained. It has a good correspondence with the experimental findings in GdRu_2Si_2 . It is noteworthy that the developed approach is formulated in a simple analytical form and can be easily applied for a description of other compounds phase diagrams.



Generalized relativistic pseudopotentials for light elements

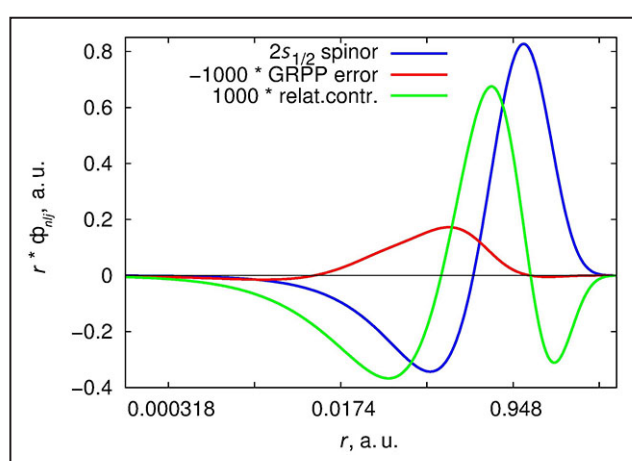
N.S. Mosyagin, A.V. Oleynichenko, A.V. Zaitsevskii, A.V. Titov
 Advanced Development Division of NRC “Kurchatov Institute” – PNPI

The construction of a new generation of generalized relativistic pseudopotentials (GRPP) with “empty atomic cores” for the elements of the first two periods of the periodic table, designed for accurate relativistic simulation of electronic structure and physical-chemical properties of their compounds has been completed in 2021. As in the case of standard (nonrelativistic) all-electron calculations, these GRPP imply an explicit description of all electrons of the atom, and their role is brought exclusively to the emulation of both one-electron and two-electron (Breit), both scalar and spin-dependent relativistic effects.

The new approach differs from the standard methods for description of such effects by the possibility of use in combination with the GRPP model for heavy atoms and by significantly higher efficiency. As shown in the Figure, the GRPP method allows one to reproduce the well-known relativistic contraction for the s-orbital with good accuracy. The GRPP error (*the red line*) is negligible even in

comparison with a quite small relativistic contraction (*the green line*) in the valence region (the region of the last maximum of the $2s_{1/2}$ spinor, shown by *the blue line*), which is most important for chemical bonding and the “valence” types of properties (for example, the dipole moment).

The constructed GRPPs have already been successfully applied at NRC “Kurchatov Institute” – PNPI and Lomonosov Moscow State University in calculation of the energetic and radiative properties for excited electronic states of the CO molecule. The carbon monoxide (CO) is the second most abundant diatomic molecule (after H₂) in the Universe. The comprehensive data on its spectral properties are needed for accurate modeling and monitoring of astrophysical, environmental and atmospheric phenomena. Information on the (singlet-triplet) CO electronic transitions forbidden in the nonrelativistic approximation is of critical importance for many applications.



Normalized radial part of the large component of the $2s_{1/2}$ spinor (the logarithmic scale is used upon the abscissa axis). The multiplied by 1 000 relativistic contraction for this orbital (obtained as the difference between relativistic and nonrelativistic calculations). The multiplied by -1 000 error of its reproducing in the calculation with the help of the generalized relativistic pseudopotentials (obtained as the difference between the calculations with Dirac–Coulomb–Breit Hamiltonian and with the generalized relativistic pseudopotentials)

1. Mosyagin N.S., Oleynichenko A.V., Zaitsevskii A.V. et al. // J. Quant. Spectrosc. Radiat. Transf. 2021. V. 263. P. 107532.
2. Mosyagin N.S., ..., Titov A.V., Zaitsevskii A.V. // Sb. tezisov XXXIII Simpoziuma “Sovremennaya khimicheskaya fizika”. M.: Doblest, 2021. P. 120.

Critical non-Abelian flux tube and holography for little string theory

E.A. levlev, A.V. Yung

Theoretical Physics Division of NRC “Kurchatov Institute” – PNPI

Non-Abelian flux tubes (vortices) were discovered in the $N = 2$ supersymmetric quantum chromodynamics (QCD) in 2003 in a joint work of A. Yung and K. Konishi with his group, and also independently by A. Hanany and D. Tong. A distinct feature of these non-Abelian strings is that they possess orientational zero modes rotating the string flux inside the $SU(N)$ group. The theory of the non-Abelian strings has been developed in the course of several years in the papers by A. Yung, M. Shifman and others. The non-Abelian string turned out to be an alternative to the Abelian Abrikosov string and allowed for a description of a non-Abelian confinement of monopoles.

Later it was shown that the non-Abelian vortex string in the four-dimensional $N = 2$ supersymmetric QCD with the gauge group $U(2)$ and $N_f = 4$ quark flavors behaves as a critical superstring. This happens because the six orientational and size moduli combine with the four translational moduli and form the ten-dimensional space necessary for the string to be critical. The string state spectrum is interpreted as the hadron spectrum of the four-dimensional $N = 2$ supersymmetric QCD.

These states were discovered with the help of the equivalence between the critical string on the conifold and the non-critical string on a half-infinite cigar described by a Wess–Zumino–Novikov–Witten model with the group $SL(2, \mathbb{R})/U(1)$. Earlier a massless hypermultiplet and lowest massive states up to spin 2 were found. The massless hypermultiplet

corresponds to the conifold complex structure modulus. All found states turned out to be baryons.

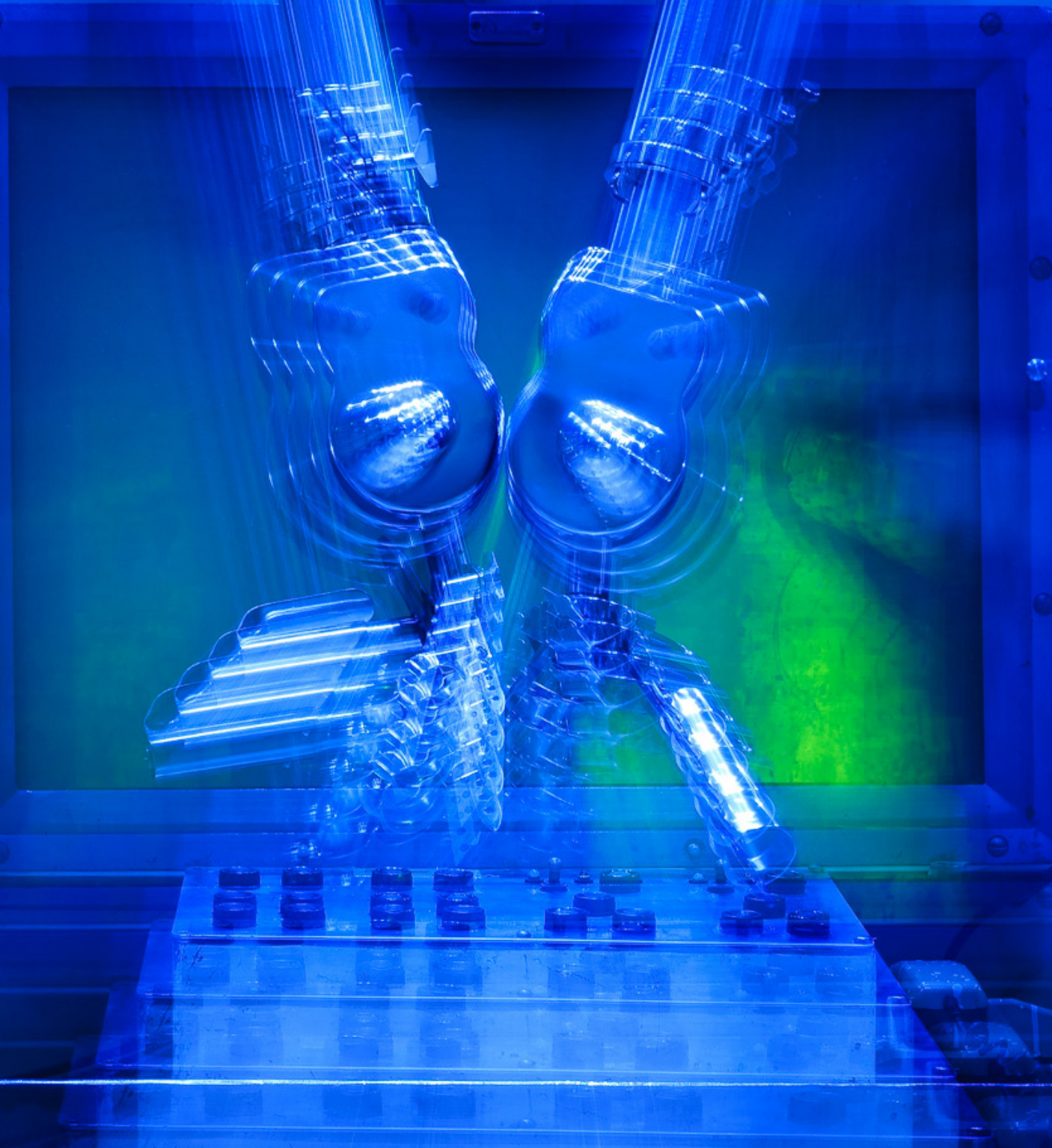
The goal of the present work is to investigate effective interactions of the hadron states. To this end we consider correlation functions of normalizable vertex operators on the $SL(2, \mathbb{R})/U(1)$ cigar. The cigar represents the extra dimensions (complementary to the “usual” four dimensions). The fact that the operators are normalizable means that the corresponding wave functions fall off along the cigar. Therefore, these states are localized in the vicinity of the tip of the cigar and do represent physical states (hadrons) living in the four dimensions.

While studying the correlation functions we determined, among other things, the decay channels of the hadron states as determined by their quantum numbers.

In this work we also compare the gauge-string duality approach based on the solitonic string with the holographic AdS/CFT-type duality for little string theories. The latter relates the off-shell field theory correlation functions to the non-normalizable cigar vertex operator correlation functions.

It was shown in this work that in most channels the holographic approach does work because the normalizable and non-normalizable vertex operators with the same conformal dimensions are related to each other by reflection from the tip of the cigar. However, it turns out that the holography does not work for the lightest hadrons with a given baryon charge.

36V



Research Based on the Use of Neutrons, Photons and Muons

- 44 Search for the new internucleon interactions in the neutron-nucleus scattering
- 45 Fission cross section of ^{236}U by neutrons with energy of 1–200 MeV and angular distributions of fission fragments
- 46 Long-range magnetic ordering in $\text{Li}_2\text{MnGeO}_4$ driven by short-range spin correlations
- 48 Studies of spin-wave dynamics and magnetic structures in multiferroics-ferroborates using neutron scattering
- 50 Magnetic structure of $\text{Mn}_{0.9}\text{Fe}_{0.1}\text{Ge}$ compound under quasihydrostatic pressure
- 51 Study of a ferrofluid with the 3% concentration of CoFe_2O_4 nanoparticles by means of polarized muons

Search for the new internucleon interactions in the neutron-nucleus scattering

V.V. Voronin, V.V. Fedorov, D.D. Shapiro
Neutron Research Division of NRC "Kurchatov Institute" – PNPI

Nowadays four fundamental interactions are known and sufficiently well studied, but the possible existence and active search for new forces, which can help to solve a number of open problems, is discussed within the extension of the Standard Model. These forces can be both spin-dependent and spin-independent.

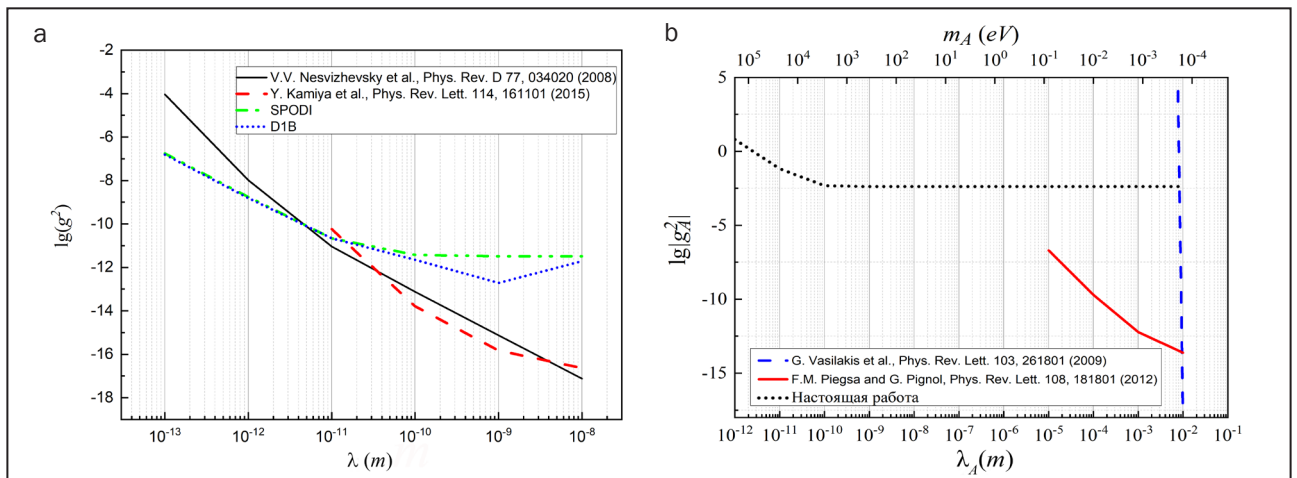
We proposed to use powder diffraction of neutrons on silicon to set constraints on the coupling constant g of the spin-independent interaction. The essence of the method is to study the dependence of the silicon scattering amplitude dependence on the momentum transfer.

In this work the calculations showing the method validity were made. The constraints of g depending on the interaction radius λ were obtained from the calibration data of the diffractometers SPODI (FRM II, Munich, Germany) and D1B (ILL, Grenoble, France). They were shown to be at the level of the best current limits (Fig. a).

To improve the constraints, we performed an experiment at the diffractometer D20 (ILL, Grenoble, France) with the silicon calibration standard NIST 640f with a mass of 1.27 g as a sample. The measurements were made with two wavelengths of 1.3 and 2.41 Å at four temperatures each (4, 6, 77, 300 K). The data obtained are currently being processed.

To set constraints on the coupling constant g_A of the spin-dependent interaction, it was proposed to use the results of the experiment of the neutron transition through the non-centrosymmetric perfect crystal in the vicinity of a Bragg reflection.

The existence of such interaction should result in the neutron spin rotation by an angle which was measured at the experiment. The constraints obtained are the most stringent at the interaction radius range of $\lambda_A = 10^{-12} - 10^{-5}$ m (Fig. b).



The constraints of g against λ (a) and of g_A against λ_A (b). The permitted area is above the lines

Fission cross section of ^{236}U by neutrons with energy of 1–200 MeV and angular distributions of fission fragments

A.S. Vorobyev¹, A.M. Gagarski², O.A. Shcherbakov¹, L.A. Vaishnene³, A.L. Barabanov⁴

¹Advanced Development Division of NRC “Kurchatov Institute” – PNPI

²Neutron Research Division of NRC “Kurchatov Institute” – PNPI

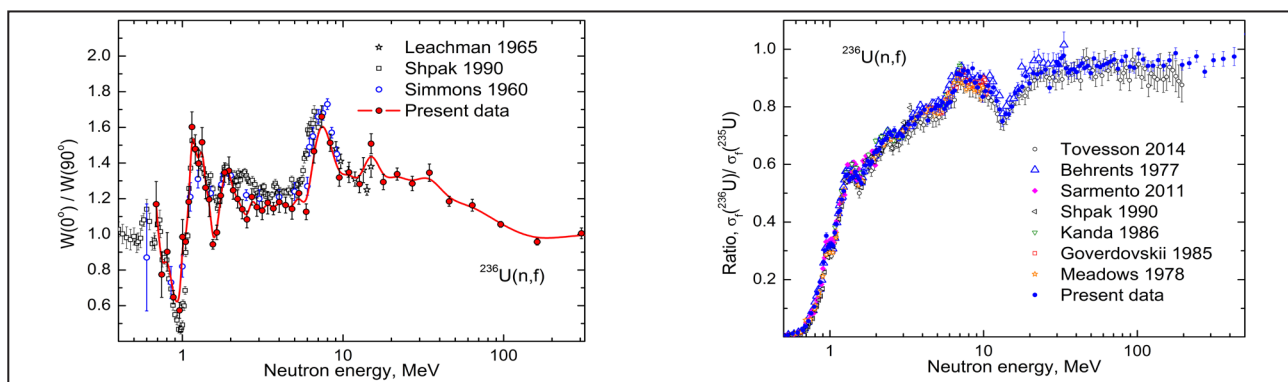
³High Energy Physics Division of NRC “Kurchatov Institute” – PNPI

⁴NRC “Kurchatov Institute”

Future plans for the development of nuclear energy are related to the implementation of a closed fuel cycle and its systems such as 4th generation nuclear power plants and accelerated driven system (ADS-systems), *i. e.* nuclear reactors driven by high-current proton accelerators with energies of about 1 GeV. The creation of such systems is designed to ensure the safety and reliability of nuclear power plants, their economic competitiveness due to lower life cycle costs compared to other energy sources, as well as more efficient use of nuclear fuel while reducing the amount of nuclear waste. However, the technical implementation of such plans is a complex and expensive task, which requires reliable and accurate nuclear data. It is important to note that obtaining new nuclear data not only makes it possible to fill in the existing gaps in the experimental database, but also to perform an assessment, and also stimulates the creation of theoretical models, as a result of which calculation codes are created, used

both for the analysis of experimental results and for engineering calculations of nuclear power plants.

Measurements of the fission cross section and angular distributions of fission fragments of the ^{236}U nucleus during interaction with neutrons with energy from 1 to 200 MeV were carried out on the GNEIS spectrometer created on the basis of the SC-1000 at the NRC “Kurchatov Institute” – PNPI. The results are shown in the Figure. Note that the angular distributions of ^{236}U fission fragments in the region of neutron energies above 15 MeV were obtained for the first time. A theoretical analysis of the data obtained is currently underway. The measurements performed completely cover both the range of 1–20 MeV (reactor spectrum), which is in demand in today's nuclear technologies and technologies of the near future, and the most difficult from an experimental point of view area of 20–200 MeV, which is critically important for the development of promising ADS technologies.



Anisotropy of angular distributions of fragments (left) and ^{236}U fission cross-section (right) in comparison with the results of other studies

1. Barabanov A.L., Vorobyev A.S., Gagarski A.M., Shcherbakov O.A., Vaishnene L.A. // Collect. Abstr. XXVIII Int. Seminar on Interaction of Neutrons with Nuclei. 2021. P. 104.
2. Barabanov A., Vorobyev A., Gagarski A., Shcherbakov O., Vaishnene L. // EPJ Web Conf. 2021. V. 256. P. 00003.

Long-range magnetic ordering in $\text{Li}_2\text{MnGeO}_4$ driven by short-range spin correlations

A.N. Korshunov, A.I. Kurbakov, A.E. Susloparova
Neutron Research Division of NRC "Kurchatov Institute" – PNPI

This work is devoted to one of the most relevant areas in modern condensed matter physics: the study of the magnetism of frustrated quasi-two-dimensional oxides with a trigonal superstructure of magnetic ions. Long-range magnetic ordering and short-range spin correlations in layered noncentrosymmetric orthogermanate $\text{Li}_2\text{MnGeO}_4$ were researched by means of polarized and unpolarized neutron scattering.

The $\text{Li}_2\text{MnGeO}_4$ compound studied in this work belongs to the A_2MXO_4 family ($\text{A} = \text{Li}, \text{Na}, \text{Ag}$; $\text{M} = \text{Be}, \text{Mg}, \text{Mn}, \text{Fe}, \text{Co}, \text{Zn}, \text{Cd}$; $\text{X} = \text{Si}, \text{Ge}$), which is quite diverse in the types of crystal structures and, most importantly, in the demonstrated properties. A composition in which the ratio $\text{A} : \text{M}^{+2}$ (M , in this

case, is a transition metal, TM) is $2 : 1$, *i.e.* ideally, two electrons per TM, is considered very promising for use in electrochemistry.

The combined Rietveld refinement of synchrotron (SpLine BM25, ESRF, France) and neutron powder diffraction data (HRPT and DMC diffractometers, PSI, Switzerland) at room temperature within the $Pmn2_1$ space group allowed for specifying the details of the crystal structure (Fig. 1). In $\text{Li}_2\text{MnGeO}_4$, all cation tetrahedra are lined up in the same direction perpendicular to the oxygen close-packed layers, and the structure is noncentrosymmetric, *i.e.* suggests the existence of interesting nonlinear physical properties. While for many related compositions, for example, $\text{Li}_2\text{MnSiO}_4$, half of the

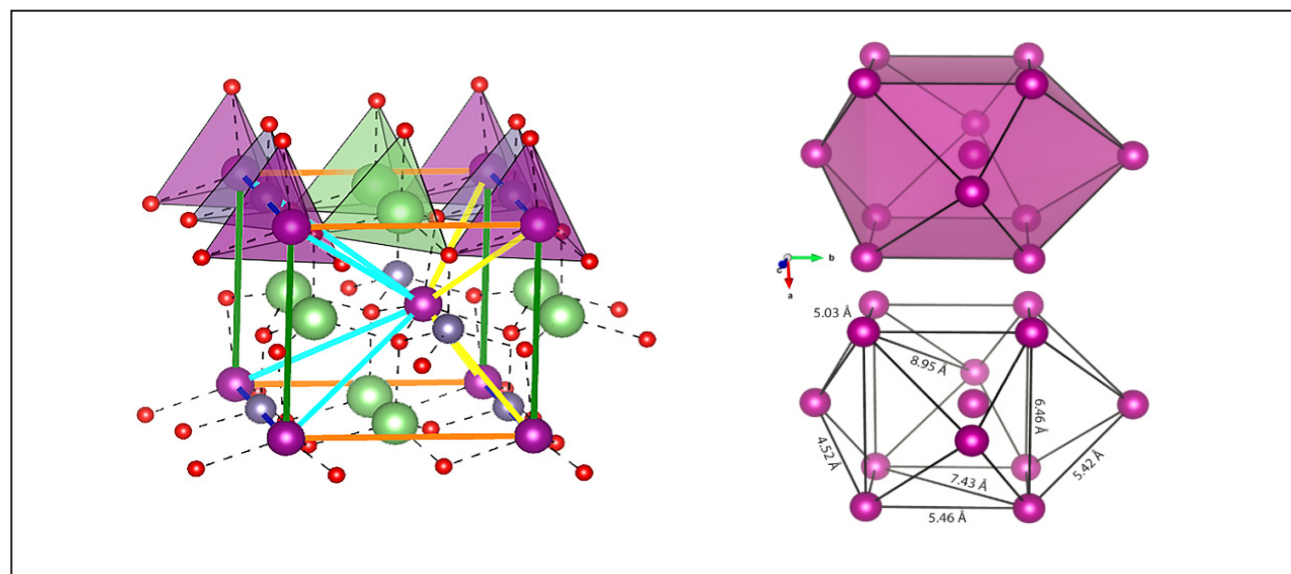


Fig. 1. Couplings between magnetic Mn^{2+} ions indicate the main spin exchange paths (on the left). Refined crystal structure of $\text{Li}_2\text{MnGeO}_4$ with the tetrahedral environment of oxygens (red balls). Magenta, green and grey balls show the Mn, Li and Ge sites respectively in the $Pmn2_1$ space group. All tetrahedra border each other only through the vertices. General view of the distorted cuboctahedron formed by 12 nearest Mn neighbors (on the right). The main distances between magnetic atoms at $T = 1.7$ K are indicated in the bottom image

tetrahedra have the opposite orientation; as a result, the parameter b doubles, which leads the system to be centrosymmetric.

According to the additional Bragg peaks in low-temperature neutron diffraction patterns a long-range antiferromagnetic (AFM) ordering with the propagation vector $\mathbf{k} = (1/2 \ 1/2 \ 1/2)$ has been found below $T_N \approx 8$ K. Symmetry analysis and subsequent full-profile refinement of neutron experimental data revealed a model of the ground state spin structure within the Cac (no. 9.41) magnetic space group (Fig. 2). It represents a noncollinear ordering of Mn atoms with a refined magnetic moment of $4.9 \ \mu_B / \text{Mn}^{2+}$ at $T = 1.7$ K, which corresponds to the saturated value for the high-spin configuration $S = 5/2$.

Diffuse magnetic scattering was detected in the neutron diffraction patterns at temperatures just

above T_N . Its temperature evolution was investigated in detail by polarized neutron scattering with the following XYZ-polarization analysis on the neutron time-of-flight spectrometer DNS (MLZ, Germany). Reverse Monte Carlo simulation of diffuse scattering data showed the development of short-range ordering in $\text{Li}_2\text{MnGeO}_4$, which is symmetry consistent with the long-range magnetic state below T_N . The reconstructed radial spin-pair correlation function $S(0) \cdot S(r)$ displayed the predominant role of AFM correlations. It was found that spin correlations are significant only for the nearest magnetic neighbors and almost disappear at $r \approx 12 \text{ \AA}$ at $T = 10$ K. Temperature dependence of the diffuse scattering implies short-range ordering long before the magnetic phase transition. As a result, an exhaustive picture of the gradual formation of magnetic ordering in $\text{Li}_2\text{MnGeO}_4$ is presented.

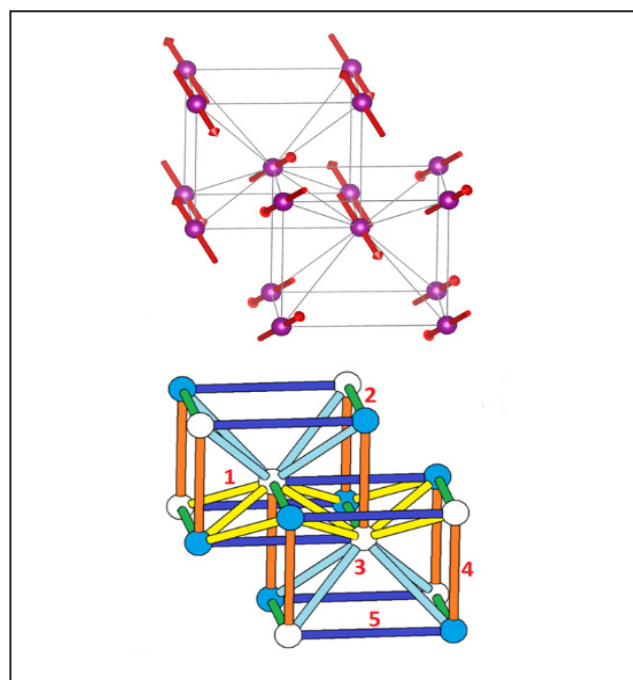


Fig. 2. Spin structure models of $\text{Li}_2\text{MnGeO}_4$ at $T = 1.7$ K. Noncollinear ordering using the Cac magnetic space group (top). Spin exchange paths of the collinear spin arrangement expected from DFT calculations; shaded and unshaded spheres represent spin-up and spin-down Mn^{2+} sites, respectively (bottom)

1. Korshunov A.N., Kurbakov A.I., ..., Susloparova A.E. et al. // Phys. Rev. B. 2020. V. 102. P. 214420.

2. Susloparova A.E., Kurbakov A.I., Pomjakushin V.Yu. // Sb. tezisov dokladov "RNIKS-2021". 2021. P. 73.

Studies of spin-wave dynamics and magnetic structures in multiferroics-ferroborates using neutron scattering

I.V. Golosovsky¹, B.Z. Malkin², A.A. Mukhin³, M.N. Popova⁴, M. Boehm⁵, A. Gukasov⁶

¹ Neutron Research Division of NRC “Kurchatov Institute” – PNPI

² Kazan (Volga region) Federal University

³ A.M. Prokhorov General Physics Institute of RAS

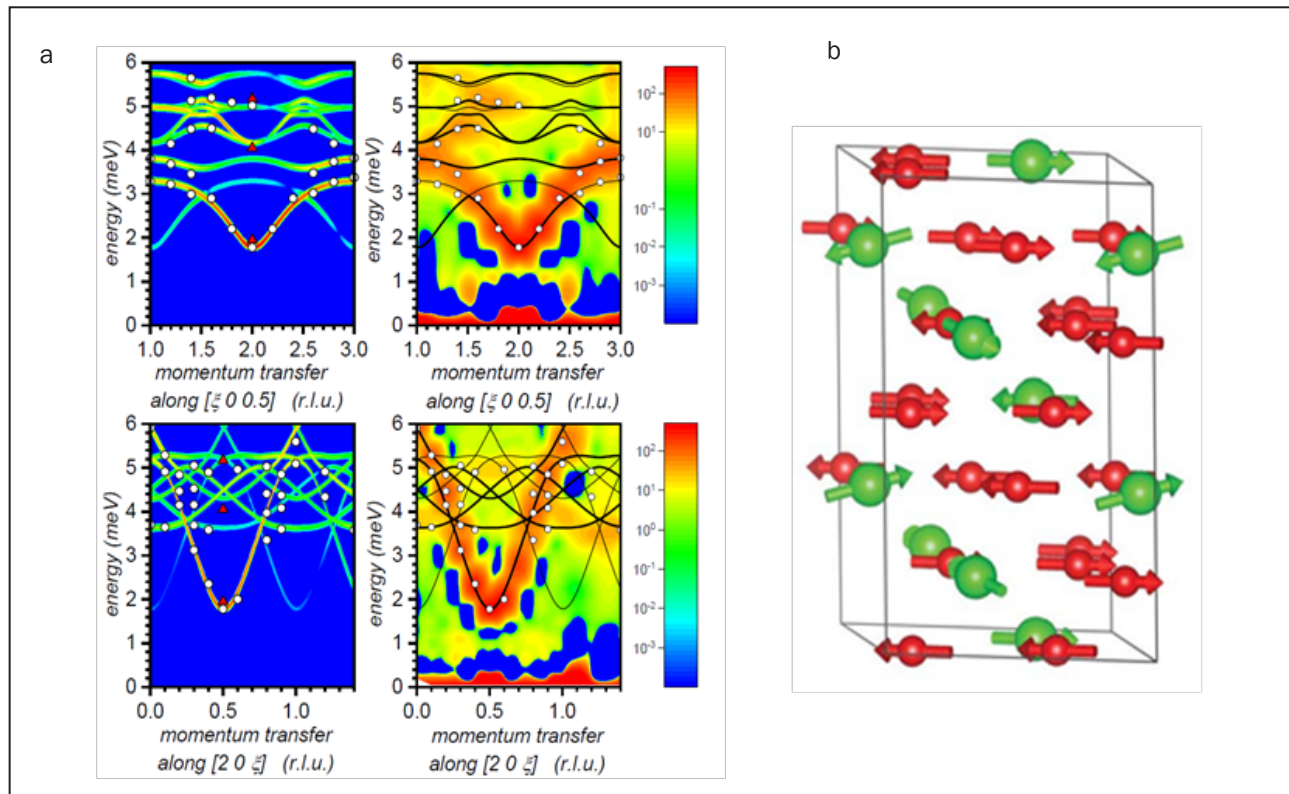
⁴ Institute of Spectroscopy of RAS

⁵ Institut Laue–Langevin, France

⁶ Laboratoire Léon Brillouin, France

The research of multiferroics – the materials in which magnetic order can be controlled by the application of an electric field and vice versa – the electric polarization can be controlled by a magnetic field, which opens up the possibility of practical application, continues in the NRC “Kurchatov Institute” – PNPI. The object of research is multiferroics-ferroborates. The interest in these materials results from the strong dependence of the

electric polarization on the applied magnetic field, which is important for the practical application. In these compounds, an “easy-plane” magnetic structure with in-plane moments, as in $\text{NdFe}_3(\text{BO}_3)_4$, or an “easy-axis” structure, with moments along the axis, as in $\text{TbFe}_3(\text{BO}_3)_4$, is realized. As a result, complex noncollinear magnetic structures in the mixed $\text{Nd}(\text{Tb})\text{Fe}_3(\text{BO}_3)_4$ system are to be expected. Indeed, using elastic scattering on single crystals, a weak



An example of spin-wave spectra in $\text{TbFe}_3(\text{BO}_3)_4$ for two different directions (a): left panel – calculation, right panel – experiment. “Easy-plane” magnetic structure in $\text{HoFe}_3(\text{BO}_3)_4$ (b)

noncollinearity of the magnetic structure was detected, which is due to the Dzyaloshinskii–Moriya interaction. This phenomenon can be called “weak antiferromagnetism” by analogy with the well-known “weak ferromagnetism”.

The experiments with inelastic neutron scattering reveal a complex dynamic of magnetic excitations. An adequate description of spin-wave spectra (Fig.) turned out to be possible only when taking into account a large number of exchange interactions, up to 12 coordination spheres. The exchange interactions and anisotropy parameters were defined from the magnon spectra. It was discovered that the

exchange interaction is highly visible even at very long distances, up to 7 Å.

In contrast to the substituted system Nd(Tb)Fe₃(BO₃)₄, in the ferroborate HoFe₃(BO₃)₄ it is impossible to determine unambiguously the direction of magnetic moments with a small number of diffraction reflections from neutron diffraction. The problem was solved by using high resolution optical spectroscopy. The proposed model (see Fig.) was confirmed by measurements on polarized neutrons (flipping ratio) and is consistent with the measured temperature dependences of the intensities of characteristic reflections.

1. Golosovsky I.V., Mukhin A.A. et al. // PRB. 2021. V. 103. P. 214412.

2. Popova M.N., Golosovsky I.V., Gukasov A., Mukhin A.A., Malkin B.Z. et al. // PRB. 2021. V. 103. P. 094411.

Magnetic structure of $\text{Mn}_{0.9}\text{Fe}_{0.1}\text{Ge}$ compound under quasihydrostatic pressure

E.V. Altynbaev, S.V. Grigoriev, D.O. Skanchenko

Neutron Research Division of NRC "Kurchatov Institute" – PNPI

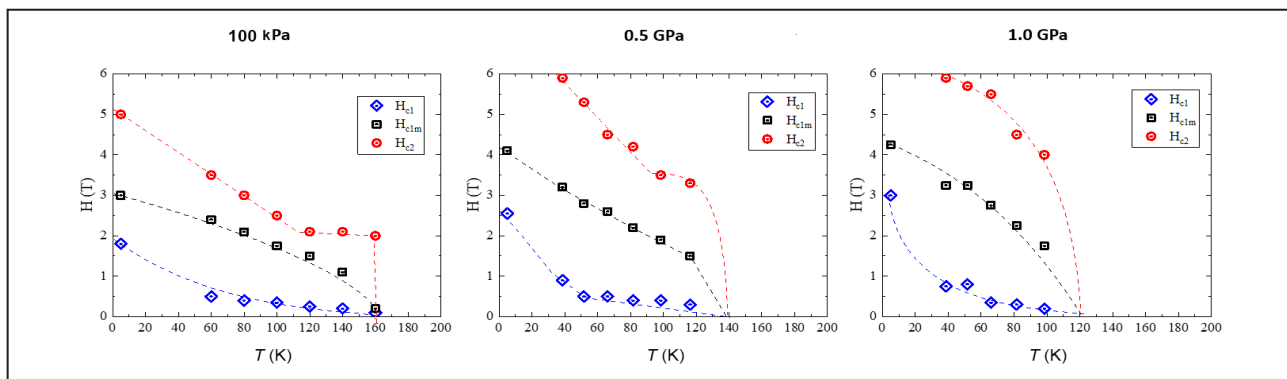
The helical magnetic structure of the $\text{Mn}_{0.9}\text{Fe}_{0.1}\text{Ge}$ compound under a quasihydrostatic pressure of up to 1 GPa was investigated by small-angle neutron scattering in a wide range of temperatures (5–300 K) and magnetic fields (0–5 T).

SANS experiments were carried out at the PA20 instrument at Laboratoire Leon Brillouin (nuclear research reactor Orphée) in Saclay, France. In order to carry out the investigation, we have developed a non-magnetic high-pressure cell that fits the standard position of the sample and allows applying the pressure up to 1.2 GPa. A slight modification of the cell opens the possibility of further pressure increase up to 2.5 GPa.

As a result of our studies, a field-temperature ($H-T$) phase diagram was constructed for the first time for the $\text{Mn}_{0.9}\text{Fe}_{0.1}\text{Ge}$ compound at various pressures up to $P = 1$ GPa. It is shown that the application of pressure at low temperatures leads to a process inverse to the process of substitution of Mn atoms by Fe atoms in the MnGe compound, namely, to an increase in the values of all critical

magnetic fields H_{c1} , H_{c1m} and H_{c2} (Fig.), which may indicate the stabilization of the magnetic system under the influence of external pressure, caused by the desire of the magnetic system to build a commensurate crystalline magnetic structure. It is shown that the wave vector of the magnetic spiral increases with increasing pressure simultaneously with a decrease in the magnetic ordering temperature, T_c , at a rate of about 40 K/GPa. This may indicate that the magnetic system is approaching a quantum phase transition to a disordered state with an increase in external pressure, which should be expected when pressure $P = 4$ GPa is applied.

Since the replacement of Mn by Fe atoms in the $\text{Mn}_{1-x}\text{Fe}_x\text{Ge}$ compound changes at least two parameters important for the stabilization of the magnetic structure, namely, the electron concentration and the cell constant, the use of high pressure allows one to separate these two components. Thus, it is possible to estimate the influence of each process on the evolution of the field-temperature phase diagram.



Temperature dependence of the critical fields corresponding to the beginning of the process of transition of a polycrystalline sample to the conical phase, H_{c1} (a), the end of the process of transition to the conical phase, H_{c1m} (b), and the transition to the ferromagnetic phase, H_{c2} (c) for the $\text{Mn}_{0.9}\text{Fe}_{0.1}\text{Ge}$ compound at $P = 100$ kPa (a), 0.5 GPa (b), 1 GPa (c)

Study of a ferrofluid with the 3% concentration of CoFe_2O_4 nanoparticles by means of polarized muons

S.I. Vorobyev, A.L. Getalov, E.N. Komarov, S.A. Kotov, G.V. Shcherbakov
High Energy Physics Division of NRC "Kurchatov Institute" – PNPI

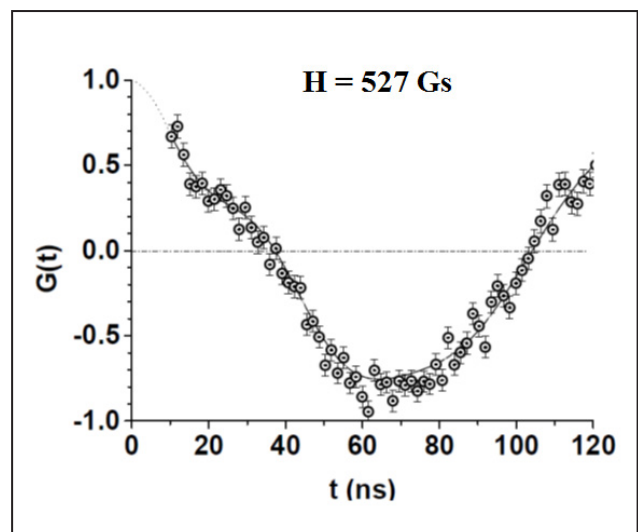
Magnetic fluids based on single-domain magnetic spinel ferrite nanoparticles dispersed in various liquid media are of particular practical and scientific interest due to their special properties, which are caused by nanoscale effects. Currently, liquids based on single-domain magnetic nanoparticles of spinel ferrites, MeFe_2O_4 (where Me are Cr, Mg, Fe, Co and Zn), dispersed in various liquid media are widely studied.

A ferrofluid sample was studied using the μ SR-setup installed at the output of the muon channel of the SC-1000 synchrocyclotron of NRC "Kurchatov Institute" – PNPI. The beam of positively charged muons with an average momentum $p_\mu = 90 \text{ MeV}/c$ and a momentum dispersion $\Delta p_\mu/p_\mu = 0.02$ (FWHM) had a longitudinal polarization $P_\mu = 0.90–0.95$.

An experimental study of a ferrofluid based on magnetic nanoparticles of CoFe_2O_4 molecules dispersed in H_2O with the nanoparticle concentration of 3% has been reported. In the study it was determined that the structure and value of magnetization of the ferrofluid depend on its viscosity. It was shown that at room temperature (290 K) and the external magnetic field of 527 Gs the observed additional magnetization is $\sim 20 \text{ Gs}$ (Fig.). A small fraction of the sample ($\sim 20\%$) shows negative

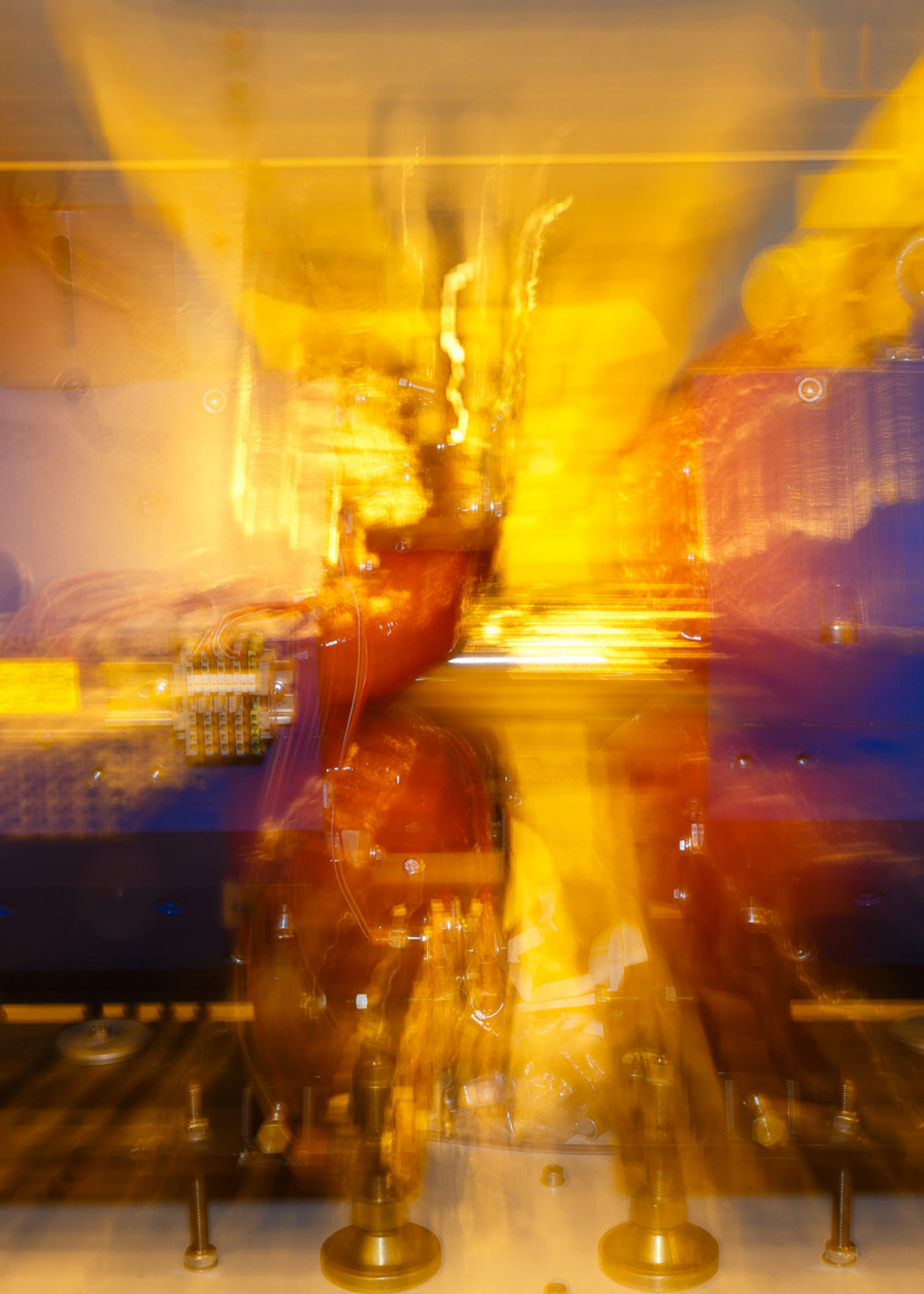
magnetization (diamagnetism). At a low temperature ($\sim 30 \text{ K}$) the sample in the magnetic field behaves like a paramagnet.

For the first time the magnetic field inside and in the near vicinity of the CoFe_2O_4 nanoparticle was measured experimentally using the μ SR method and its value was found to be $1.96 \pm 0.44 \text{ kGs}$. Thus, a direct measurement of the magnetization of a nanoscale object was made.



Function $G(t)$ in the ZFC mode in the external magnetic field $H = 527 \text{ Gs}$; the spectra are added at temperatures from 26 to 100 K

1. Vorob'ev S.I., ..., Getalov A.L., ..., Komarov E.N., Kotov S.A., ..., Scherbakov G.V. // Magnetochemistry. 2021. V. 7. P. 104.
 2. Vorobyev S.I., ..., Getalov A.L., ..., Komarov E.N., Kotov S.A., ..., Shcherbakov G.V. Preprint NRC "Kurchatov Institute" – PNPI 3049. Gatchina, 2021. 14 p.



Research Based on the Use of Protons and Ions. Neutrino Physics

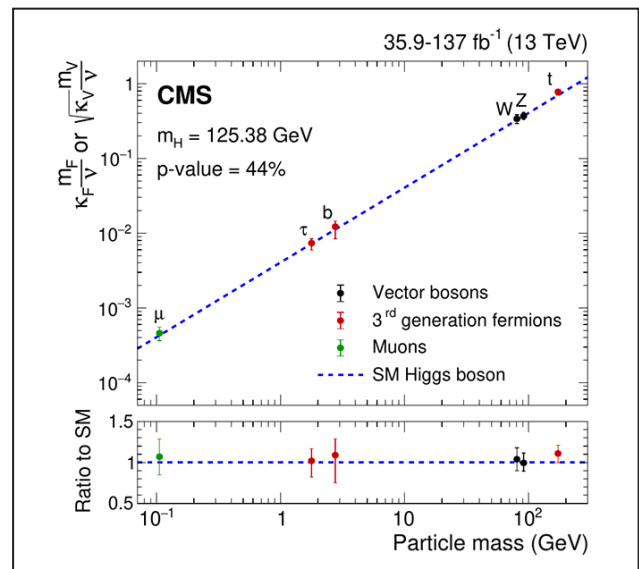
- 54 First evidence for Higgs boson decay into muons obtained by CMS experiment
- 55 First direct observation of the “dead cone” effect in quantum chromodynamics in hard proton-proton interactions at the Large Hadron Collider
- 57 Search for associated production of a Z-boson with dark matter candidates in the ATLAS experiment
- 58 Measurement of the polarisation of single top quarks and antiquarks in the ATLAS experiment
- 59 Study of rare decays of beauty hadrons
- 60 First measurement of momentum transfer dependence of coherent J/ ψ photoproduction in Pb–Pb ultraperipheral collisions at the Large Hadron Collider and 3D imaging of nuclear gluons
- 62 Observation of odderon exchange from proton-proton and proton-antiproton elastic scattering data in the D0 and TOTEM experiments
- 63 Shell effect in the charge radii of the neutron-rich mercury isotopes
- 65 Shape staggering in neutron-deficient bismuth isotopes
- 66 Results of the Neutrino-4 experiment on the search for sterile neutrino
- 67 Direct ultraprecision measurement of the $^{187}\text{Re} - {}^{187}\text{Os}$ mass difference as a prologue for determining the effective mass of the antineutrino
- 68 Precision measurements of the ${}^{210}\text{Bi}$ β -spectrum for neutrino physics tasks
- 69 Spectrum of protons in collisions of heavy ions ${}^{12}\text{C} + {}^9\text{Be}$ at energies of 0.3–2.0 GeV/nucleon in terms of the hydrodynamic approach

First evidence for Higgs boson decay into muons obtained by CMS experiment

A.A. Vorobyev, V.T. Kim, Yu.M. Ivanov, S.S. Volkov, G.E. Gavrilov, V.L. Golovtsov, E.V. Kuznetsova, P.M. Levchenko, V.A. Murzin, V.A. Oreshkin, I.B. Smirnov, D.E. Sosnov, V.V. Sulimov, L.N. Uvarov
*High Energy Physics Division of NRC "Kurchatov Institute" – PNPI,
CMS Collaboration*

The main goals of modern high energy physics are the search for the effects of new physics and precision tests of the Standard Model (SM). Particularly relevant in this regard is the study of the properties of the SM Higgs boson, discovered by the ATLAS and CMS experiments in 2012. One of the key directions of such research is the study of the symmetry of fermion generations, *i.e.*, quarks and leptons. At present the decays of the Higgs boson into all three generations of quarks are well studied. In the case of leptons, only the decay into the leptons of the third generation (heavy τ -leptons) was observed. Since the decay probability of the Higgs boson, according to the SM, is proportional to the lepton mass, the number of expected decays into second-generation leptons, muons, should be more than an order of magnitude smaller than that into heavy leptons, which makes the search for such a decay extremely difficult.

Analysis of the data from the CMS experiment collected at the second run of the Large Hadron Collider in 2015–2018 with 137 fb^{-1} at 13 TeV yields the first evidence of a direct decay of the Higgs boson into second-generation leptons $H \rightarrow \mu\mu$ at a significance level of 3.0σ . The most accurate value for the coupling constant of the Higgs boson with muons was also obtained. The signal strength was $1.19^{+0.40}_{-0.39}(\text{stat.})^{+0.15}_{-0.14}(\text{syst.})$. The obtained results are within the existing uncertainties in accordance with the expectations of the SM (Fig.).



Coupling constants for fermions (F) and bosons (V) with modification coefficients k_F and k_V and their ratios to the expected in the Standard Model as a function of particle mass

One of the most important roles in the CMS experiment study of the SM Higgs boson properties is played by the CMS EndCap muon system (EMU). NRC “Kurchatov Institute” – PNPI made a significant contribution to the EMU design, development, construction maintenance, operation and upgrade. The Institute scientists and engineers are actively involved in the maintenance and operation of the CMS muon system, as well as in the physical analysis of CMS data.

First direct observation of the “dead cone” effect in quantum chromodynamics in hard proton-proton interactions at the Large Hadron Collider

Yu.L. Dokshitzer¹, S.I. Troyan¹, V.A. Khoze¹, M.B. Zhalov², V.V. Ivanov², E.L. Kryshen², M.V. Malaev², V.N. Nikulin², A.Yu. Ryabov², V.G. Ryabov², Yu.G. Ryabov², A.V. Khanzadeev²

¹ Theoretical Physics Division of NRC “Kurchatov Institute” – PNPI

² High Energy Physics Division of NRC “Kurchatov Institute” – PNPI

One of priority fundamental problems of relativistic nuclear physics and the physics of strong interactions in general is an investigation of the new extreme state of matter of the high-temperature quark-gluon plasma (QGP), which is formed in collisions of ultrarelativistic ions at hadron and ion colliders. One of main methods of diagnostics of QGP is an analysis of energy losses of relativistic quarks, which are created in hard parton-parton interactions in the collision zone and traverse the region of the formed QGP. To estimate the magnitude of radiative energy losses and transport coefficients characterizing the viscosity of the QGP matter, it is essential to take into account the “dead cone” effect, which constitutes the suppression of gluon radiation by relativistic heavy quarks in a narrow cone around the direction of the quark motion, whose aperture depends on the ratio of the quark mass M to its energy E . While in perturbative QCD the “dead cone” effect was predicted back in 1991 (Dokshitzer Yu.L., Troyan S.I., Khoze V.A. // J. Phys. G: Nucl. Part. Phys. 1991. V. 17. P. 1602), its observation has been challenging in many experiments. Primarily, it was hindered by difficulties in reconstructing the true direction of the quark motion and the precise determination of the cone size as well as the identification and removal from the cone region the particles that are not related to gluon emission.

In the ALICE experiment and with participation of scientists of NRC “Kurchatov Institute” – PNPI, a detailed investigation of hadron multiplicity in events of proton-proton interactions with production of hadron jets initiated by massive charm quarks has been carried out. Precision particle detectors at ALICE, the development of methods of experi-

mental data analysis, and detailed modeling of proton interactions at Large Hadron Collider energies combined with the existing computer capabilities have allowed one to reconstruct the process of gluon emission by charm quarks. Figure 1 shows schematically such a reconstruction.

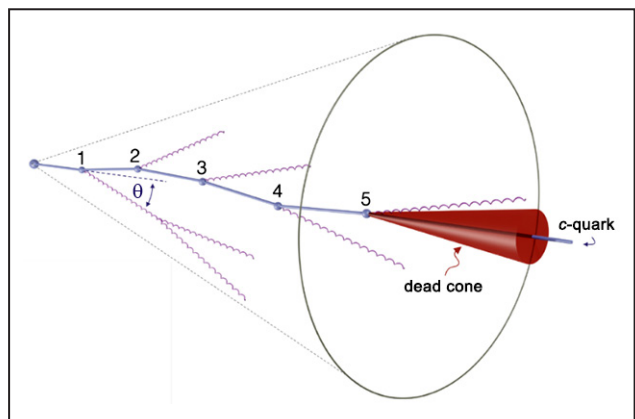


Fig. 1. Schematic reconstruction of the process of gluon emission by c-quarks: the solid line is the trajectory of the c-quark motion from the proton-proton interaction vertex; the wavy lines denote emitted gluons

Figure 2 shows the extracted from the data ratio $R(0)$ of the angular distributions of emitted gluons in jets initiated by a heavy charm quark with the energy E to that in inclusive jets. In the latter case, the “dead cone” effect is essentially absent because light quarks with $M/E \ll 1$ and massless gluons emit forward gluons with a logarithmically increasing probability.

These results convincingly demonstrate a two-fold suppression of gluon emission in the region of small angles by heavy charm quarks compared to the emission in the same region by light quarks.

Thus, for the first time, the ALICE experiment not only confirmed the theoretically predicted “dead cone” effect but also clearly demonstrated that kinematics of produced hadrons reproduces the kinematics of emitted QCD partons even in such

narrow angles, hence, justifying a hypothesis of the local parton-hadron duality (LHPD) formulated by the B.P. Konstantinov Leningrad Institute of Nuclear Physics theorists nearly 40 years ago.

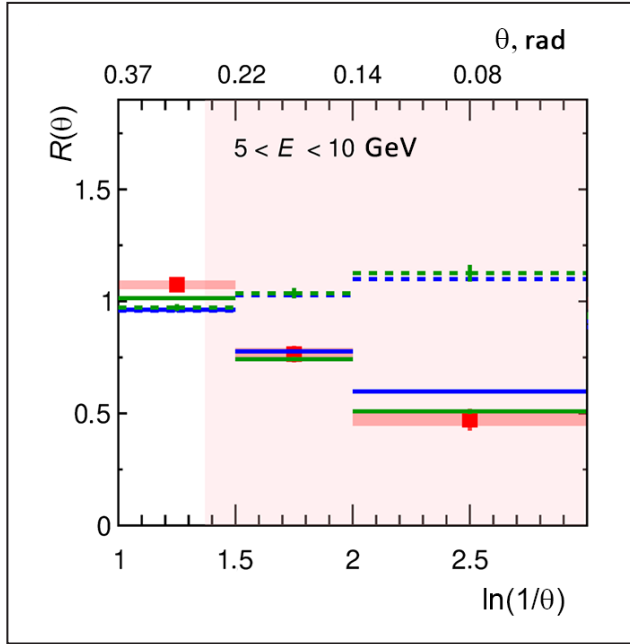


Fig. 2. Ratio $R(\theta)$ of the angular distributions of emitted gluons in jets initiated by a heavy charm quark with the energy E to that in inclusive jets. The red solid squares with pink strips show the values of $R(\theta)$ extracted from the data of the ALICE experiment; the blue and green solid curves present the results of calculations using event generators SHERPA and PYTHIA including the “dead cone” effect, while the dashed lines give the results without its account

Search for associated production of a Z-boson with dark matter candidates in the ATLAS experiment

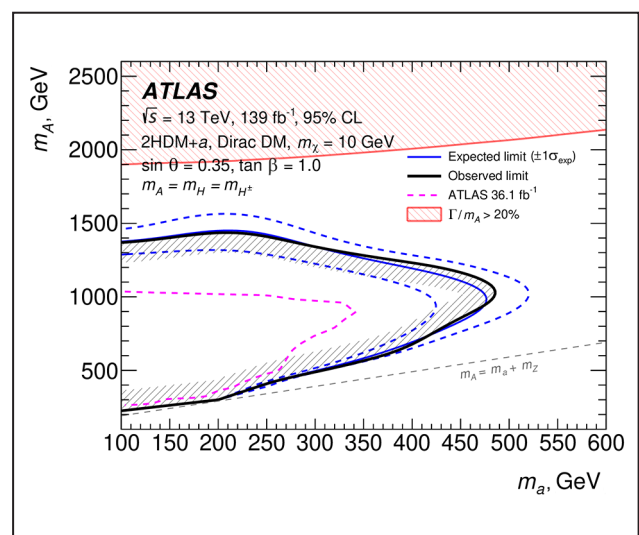
S.G. Barsov, A.E. Ezhilov, M.P. Levchenko, V.P. Maleev, Yu.G. Naryshkin,
D. Pudzha, V.M. Solovyev, O.L. Fedin, V.A. Schegelsky

High Energy Physics Division of NRC “Kurchatov Institute” – PNPI,
ATLAS Collaboration

Search for dark matter (DM) particles is one of the most important goals in particle physics today. Existence of the DM follows from the astrophysical observations. One of the most acknowledged hypotheses is that DM candidates are WIMPs – weakly interacting massive particles. At the Large Hadron Collider (LHC), searches for WIMP-like DM production rely on visible particles being produced in association with invisible DM candidates, whose experimental signature is a missing transverse momentum in the event. In the ATLAS experiment a search for DM candidates was performed in associative production with a gauge Z-boson (so-called mono-Z channel), followed by its decay to a pair of electrons or muons.

The analysis is performed using proton-proton collisions at a centre-of-mass energy of 13 TeV, delivered by the LHC, corresponding to an integrated luminosity of 139 fb^{-1} and recorded by the ATLAS experiment. All known Standard Model (SM) processes have been accounted. Transverse mass distribution is used as the discriminating observable. Obtained results are compatible with the SM predictions within statistical and systematic uncertainties. The interpretation was performed in the context of simplified DM models and the exclusion limits on the DM mass versus the mediator mass with the coupling's values of $g_\chi = 1.0$, $g_a = 0.25$ and $g_\ell = 0$, when assuming an axial-vector mediator and vector mediators have been obtained. Furthermore, there was tested a two-Higgs-doublet model (2HDM) that includes an additional pseudoscalar mediator a and called 2HDM + a . Exclusion limits within the context of 2HDM + a models with different parameter choices and in various planes have been derived.

Figure shows the obtained limits in (m_A, m_a) plane. The highest excluded m_A value is about 1.4 TeV for $m_a = 100 \text{ GeV}$, and the highest excluded m_a is about 480 GeV for $m_A = 1.05 \text{ TeV}$. Comparison of the cross section upper limits obtained in direct-detection experiments with exclusion limits obtained in the frame of simplified DM models for the spin-dependent WIMP-proton scattering cross-section or the spin-independent WIMP-nucleon scattering cross-section was performed. The upper limits, obtained in mono-Z channel at the ATLAS experiment are particularly competitive for low DM masses: $m_{\text{DM}} < 300 \text{ GeV}$, for spin-dependent and $m_{\text{DM}} < 2 \text{ GeV}$ for spin-independent cross-sections, where the experiments based on recoil measurements have limited sensitivity.



Exclusion limits within the context of 2HDM + a models for some fixed parameters in (m_A, m_a) plane, obtained in the ATLAS experiment. The solid blue line indicates the expected limit in the absence of signal, and the dashed blue area the corresponding $\pm 1\sigma$ uncertainty band

Measurement of the polarisation of single top quarks and antiquarks in the ATLAS experiment

S.G. Barsov, A.E. Ezhilov, M.P. Levchenko, V.P. Maleev, Yu.G. Naryshkin,
D. Pudzha, V.M. Solovyev, O.L. Fedin, V.A. Schegelsky

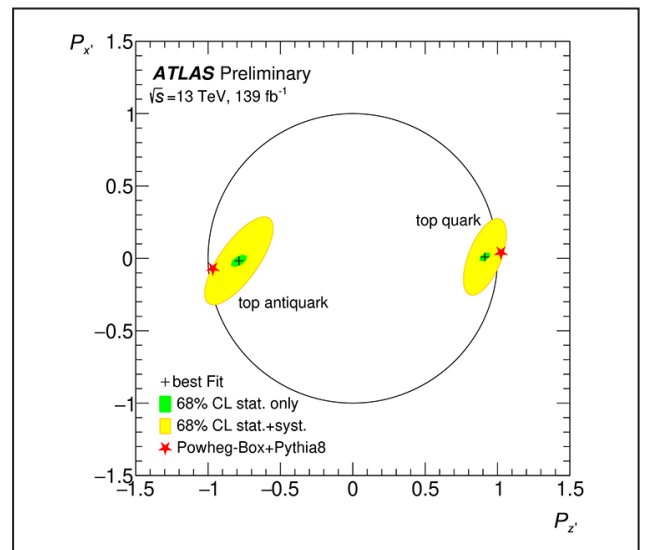
High Energy Physics Division of NRC “Kurchatov Institute” – PNPI,
ATLAS Collaboration

Single-top-quark production through the electroweak charged current at hadron colliders mostly proceeds, according to the Standard Model (SM) prediction, via three modes: the exchange of virtual W -boson in the t - or in the s -channel, and the associated production of a top quark and a W -boson. At the Large Hadron Collider (LHC), in proton-proton collision data, the t -channel is the dominant process and the subject of the measurements presented in this work. In this process, a light-flavour quark from one of the colliding protons interacts with a b -quark from another proton via a space-like virtual W -boson, producing a top quark and a recoiling light-flavour quark, called a “spectator quark”.

Single-top-quark production yields a large sample of highly polarised top quarks and top antiquarks. In the t -channel process, top quarks are expected to be mostly polarised along the direction of the spectator quark, while top antiquarks – in the opposite direction. In the SM, the expected values of the polarisations of top quarks and top antiquarks along the direction of the spectator quark are 0.90 and -0.86 respectively.

Measurement of the polarisation of single top quarks and antiquarks using an integrated luminosity of 139 fb^{-1} of proton-proton collision data at a centre-of-mass energy of 13 TeV was performed in the ATLAS experiment at the LHC. The $t \rightarrow Wb \rightarrow l^{\pm}vb$ decay mode of the top quark and charge-conjugate decay mode of the top antiquark were used in the analysis. The lepton l^{\pm} could be either an electron or a muon. The polarisation vector was defined in the orthogonal coordinate system with z -axis direction along the direction of the momentum of the spectator quark. Information on the pin of the top quark is transmitted to

the decay products, and therefore can be extracted from their angular distributions. Spin analysing power of charged leptons is close to 1, therefore this analysis was based on angular distributions of charged leptons from top quarks and antiquarks decays. The variable Q depending on the cosines of polar angles of the charged-lepton momentum in the orthogonal coordinate system was constructed. Components of the polarisation vector were defined via a fit to the Q distribution in data. Figure shows measured x - and z -components of top quarks and antiquarks polarisation vectors in the two-dimensional polarisation parameter space. Measured z -components are 0.91 ± 0.10 and -0.79 ± 0.16 for top quarks and antiquarks respectively. The extracted polarisations are consistent with the SM expectation.



Measured x - and z -components of top quarks and antiquarks polarisation vectors in the two-dimensional polarisation parameter space

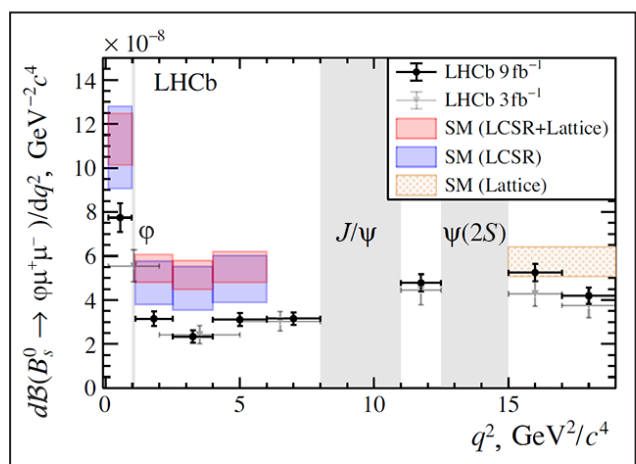
Study of rare decays of beauty hadrons

G.D. Alkhazov, A.V. Andreianov, N.F. Bondar, A.A. Vorobyev, N.I. Voropaev, A.A. Dzyuba, K.A. Ivshin, D.S. Ilin, A.G. Inglessi, S.N. Kotriakhova, P.V. Kravchenko, O.E. Maev, D.A. Maisuzenko, N.R. Sagidova, A.N. Solovev, I.N. Solovyev, A.D. Chubykin, V.V. Chulikov
*High Energy Physics Division of NRC “Kurchatov Institute” – PNPI,
LHCb Collaboration*

In the Standard Model of particle physics decays of beauty mesons with emission of $\mu^+\mu^-$ pairs in the final state are described with the loop diagrams. Such processes are very suppressed. Nevertheless, the differential characteristics of such decays can be theoretically predicted with good accuracy. The deviation of experimentally obtained values from theoretical predictions will be an evidence of the existence of new fundamental particles and interactions that go beyond the scope of modern theory. The goal of the presented analysis is to study the differential characteristics of rare decays $B_s^0 \rightarrow \varphi\mu^+\mu^-$, as well as the search for previously unobserved decays of such type.

Measurement of angular distributions and mass dependence for the decay $B_s^0 \rightarrow \varphi(\rightarrow K^+K^-)\mu^+\mu^-$ is done for the data-sample collected by LHCb experiments during the first and the second runs of the Large Hadron Collider in 2011–2018. Energies in the center-of-mass system of interacting protons are 7, 8 and 13 TeV. So-called multivariate analysis methods are used to identify $1\,530 \pm 52$ candidates for this decay. The analysis of mass and angular distributions is performed for selected events. In particular, the differential branching fraction $B_s^0 \rightarrow \varphi\mu^+\mu^-$ is obtained for $B_s^0 \rightarrow \varphi\mu^+\mu^-$ decay as a function of q^2 – squared mass of the di-muon pair (Fig.). The mass range of the K^+K^- system above the mass of φ resonance is also investigated.

Comparison of the experimentally obtained $d\mathcal{B}(B_s^0 \rightarrow \varphi\mu^+\mu^-)/dq^2$ distributions with the set of theory predictions show a disagreement between them at the low- q^2 region. The statistical significance of the evidence is at the level of 3.6 standard deviations. In addition, rare decay $B_s^0 \rightarrow f'_2(1\,525)\mu^+\mu^-$ is observed for the first time. The measurement is done with the large contribution from physicists of NRC “Kurchatov Institute” – PNPI.



Differential branching fraction for the $B_s^0 \rightarrow \varphi\mu^+\mu^-$ decay as a function of the squared mass of the di-muon pair overlaid with Standard Model predictions using light cone sum rules and lattice quantum-chromodynamics calculations. The results from the previous LHCb are shown with gray marker

1. LHCb Collab., Alkhazov G., ..., Andreianov A., ..., Bondar N., ..., Chubykin A., Chulikov V., ..., Dzyuba A., ..., Ilin D., ..., Inglessi A., ..., Ivshin K., ..., Kotriakhova S., Kravchenko P., ..., Maev O., ..., Maisuzenko D., ..., Sagidova N., ..., Solovev A., Solovyev I., ..., Vorobyev A., ..., Voropaev N. et al. // Phys. Rev. Lett. 2021. V. 127. P. 151801.
2. LHCb Collab., Alkhazov G., ..., Andreianov A., ..., Bondar N., ..., Chubykin A., Chulikov V., ..., Dzyuba A., ..., Ilin D., ..., Inglessi A., ..., Ivshin K., ..., Kotriakhova S., Kravchenko P., ..., Maev O., ..., Maisuzenko D., ..., Sagidova N., ..., Solovev A., Solovyev I., ..., Vorobyev A., ..., Voropaev N. et al. // JHEP. 2021. V. 11. P. 43.

First measurement of momentum transfer dependence of coherent J/ψ photoproduction in Pb–Pb ultraperipheral collisions at the Large Hadron Collider and 3D imaging of nuclear gluons

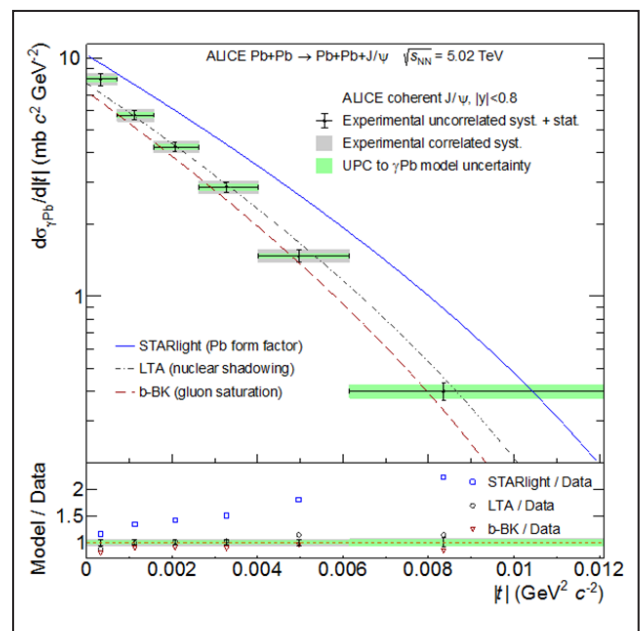
V.A. Guzey, M.B. Zhalov, E.L. Kryshen, V.V. Ivanov, M.V. Malaev,
 V.N. Nikulin, A.Yu. Ryabov, V.G. Ryabov, Yu.G. Ryabov, A.V. Khanzadeev
*High Energy Physics Division of NRC “Kurchatov Institute” – PNPI,
 ALICE Collaboration*

An important part of the heavy-ion program at the Large Hadron Collider (LHC) is studies of ultraperipheral collisions (UPCs), when colliding beams intersect at large impact parameters $b \gg R_A + R_B$ (R_A , R_B denote the radii of the involved nuclei). In this case, the short-range strong interaction is suppressed and the reaction proceeds through emission of quasireal photons, which is usually treated in the Waizsäcker–Williams equivalent photon approximation. The high intensity and energy of the resulting photon flux provide photon-photon and photon-nucleus (photon-proton) interactions at unprecedentedly high energies, which enables one to address open questions of the proton and nucleus structure in quantum chromodynamics and also to search for signals of new physics.

The focus of UPC measurements at the LHC has been exclusive photoproduction of charmonia (J/ψ , ψ') and light ρ mesons. The former provided new constraints on the nuclear gluon distribution $g_A(x, Q^2)$ at small x (x is the momentum fraction of the nucleus carried by gluons) down to $x \sim 6 \cdot 10^{-4}$. These measurements, which are usually presented in the form of the UPC cross section integrated over the momentum transfer t for various values of the J/ψ rapidity y (central and forward), helped to establish the significant suppression of $g_A(x, Q^2)$ at small x compared to its free proton counterpart because of the gluon nuclear shadowing.

The ALICE Collaboration, where scientists of NRC “Kurchatov Institute” – PNPI play an important and active role, has for the first time measured the t dependence of coherent J/ψ photoproduction in Pb–Pb UPCs in the central rapidity region $|y| < 0.8$ at 5.02 TeV, which corresponds to

the small- x range $x \sim (0.3\text{--}1.4) \cdot 10^{-3}$. It extended the previous UPC results at the LHC by providing information on the spatial distribution of nuclear gluons as a function of the impact parameter, which can be readily obtained by a two-dimensional Fourier transform of the measured t dependence. Thus, this measurement gave insight into the three-dimensional structure of the nuclear gluon distribution.



The results of the ALICE experiment for the t dependence of the photonuclear cross section in six bins of t

Figure shows the ALICE results for the t dependence of the photonuclear cross section in six bins of t . The data clearly deviate from the t dependence given by the nuclear form factor squared $|F_A(t)|^2$, which is shown by the blue solid curve and which is implemented in the commonly used

Monte Carlo generator Starlight. At the same time, the ALICE data agree well with predictions of two theoretical approaches, where the effect of nuclear shadowing is correlated with the t dependence. In the approach developed at NRC “Kurchatov Institute” – PNPI, which is based on the leading twist approximation (*the green dot-dashed curve labeled “LTA”*), nuclear shadowing is stronger at small impact parameters closer to the center of the nucleus because of the stronger nucleon overlap (higher nuclear density) there. This leads to broadening of the gluon distribution in impact parameter space, which translates into a modified, narrower t dependence compared to that given by $|F_A(t)|^2$.

A similar trend is predicted in the approach based on the color dipole model, where the scattering amplitude is obtained from the impact-parameter dependent solution of the Balitsky–Kovchegov equation, which incorporates gluon saturation effects (*the red dashed curve labeled “b-BK”*). *The lower panel* of the Figure presents the ratio of the model predictions to the data.

These results allow one to determine the nuclear gluon distribution both in the space of x and the impact parameter and, hence, pave the way to a 3D imaging of nuclear gluons using coherent photoproduction of charmonia at the LHC.

1. Guzey V., Kryshen E., ..., Zhalov M. // Phys. Lett. B. 2021. V. 816. P. 136202.
2. ALICE Collab., Ivanov V.V., Khanzadeev A.V., Kryshen E.L., Malaev M.V., Nikulin V.N., Ryabov A.Yu., Riabov V.G., Ryabov Yu.G., Zhalov M.B. // Phys. Lett. B. 2021. V. 817. P. 136280.

Observation of odderon exchange from proton-proton and proton-antiproton elastic scattering data in the D0 and TOTEM experiments

G.D. Alkhazov, A.A. Lobodenko, P.V. Neustroev, L.N. Uvarov, S.L. Uvarov

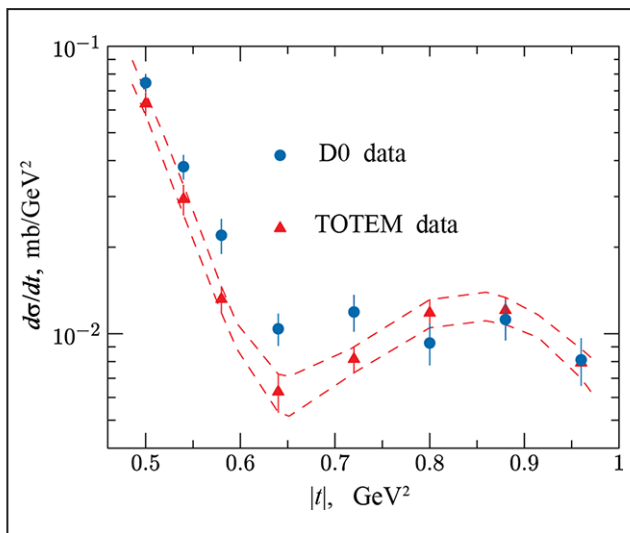
High Energy Physics Division of NRC "Kurchatov Institute" – PNPI,

Collaborations D0 and TOTEM

We present an analysis comparing the $p\bar{p}$ elastic cross section as measured by the D0 Collaboration at a centre-of-mass energy of 1.96 TeV to that in pp collisions as measured by the TOTEM Collaboration at 2.76, 7, 8 and 13 TeV using a model-independent approach. The TOTEM cross sections, extrapolated to a centre-of-mass energy of $\sqrt{s} = 1.96$ TeV, are compared with the D0 measurement in the region of the diffractive minimum and the second maximum of the pp cross section (Fig.). The two data sets disagree at the 3.4σ level and thus provide evidence for the t -channel exchange of a colourless, C-odd gluonic compound, also known as the odderon.

Note that the TOTEM Collaboration has performed also an analysis of the total cross section and the ratio of the real to imaginary parts of the forward elastic strong interaction amplitude in pp scattering and obtained an independent evidence of the same C-odd exchange with the significance between 3.4σ and 4.6σ .

The combined significance of the two analyses of the D0 and TOTEM data is larger than 5σ and is interpreted as the first observation of the exchange of a colourless, C-odd gluonic compound.



Comparison between the D0 $p\bar{p}$ cross section as a function of $|t|$ (the four-momentum transferred squared) measured at $\sqrt{s} = 1.96$ TeV (blue circles) and the TOTEM pp cross section measured at $\sqrt{s} = 2.76, 7, 8$ and 13 TeV, and extrapolated to $\sqrt{s} = 1.96$ TeV (red triangles). The dashed lines show the $\pm 1\sigma$ uncertainty band on the extrapolated pp cross section

Shell effect in the charge radii of the neutron-rich mercury isotopes

A.E. Barzakh, D.V. Fedorov, P.L. Molkanov, M.D. Seliverstov
 High Energy Physics Division of NRC “Kurchatov Institute” – PNPI,
 IS598 Collaboration

Isotope shifts and hyperfine splittings of the atomic transition $\lambda = 254$ nm in $^{206-208}\text{Hg}$ were measured with the in-source resonance ionization spectroscopy at the ISOLDE facility. Isotopic changes in the mean-square charge radius ($\delta\langle r^2 \rangle$), magnetic and quadrupole moments of the studied nuclei were derived from the experimental data. For investigation of the mercury isotopes the new modification of the ion source, versatile arc discharge and laser ion source (VADLIS), was used.

Analysis of the magnetic moments (μ) for the nuclei with $N = 127$ ($\mu(^{207}\text{Hg})$ included) demonstrated that their Z -dependence is determined by the particle-quadrupole-vibration coupling mechanism. In the second order of perturbation theory the g -factor, $g = \mu/I$, correction due to particle-vibration coupling is proportional to the inverse square of the energy of the lowest vibrational 2^+ state in the even-even nucleus with the same proton number, $E(2^+)^{-2}$. The agreement of the $g(vg_{9/2})$ and

the $E(2^+)^{-2}$ evolution with Z supports the interpretation of the mechanism behind the variation in the g -factors of the $N = 127$ isotones (Fig. 1).

The characteristic kink in the charge radii at the $N = 126$ neutron shell closure has been revealed, along with the odd-even staggering (OES), where an odd- N isotope has a smaller charge radius than the average of its two even- N neighbors (Fig. 2).

The new data were analyzed via both spherical relativistic Hartree–Bogoliubov (RHB) and spherical nonrelativistic Hartree–Fock (NRHF) approaches, together with the traditional magic- Z theoretical benchmark of the lead isotopic chain. To quantify the shell effect at $N = 126$, the special kink indicator was used:

$$\Delta R^{(3)}(A) = 0.5[R(A + 2) + R(A - 2)] - R(A),$$

where $R(A) = \langle r^2 \rangle^{1/2}(A)$ is the charge radius of the isotope with mass A of the element under consideration.

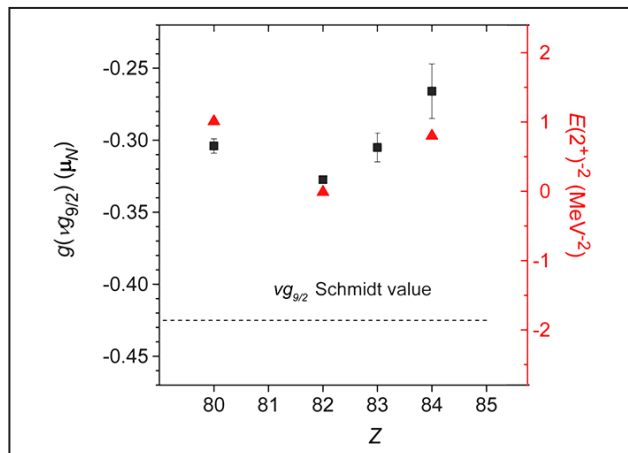


Fig. 1. The observed correlation between the values of $E(2^+)^{-2}$ and g -factors values: black squares – experimental g -factors for $N = 127$ isotones ($vg_{9/2}$); dashed line shows the Schmidt value for $vg_{9/2}$ shell; red triangles – $E(2^+)^{-2}$ values in the corresponding even-even nuclei with $N = 126$

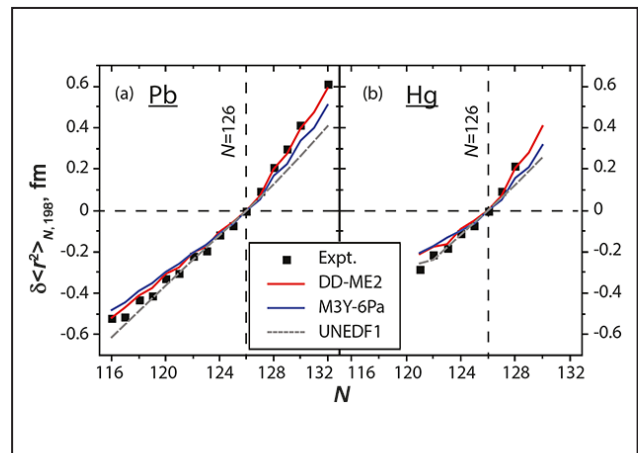


Fig. 2. Comparison of experimental and theoretical $\delta\langle r^2 \rangle$ values for Pb (a) and Hg (b) isotopes: black squares – experimental values; lines – theoretical approaches, within which the results were obtained

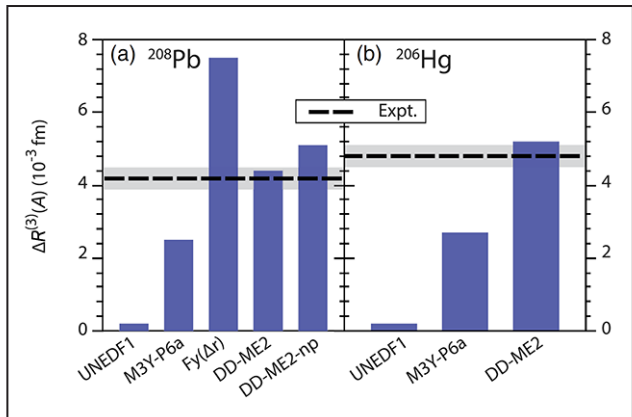


Fig. 3. Comparison of the experimental and theoretical $\Delta R^3(A)$ values for the isotopes of lead (a) and mercury (b). Experimental values are shown by *dashed line* with experimental uncertainty depicted as translucent gray bars. Blue bars present the values obtained in the framework of the corresponding theoretical approaches

Shell effect is absent when $\Delta R^3(A) = 0$.

In Figure 3 experimental and theoretical values of this indicator are compared. Theoretical calculations were performed in the framework of the different approaches: NRHF with UNEDF1 functional, NRHF with M3Y-P6a functional (with modified spin-orbital interaction), NRHF with Fayans functional [Fy(Δr)], RHB with DD-ME2 functional. The bar with the designation DD-ME2-np corresponds to the RHB (DD-ME2) calculations without pairing. Evidently, the RHB (DD-ME2) calculations best reproduce the kink, while the NRHF (M3Y-P6a)

and NRHF [Fy(Δr)] results underestimate and overestimate its magnitude, respectively.

Contrary to previous interpretations, it was demonstrated that both the kink at $N = 126$ and the odd-even staggering in its vicinity can be described predominately at the mean-field level and that pairing does not play a crucial role in their origin. A new OES mechanism is suggested, related to the staggering in the occupation of the different neutron orbitals in odd- and even- A nuclei, facilitated by particle-vibration coupling for odd- A nuclei.

1. Day Goodacre T., ..., Barzakh A.E., ..., Fedorov D.V., ..., Molkanov P.L., ..., Seliverstov M.D. et al. // Phys. Rev. Lett. 2021. V. 126. P. 032502.
2. Day Goodacre T., ..., Barzakh A.E., ..., Fedorov D.V., ..., Molkanov P.L., ..., Seliverstov M.D. et al. // Phys. Rev. C. 2021. V. 104. P. 054322.

Shape staggering in neutron-deficient bismuth isotopes

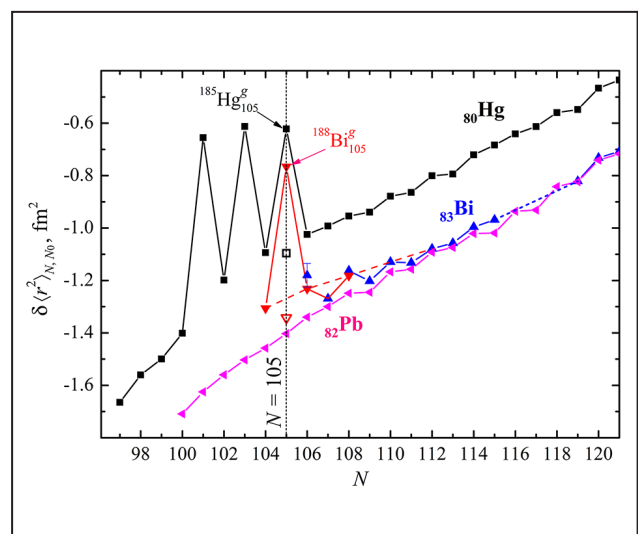
A.E. Barzakh, D.V. Fedorov, P.L. Molkanov, V.N. Panteleev, M.D. Seliverstov
 High Energy Physics Division of NRC “Kurchatov Institute” – PNPI,
 IS598 Collaboration

Isotope shifts and hyperfine splittings of the atomic transition $\lambda = 306.9$ nm in $^{187-191}\text{Bi}$ were measured by the in-source resonance ionization spectroscopy at the ISOLDE facility. Isotopic changes in the mean-square charge radius ($\delta\langle r^2 \rangle$), magnetic and quadrupole moments of the studied nuclei were derived from the experimental data by means of the advanced atomic calculations. It is the ultrasensitive in-source spectroscopy that enables us to study nuclei with the yield less than 1 ion per 10 s.

Nuclear shape staggering effect was found for the first time in the mercury isotopic chain: the ground states of the odd- N isotopes with $N = 101, 103, 105$ proved to be strongly deformed, whereas their even- A neighbors ($N = 102, 104, 106$) keep the near-spherical shape (Fig.). This phenomenon was characterized as one of the most remarkable discoveries in nuclear structure physics in the last 50 years.

Fifty years after this discovery, we found the second example of such an unusual behavior – shape staggering in the neutron-deficient bismuth isotopes. Ground state of ^{188}Bi is strongly deformed, whereas $^{187},^{189}\text{Bi}$ and high-spin isomer of ^{188}Bi are near spherical. This effect reveals itself in the saw-tooth isotopic dependency of the nuclear radii, similar to that observed earlier in the mercury chain. It should be noted that shape staggering in bismuth nuclei takes place at the same neutron number ($N = 105$; see Fig.) as in the mercury isotopes.

In the same experiment electric quadrupole moment for $^{188}\text{Bi}^g$ was measured. The deformation



Changes in the mean-square charge radii for bismuth (blue triangles – literature data; red triangles – present work), mercury (black squares) and lead (violet triangles) isotopes. Full and hollow symbols label the ground states and isomers, respectively. Data for each chain are shifted along the Y axis to improve visibility

parameter derived from this quadrupole moment ($\beta_0 = 0.25(7)$) perfectly agrees with the deformation parameter extracted from the $\delta\langle r^2 \rangle$ values ($\beta_1 = 0.28(2)$). This coincidence unambiguously confirms the interpretation of the observed effect.

It was found also that the $\delta\langle r^2 \rangle$ values for bismuth isotopes with $N < 112$ markedly deviate from the radii isotopic trend for spherical lead nuclei (see dashed line in Fig.). Theoretical analysis in the Hartree–Fock–Bogoliubov framework explains this deviation by the mixing of configurations with different deformation.

Results of the Neutrino-4 experiment on the search for sterile neutrino

A.P. Serebrov¹, V.G. Ivochkin¹, R.M. Samoilov¹, A.K. Fomin¹, V.G. Zinoviev¹, A.V. Chernyj¹, O.M. Zherebtsov¹, M.E. Chaikovskii¹, M.E. Zaytsev¹, A.A. Gerasimov¹, V.V. Fedorov¹, P.V. Neustroev², S.S. Volkov², V.L. Golovtsov², A.L. Petelin³, A.L. Izhutov³, A.A. Tuzov³, S.A. Sazontov³, M.O. Gromov³, V.V. Afanasiev³, M.E. Zaytsev⁴

¹ Neutron Research Division of NRC “Kurchatov Institute” – PNPI,
Neutrino-4 Collaboration

² High Energy Physics Division of NRC “Kurchatov Institute” – PNPI

³ Joint Stock Company “State Scientific Center – Research Institute of Atomic Reactors”

⁴ Dimitrovgrad Engineering Institute of Technology – Branch of National Research
Nuclear University MEPhI

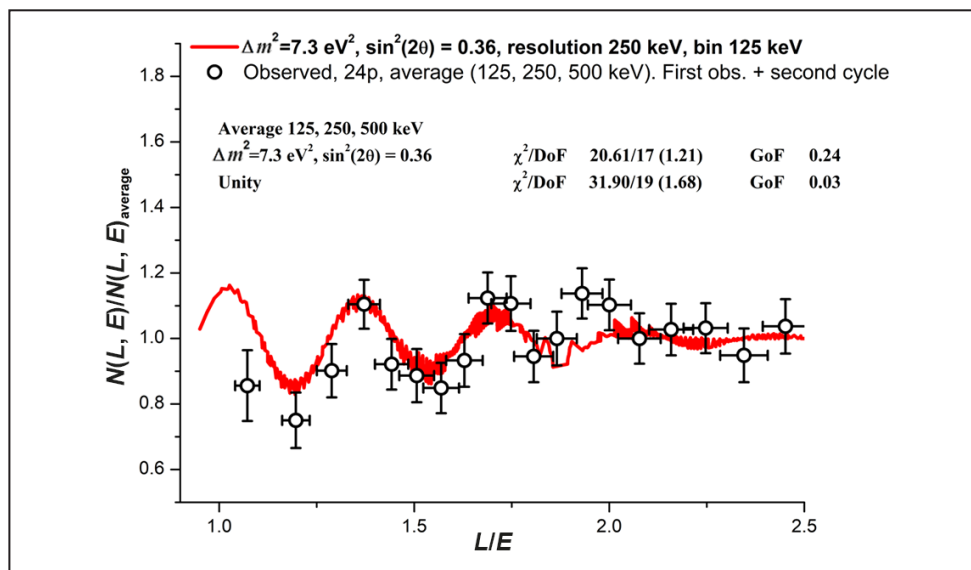
The experiment Neutrino-4 had started in 2014 with a detector model and then was continued with a full-scale detector in 2016–2021. Measurements of the flux and spectrum of the reactor anti-neutrinos as a function of distance to the center of the active zone of the SM-3 reactor (Dimitrovgrad, Russia) in the range of 6–12 m were made. Using all the collected data, we performed a model-independent analysis to determine the oscillation parameters Δm_{14}^2 and $\sin^2 2\theta_{14}$.

The dependence of

$$R_{ik}^{\text{exp}} = (N_{ik} \pm \Delta N_{ik})L_k^2 / K^{-1} \sum_k^K (N_{ik} \pm \Delta N_{ik})L_k^2$$

on L/E_ν , obtained using the method of coherent summation of measurement results allows to directly demonstrate the oscillation effect (Fig.).

The analysis of possible systematic errors and Monte Carlo simulation of the experiment, which considers the possibility of the effect manifestation at the present precision level, were performed. As a result of the analysis, we can conclude that at the currently available statistical accuracy we observe the oscillations at the 2.9σ level with parameters $\Delta m_{14}^2 = (7.30 \pm 0.13_{\text{stat}} \pm 1.16_{\text{syst}}) \text{ eV}^2 = (7.30 \pm 1.17) \text{ eV}^2$ and $\sin^2 2\theta_{14} \approx 0.36 \pm 0.12_{\text{stat}}$ (2.9σ).



Dependence of the R ratio on L/E for the neutrino signal. The red curve is the expected dependence with oscillation parameters $\Delta m_{14}^2 = 7.3 \text{ eV}^2$ and $\sin^2 2\theta_{14} = 0.36$, corresponding to the best approximation. Reliability level of observation of oscillations is 2.9σ . Experimental points are presented as the average of three samples with different widths of energy bins (125, 250 and 500 keV)

Direct ultraprecision measurement of the $^{187}\text{Re} - ^{187}\text{Os}$ mass difference as a prologue for determining the effective mass of the antineutrino

S.A. Eliseev, Yu.N. Novikov, P.E. Filianin

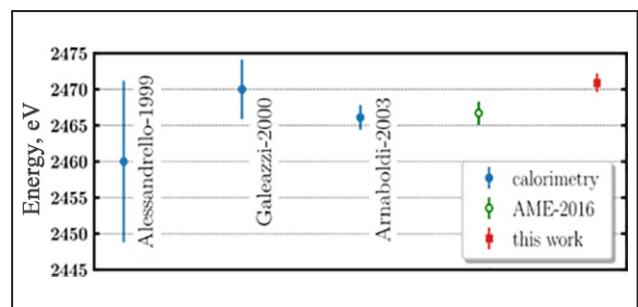
High Energy Physics Division of NRC "Kurchatov Institute" – PNPI,
PENTATRAP Collaboration

Nuclide ^{187}Re is characterized by the smallest of all known β -decay energy between the ground states of nuclei, which according to the literature data is about 2.5 keV. This corresponds to the smallest mass difference of $^{187}\text{Re} - ^{187}\text{Os}$. Therefore, it is considered as one of the best candidates for determining the absolute value of the effective antineutrino mass. The specified value of the ^{187}Re decay energy is many times less than the decay energy of tritium (18.6 keV), which is actively used by the KATRIN installation to determine the desired mass. The difference in the masses of the nuclide pair under discussion was measured earlier by our group at the SHIPTRAP installation (GSI Helmholtz Center for Heavy Ion Research, Darmstadt), and upon the commissioning of the PENTATRAP system it was transferred to the Max Planck Institute for Nuclear Physics in Heidelberg.

The PENTATRAP system is a tower of five Penning ion traps, in which the resonant excitation frequencies of individual highly charged ions $^{187}\text{Re}^{29+}$ and $^{187}\text{Os}^{29+}$ are measured. These ions are formed by irradiating the material with a powerful electron beam and are carried into the trap area by a formed beam stretched in the ion channel from the electron gun through a magnetic mass separator. One osmium ion and two rhenium ions are simultaneously launched into three traps in which their cyclotron frequencies are measured. Then the same ions are moved to another set of three traps. This configuration of the experiment makes it possible to eliminate the temporary inaccuracy of the magnetic field, that significantly reduces the systematic uncertainty of measurements and increases their precision.

PENTATRAP allows to measure masses with great accuracy, largely due to the fact that measurements are carried out for ions with big charges.

However, for the purposes of neutrino physics, it is necessary to know the masses of neutral atoms whose beta decay spectrum (with the departure of antineutrinos) is measured by a microcalorimeter. To move from the difference of ionic masses to the difference of neutral masses, it is necessary to calculate the differences in the binding energies of the electrons in each ion of the pair, which is done with very good accuracy using the Dirac–Hartree–Fock method.



The decay energy values are plotted on the Y-axis in eV units, and different experiments are plotted on the X-axis. The point with the value obtained in the present experiment is shown in red

This recalculation was performed by the PENTATRAP Collaboration for both the above-mentioned nuclide pairs in 2021. For the mass difference of the neutral ground states ^{187}Re and ^{187}Os , the value $\Delta M = 2470.9 \pm 1.3$ eV was obtained. This direct measurement puts an end to the question of the mass difference (the decay energy endpoint of ^{187}Re), the spread of values of which was caused by various previous experiments (Fig.). The obtained value of the β -decay endpoint energy with an accuracy of 1 eV opens up the possibility of obtaining the effective antineutrino mass with the same accuracy in the analysis of the microcalorimetric spectrum.

Precision measurements of the ^{210}Bi β -spectrum for neutrino physics tasks

A.V. Derbin, I.S. Drachnev, I.M. Kotina, I.S. Lomskaya, M.S. Mikulich,
V.N. Muratova, N.V. Niyazova, D.A. Semenov, M.V. Trushin, E.V. Unzhakov, E.A. Chmel
Neutron Research Division of NRC "Kurchatov Institute" – PNPI

The isotope ^{210}Bi is an element of ^{238}U natural decay chain. As decay product of ^{222}Rn gas and subsequent long-lived ^{210}Pb , the ^{210}Bi isotope is present inside and on the surface of all structural materials. At present, accurate measurement of ^{210}Bi β -spectrum is necessary for background simulation of modern neutrino and dark matter detectors, as well as for other low-background experiments. The shape of ^{210}Bi β -spectrum is very similar to the spectrum of recoil electrons from the scattering of solar CNO-neutrinos.

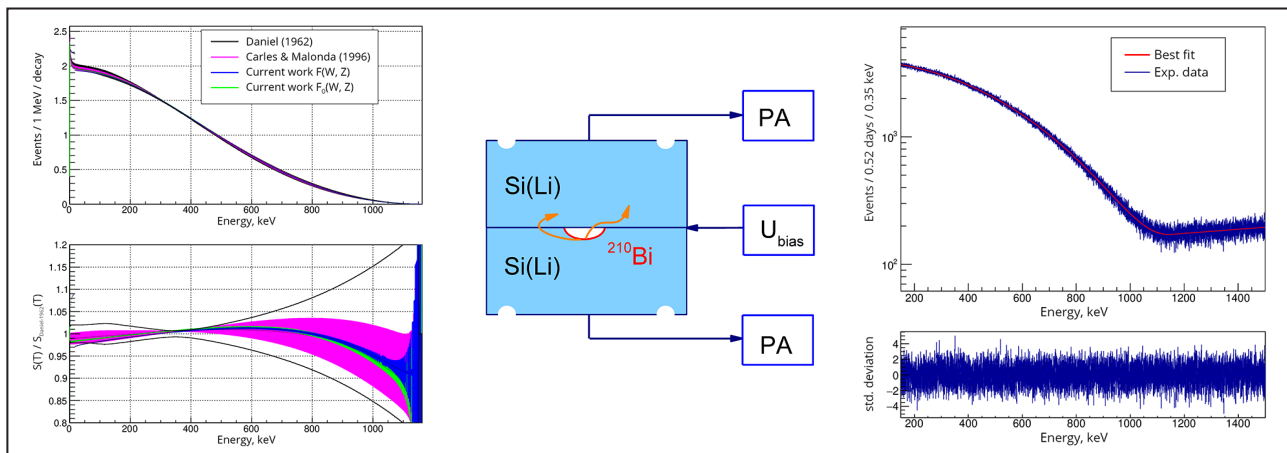
The Borexino international collaboration, in which scientists from NRC "Kurchatov Institute" – PNPI participate, presented the results of the detection of neutrinos emitted in the reactions of the CNO-cycle on the Sun. A significant contribution of NRC "Kurchatov Institute" – PNPI is related to the precision measurement of the ^{210}Bi β -spec-

trum required for analyzing the solar CNO neutrino flux.

The β -spectrum was measured with two types of Si-spectrometers developed and manufactured at NRC "Kurchatov Institute" – PNPI (Fig.). To register electrons in a spectrometer designed according to the classical "target-detector" scheme, a Si(Li)-detector 15 mm in diameter and 7 mm thick was used. The main difference of the new $4\pi\beta$ -spectrometer is the response function, which is close to Gaussian, which does not require careful consideration of electron backscattering from the crystal surface.

As a result of two independent measurements, the values of the nuclear form factor parameters are determined with an accuracy better than a percent and are consistent with each other.

The work was supported by the RFBR grant No. 19-02-00097.



The spectrum of ^{210}Bi measured in the "target-detector" scheme, in comparison with the results of other works (on the left); a circuit of a $4\pi\beta$ -spectrometer with Si(Li)-detectors, preamplifiers (PA) and bias voltage (U_{bias}) (center); the spectrum of ^{210}Bi measured by the $4\pi\beta$ -spectrometer and the result of fitting with the theoretical shape of the β -spectrum (on the right)

1. Alekseev I.E., Baklanov S.V., Derbin A.V., Drachnev I.S., Kotina I.M., Lomskaya I.S., Muratova V.N., Niyazova N.V., Semenov D.A., Trushin M.V., Unzhakov E.V. // J. Phys.: Conf. Ser. 2021. V. 2103. P. 012144.
2. Baklanov S.V., Derbin A.V., Drachnev I.S., Kotina I.M., Lomskaya I.S., Muratova V.N., Niyazova N.V., Semenov D.A., Trushin M.V., Unzhakov E.V., Chmel E.A. // Instrum. Exp. Tech. 2021. V. 64. P. 190.

Spectrum of protons in collisions of heavy ions $^{12}\text{C} + ^9\text{Be}$ at energies of 0.3–2.0 GeV/nucleon in terms of the hydrodynamic approach

A.T. Dyachenko, I.A. Mitropolsky

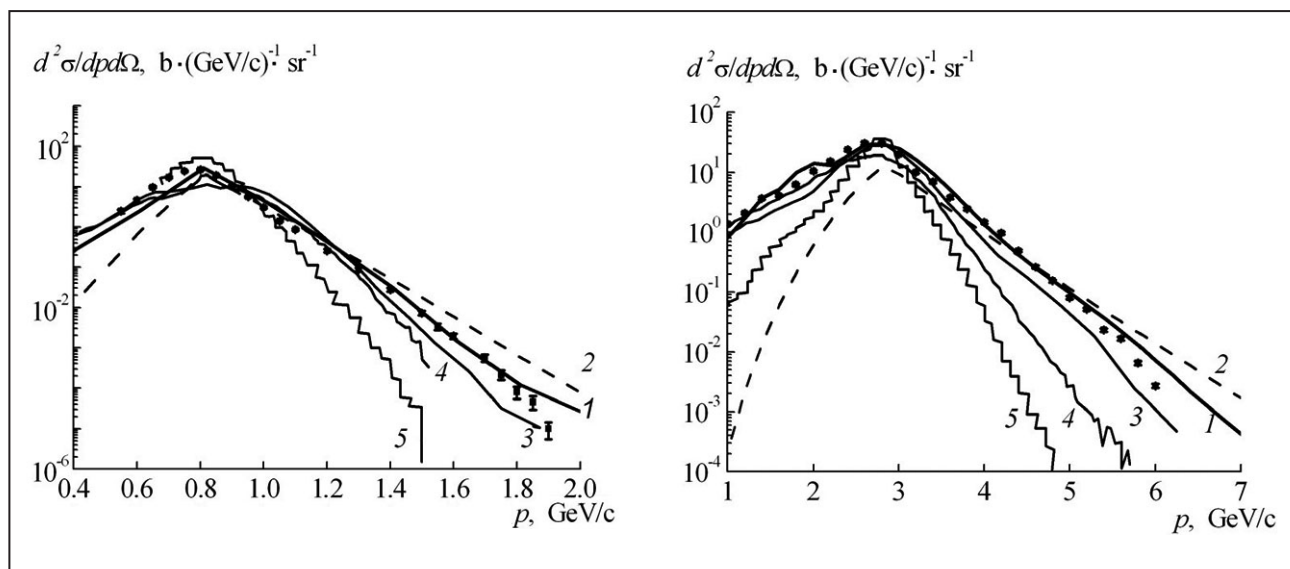
High Energy Physics Division, Neutron Research Division of NRC “Kurchatov Institute” – PNPI

In an effort to develop the hydrodynamic approach with a nonequilibrium state equation, collisions of ^{12}C nuclei with a beryllium target are considered at energies of incident carbon nuclei of 0.3–2.0 GeV/nucleon with proton emission at an angle of 3.5° .

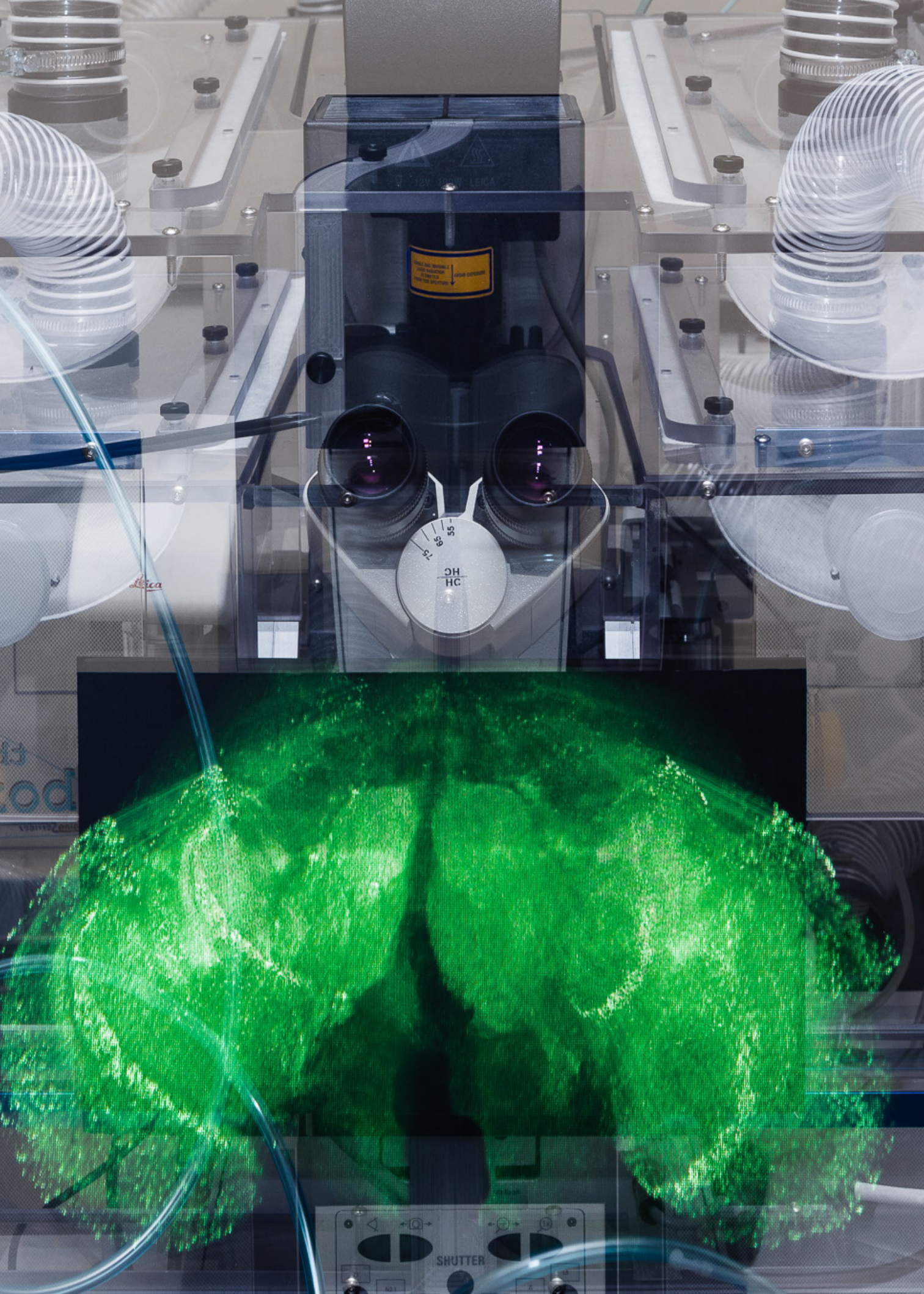
The proton spectra contain a high-energy cumulative part that we had previously described in terms of the hydrodynamic approach, with allowance for the microcanonical distribution correction and the soft part of the spectrum that contains a contribution from fragmentation.

In this work, we took into account the contribution of protons from fragmentation based on a statistical mechanism. In Figure, the calculation results

are compared with experimental data. In the region of small momentum at all energies, our calculation reproduces experimental data, which is due to the contribution from protons formed as a result of fragmentation for overlapping and non-overlapping parts of colliding nuclei. The correction for the microcanonical distribution is manifested in the high-momentum region of proton distributions. If one does not take into account the contribution from fragmentation and does not adjust for the microcanonical distribution (dashed curves 2), then in the soft region of the spectrum, the calculated criteria underestimate the experimental data, and in the cumulative region they go above the experimental points.



Proton momentum distributions in the reaction $^{12}\text{C} + ^9\text{Be} \rightarrow p + X$ at the ^{12}C ion energy of 0.3 GeV/nucleon (left) and 2.0 GeV/nucleon (right): curve 1 – our calculations; dashed curve 2 – our calculations with no microcanonical distribution correction and allowance for the contribution from fragmentation; dots – experimental data (Abramov B.M. et al., 2015); curves 3–5 – the results from calculations using the transport codes (ibid): curve 3 – the cascade model; curve 4 – the transport model of quark-gluon strings; curve 5 – the quantum molecular dynamics model integrated into the GEANT4 software package



SHUTTER

Biological Research

- 72** Evaluation of haptoglobin and its proteoforms as glioblastoma markers
- 73** Genetic analysis of the function of the Hsm3 protein in the complex in the yeast *Saccharomyces cerevisiae*
- 74** Transcriptomic profiles reveal downregulation of low-density lipoprotein particle receptor pathway activity in patients surviving severe COVID-19
- 75** Ambroxol increases glucocerebrosidase (GCase) activity and restores GCase translocation in primary patient-derived macrophages in Gaucher disease and Parkinsonism
- 76** Morphofunctional consequences of swiss cheese knockdown in glia of *Drosophila melanogaster*
- 77** Loss of swiss cheese in neurons contributes to neurodegeneration with mitochondria abnormalities, reactive oxygen species acceleration and accumulation of lipid droplets in drosophila brain
- 78** Multifaceted mechanism of amicoumacin A inhibition of bacterial translation
- 79** Differential contribution of protein factors and 70S ribosome to elongation
- 80** Targeting evolution of antibiotic resistance by SOS response inhibition
- 81** Antibacterial properties of fucoidans from the brown algae *Fucus vesiculosus* of the Barents Sea
- 83** Long-term monitoring of the development and extinction of IgA and IgG responses to SARS-CoV-2 infection
- 85** Delivery of functional exogenous proteins by plant vesicles into human cells *in vitro*

Evaluation of haptoglobin and its proteoforms as glioblastoma markers

S.N. Naryzhny¹, N.L. Ronzhina¹, O.K. Legina¹, N.V. Klopov¹, R.A. Pantina¹, E.S. Zorina², M.G. Zavialova², V.G. Zgoda², F.Yu. Kabachenko³

¹ Molecular and Radiation Biophysics Division of NRC “Kurchatov Institute” – PNPI

² V.N. Orekhovich Research Institute of Biomedical Chemistry

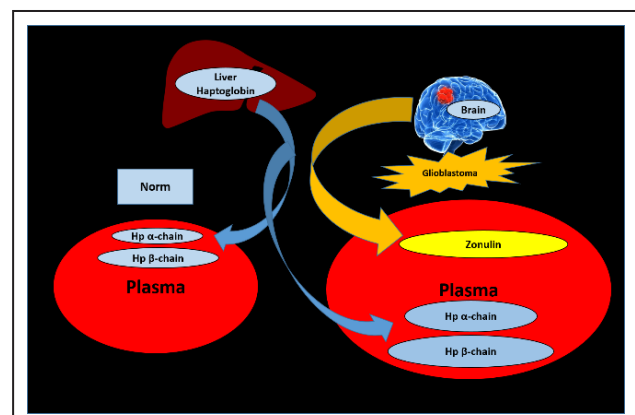
³ Peter the Great Saint Petersburg Polytechnic University

Haptoglobin (Hp) is a blood plasma glycoprotein that plays a critical role in tissue protection and the prevention of oxidative damage. Haptoglobin is an acute-phase protein, its concentration in plasma changes in pathology, and the test for its concentration is part of normal clinical practice. Haptoglobin is a conservative protein and is the subject of research as a potential biomarker of many diseases, including malignant neoplasms. The Human Hp gene is polymorphic and controls the synthesis of three major phenotypes: homozygous Hp1-1 and Hp2-2, and heterozygous Hp2-1, determined by a combination of allelic variants that are inherited. Numerous studies indicate that the phenotype of haptoglobin can be used to judge the individual's predisposition to various diseases. In addition, Hp undergoes various posttranslational modifications (PTMs). Glioblastoma multiform (GBM) is the most malignant primary brain tumor.

In our study, we have analyzed the state of Hp proteoforms in plasma and cells using 1D (SDS-PAGE) and 2D electrophoresis (2DE) with the following mass spectrometry (LC ES-MS/MS) or western blotting. We found that the levels of α 2- and

β -chain proteoforms are upregulated in the plasma of GBM patients. An unprocessed form of Hp2-2 (PreHp2-2, zonulin) with unusual biophysical parameters (pI/Mw) was also detected in the plasma of GBM patients and glioblastoma cells (Fig.).

Altogether, this data shows the possibility to use proteoforms of haptoglobin as a potential GBM-specific plasma biomarker.



Graphical representation of the possible entry into the blood of processed forms of haptoglobin from the liver and the unprocessed form of haptoglobin (zonulin) from a brain tumor

1. Naryzhny S.N., Ronzhina N.L., Zorina T.S., Kabachenko F.Yu., Zavialova M.G., Zgoda V.G., Klopov N.V., Legina O.K., Pantina R.A. // Int. J. Mol. Sci. 2021. V. 22. P. 6533.

2. Naryzhny S.N., Legina O.K. // Biomed. Chem. 2021. V. 67. No. 2. P. 105.

Genetic analysis of the function of the Hsm3 protein in the complex in the yeast *Saccharomyces cerevisiae*

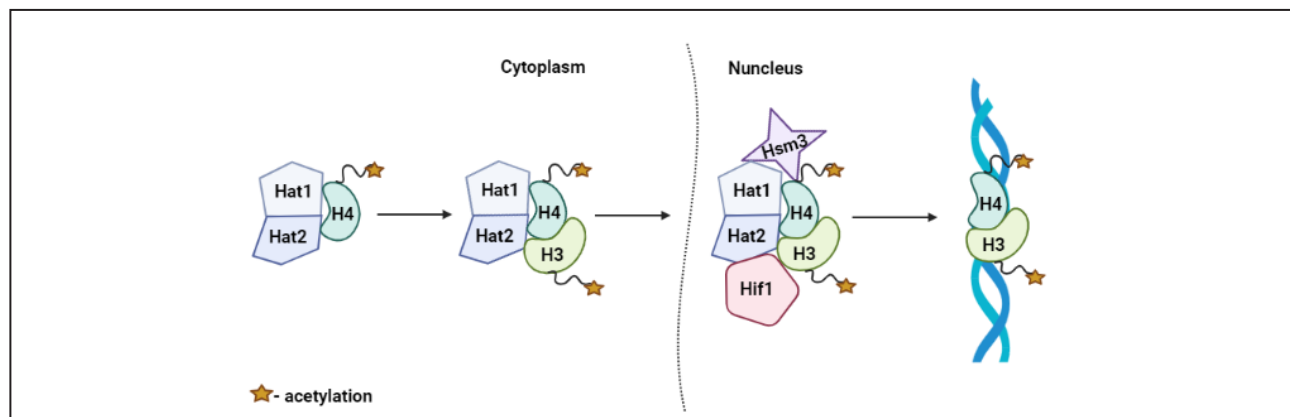
T.A. Evstyukhina, E.A. Alekseeva, D.V. Fedorov, V.T. Peshekhonov, V.G. Korolev
 Molecular and Radiation Biophysics Division of NRC “Kurchatov Institute” – PNPI

In the yeast nuclear compartment, the NuB4 nuclear complex consists of three proteins: Hat1, Hat2 and Hif1, and interacts with a number of other factors. In particular, the NuB4 complex was shown to physically interact with Hsm3p. Previously it was shown that the *HSM3* gene is involved in the control of replicative and reparative spontaneous mutagenesis and adaptive mutagenesis, and *hsm3Δ* mutants increase the frequency of mutations induced by various mutagens. Previously it was believed that the *HSM3* gene controls only some minor repair processes in the cell, but later it was suggested that it performs a chaperone function involving the assembly of proteasomes.

In this study, we performed a genetic analysis of the properties of three *hsm3Δ*, *hif1Δ* and *hat1Δ* mutants. We presented evidence that a significant increase in dNTP levels suppresses *hsm3*- and

hif1-dependent mutagenesis. In addition, *hsm3Δ* and *hif1Δ* mutations significantly reduce the efficiency of induction of RNR (ribonucleotide reductase) gene expression after UV irradiation. This decrease in expression causes the switching of precise polymerases to the highly misguided Polη polymerase during DNA repair synthesis and determines high UV-induced mutagenesis, especially at non-bipyrimidine sites (NBP sites) in *hsm3* and *hif1* mutants.

Thus, we proved that Polη is responsible for *hsm3*- and *hif1*-dependent mutagenesis. The results presented in this work show that the genetic properties of the *hsm3* mutation are completely similar to those of the *hif1* and *him1* mutations. Based on this, it was concluded that the Hsm3 protein, like the Hif1 protein, can be a functional subunit of the NuB4 complex and participate in the assembly of chromatin during the repair process (Fig.).



A model describing the potential mechanism of action of Hsm3p within the NuB4 complex. It describes the approximate mechanism of action of Hsm3p as a subunit of the NuB4 histone acetyltransferase complex. Most likely, Hsm3p is included in the Hat1p/Hat2p complex, as is Hif1p

Transcriptomic profiles reveal downregulation of low-density lipoprotein particle receptor pathway activity in patients surviving severe COVID-19

I.N. Vlasov¹, A.A. Panteleeva^{2, 3}, T.S. Usenko^{2, 3}, M.A. Nikolaev^{2, 3}, A.D. Izumchenko², E.G. Gavrilova³, I.V. Shlyk³, V.V. Miroshnikova^{2, 3}, M.I. Shadrina¹, Yu.S. Polushin³, S.N. Pchelina^{2, 3, 4}, P.A. Slonimsky¹

¹ NRC “Kurchatov Institute” – Institute of Molecular Genetics

² Molecular and Radiation Biophysics Division of NRC “Kurchatov Institute” – PNPI

³ Pavlov First Saint Petersburg State Medical University

⁴ Kurchatov Genome Center – PNPI

Coronavirus infection (COVID-19) is caused by severe acute respiratory syndrome coronavirus 2 (SARS-CoV-2) from the HCoV family of coronaviruses.

To identify genetic biomarkers of death in severe COVID-19 requiring intensive care and resuscitation, for the first time, we conducted a transcriptome analysis study in patients at the time of admission to the intensive care unit with a prospective assessment of the outcome of the disease in the acute period (30 days). We obtained peripheral blood lymphocytes from five patients who survived severe COVID-19 and three patients who died of infection in the intensive care unit. RNA sequencing was conducted for each sample. Raw data was processed by bioinformatics approaches using three different pipelines. As a result, lists of differentially expressed genes (DEGs) were identified for each pipeline – 1038, 866, 516, respectively, as well as a list of 361 DEGs common to all three pipelines used in the study.

At the next stage, an analysis of the enrichment of the functional groups of genes was carried out

for the list of DEGs of three pipelines and for 361 common DEGs. As a result, the pathways common to all pipelines were identified: the activation pathway of low-density lipoprotein receptors (GO: 0005041), leukocyte differentiation (GO: 0002521) and the activity of the cargo receptor (GO: 0038024). We have shown for the first time a decrease in the level of expression of the *STAB1*, *PPARG*, *CD36*, *ITGAV* and *ANXA2* genes, the products of which are involved in cholesterol metabolism, in survivors compared with the non-survivors. The study allowed for the first time to identify genes differentially expressed in peripheral blood lymphocytes of patients with severe COVID-19 with different outcomes (died/survived). Our data confirm the important role of changes in cholesterol metabolism in determining the outcome of coronavirus infection.

The study was carried out with financial support from Kurchatov Genome Center – PNPI under the program for development of world leading genetic research centers (agreement No. 075-15-2019-1663).

Ambroxol increases glucocerebrosidase (GCase) activity and restores GCase translocation in primary patient-derived macrophages in Gaucher disease and Parkinsonism

A.E. Kopytova¹, G.N. Rychkov^{1, 2, 3}, M.A. Nikolaev^{1, 4}, G.V. Baydakova⁵, A.A. Cheblokov¹, K.A. Senkevich^{1, 4}, D.A. Bogdanova¹, O.I. Bolshakova¹, I.V. Miliukhina^{1, 4, 6}, V.A. Bezrukikh⁷, G.N. Salogub⁷, S.V. Sarantseva¹, T.S. Usenko^{1, 4}, E.Yu. Zakharova⁵, A.K. Emelyanov^{1, 4, 6}, S.N. Pchelina^{1, 4, 6}

¹ Molecular and Radiation Biophysics Division of NRC “Kurchatov Institute” – PNPI

² Peter the Great Saint Petersburg Polytechnic University

³ Kurchatov Genome Center – PNPI

⁴ Pavlov First Saint Petersburg State Medical University

⁵ Research Center for Medical Genetics

⁶ Institute of Experimental Medicine

⁷ V.A. Almazov National Medical Research Center

Mutations in the glucocerebrosidase gene (*GBA1*) encoding the lysosomal enzyme glucocerebrosidase (GCase) cause Gaucher disease (GD) and are the most commonly known genetic risk factor for Parkinson disease (PD). Due to *GBA1* mutations the folding and transport of GCase to lysosomes is disrupted, as a result the activity of this enzyme decreases. The connection between these diseases makes it promising to develop strategies aimed at therapy for GD including neuronopathic forms and potentially for PD associated with mutations in the *GBA1* gene (GBA-PD).

There are currently no neuroprotective therapies for patients with PD, as well as no therapies for PD with the nervous system involvement. Pharmacological chaperones (PCs) are small molecules able to stabilize and refold misfolded GCase that can potentially be used as activators of the enzymatic activity of GCase. The main problem is that most of the known PCs for GCase are inhibitors of the active site of the enzyme. According to literature data, ambroxol (ABX) is a metabolite of bromhexine that has been used for more than 50 years as a mucolytic agent in the treatment of hyaline membrane

disease. ABX is considered as one of the promising GCase PCs, however, the mechanism of its action has not been described and it remains unknown to what extent its interindividual efficacy varies.

The results showed that primary macrophages are a suitable model for testing the effectiveness of drugs that affect the GCase activity not only for GD patients, but also for GBA-PD. In primary macrophages from GD patients we demonstrated effective restoration of enzymatic activity and the GCase protein level, its increased transport to lysosomes, decreased concentration of lysosphingolipids after ABX treatment. Molecular modeling *in silico* of the binding of ABX to the mutant form of GCase N370S suggests that ABX can act both as an enzyme inhibitor and allosteric PC, which confirms the hypothesis that ABX may be more effective compared to PC of the inhibitory-activator type. The identification of new potential binding sites of compounds located on the surface of GCase opens up the prospect for virtual screening of new non-inhibitory PC.

The study was supported by the Russian Foundation for Basic Research No. 17-75-20159.

Morphofunctional consequences of swiss cheese knockdown in glia of *Drosophila melanogaster*

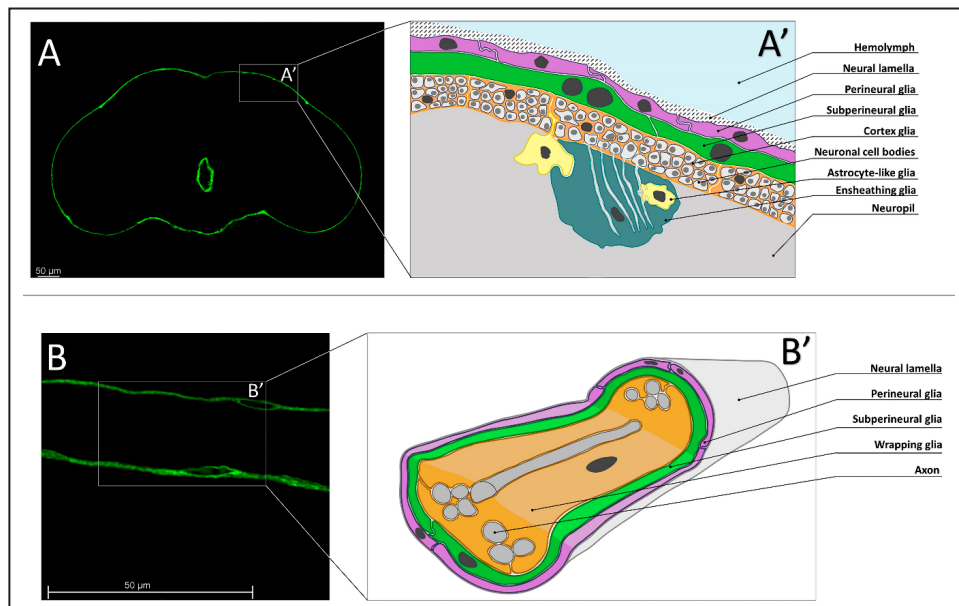
E.V. Ryabova, P.A. Melentev, A.E. Komissarov, N.V. Surina, E.A. Ivanova, S.V. Sarantseva
Molecular and Radiation Biophysics Division of NRC "Kurchatov Institute" – PNPI

Glial cells are extremely important for functioning of the nervous system, and their physiology is under control of various genes. Different insects, in particular *Drosophila melanogaster*, are used to study aspects of glial cell functioning (Fig.). We studied the consequences of the suppression of the swiss cheese gene expression in the superficial glia (perineurial and subperineurial), as well as in the underlying glial types – the glia of the central nervous system cortex and the wrapping glia of the peripheral nervous system. These types of glial cells ensure homeostasis in the nervous tissue, protecting it from the external influences and regulating neuron metabolism.

We elucidated that the knockdown of the swiss cheese gene in the subperineurial glia induces morphological changes in these cells. At the

same time, the number of the subperineurial glia nuclei is reduced, possibly, due to apoptosis. The knockdown of the studied gene in the wrapping glia causes morphological changes of structures formed by these cells. We characterised changes of the transcriptome under suppression of swiss cheese expression in these types of glia, and we also found elevation of the reactive oxygen species level. The revealed changes were accompanied by a decline in the locomotor activity of flies, which was analysed in the negative geotaxis test.

The obtained results suggest the importance of the swiss cheese gene expression in several types of glial cells to provide protection of the nervous tissue from the oxidative stress and for control of the locomotor activity of individuals.



Types of glia cells in the *Drosophila melanogaster* nervous system:
A, B – confocal microscopy images of a brain and an abdominal nerve of an adult specimen, where subperineurial glia is marked with green fluorescent protein (GFP);
A', B' – schemes of glia cells in a brain and abdominal nerves of a *Drosophila melanogaster* adult.
Scale bar – 50 μm

Loss of swiss cheese in neurons contributes to neurodegeneration with mitochondria abnormalities, reactive oxygen species acceleration and accumulation of lipid droplets in drosophila brain

P.A. Melentev, E.V. Ryabova, N.V. Surina, D.R. Zhmujdina, A.E. Komissarov,

E.A. Ivanova, S.V. Sarantseva

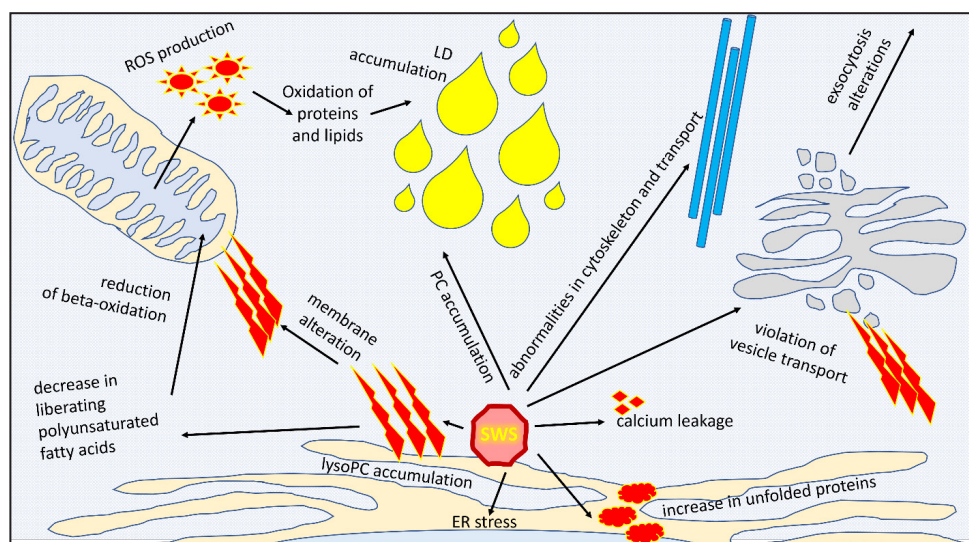
Molecular and Radiation Biophysics Division of NRC "Kurchatov Institute" – PNPI

The fruit fly *Drosophila melanogaster* is widely used as a model for studying genetical bases and physiological mechanisms of development of various neuropathologies.

In our work carried out in MRBD of NRC "Kurchatov Institute" – PNPI we created a model that recapitulates the cause of development of the neurodegenerative syndromes induced by human NTE/PNPLA6 protein dysfunction. By the means of suppression of swiss cheese expression in the neurons of *Drosophila melanogaster* imago, we induced neurodegeneration in the brain of individuals. It caused a decline of their life expectancy, as well as a decrease of the locomotor activity and memory alteration. At the same time, the level of reactive oxygen species increased in the brain,

lipid droplets accumulated, and the signal intensity of fluorescently labelled mitochondria decreased, even though the mitochondria morphology was similar to the control. In contrast, the number of fragmented round mitochondria increased in wing long axons, which could be attributed to unfunctional ones according to literature data.

These results suggest that oxidative stress develops, and lipid metabolism alters in response to neuronal dysfunction of SWS/NTE/PNPLA6. We assume that the pathological process affects mitochondria, lipid droplets and endoplasmic reticulum in several neurodegeneration diseases, such as hereditary spastic paraplegia. The swiss cheese and its orthologues, including NTE/PNPLA6, are important regulators of this process (Fig.).



Schematic representation of pathological processes that develop in the cell upon dysfunction of SWS/NTE/PNPLA6 in neurons. Endoplasmic reticulum (ER), mitochondrion, Golgi apparatus, lipid droplets (LD), microtubules, reactive oxygen species (ROS) are shown

Multifaceted mechanism of amicoumacin A inhibition of bacterial translation

E.M. Maksimova, D.S. Vinogradova, P.S. Kasatsky, A.V. Paleskava, A.L. Konevega
Molecular and Radiation Biophysics Division of NRC "Kurchatov Institute" – PNPI

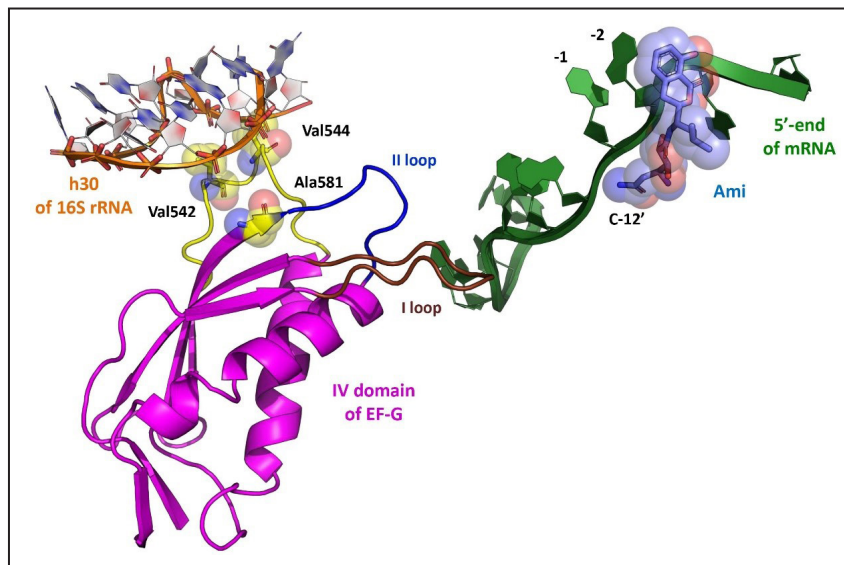
Spread of antibiotic resistance in bacteria is one of the most urgent issues in medicine, since well-known and long used antibiotics are losing their efficacy over time. One of the ways to overcome this problem is thorough study of antibacterials and the resistance mechanisms to them.

In this work, we performed a kinetic and thermodynamic investigation of amicoumacin A (Ami) influence on the main steps of polypeptide synthesis.

Ami halts bacterial growth by inhibiting the ribosome during translation. Ami binds in the vicinity of the E-site codon and stabilizes mRNA, which is relatively unusual and implies a unique way of translation inhibition. We show that Ami reduces the rate of the functional canonical 70S initiation complex formation by 30-fold. Additionally, our results indicate that Ami promotes the formation of erroneous 30S initiation complexes; however, IF3

prevents them from progressing towards translation initiation. During early elongation steps, Ami does not compromise EF-Tu-dependent A-site binding or peptide bond formation. On the other hand, Ami reduces the rate of peptidyl-tRNA movement from the A to the P site and significantly decreases the amount of the ribosomes capable of polypeptide synthesis.

Our data indicate that Ami progressively decreases the activity of translating ribosomes that may appear to be the main inhibitory mechanism of Ami. Indeed, the use of EF-G mutants that confer resistance to Ami (G542V, G581A or ins544V) leads to a complete restoration of the ribosome functionality. It is possible that the changes in translocation induced by EF-G mutants compensate for the activity loss caused by Ami.



The model of amicoumacin A (Ami) arrangement at the E site of the ribosome complex. The model presents Ami interaction (light blue) with the 5'-end of mRNA (green) and the implied interaction of the 16S rRNA (orange) with EF-G (magenta) amino acids (yellow), providing resistance to Ami. The EF-G conserved loops I and II are shown in brown and blue, respectively. The P-site tRNA is shown in light gray (PDB: 4V7D, 4V5F, 4W2F, 4V90)

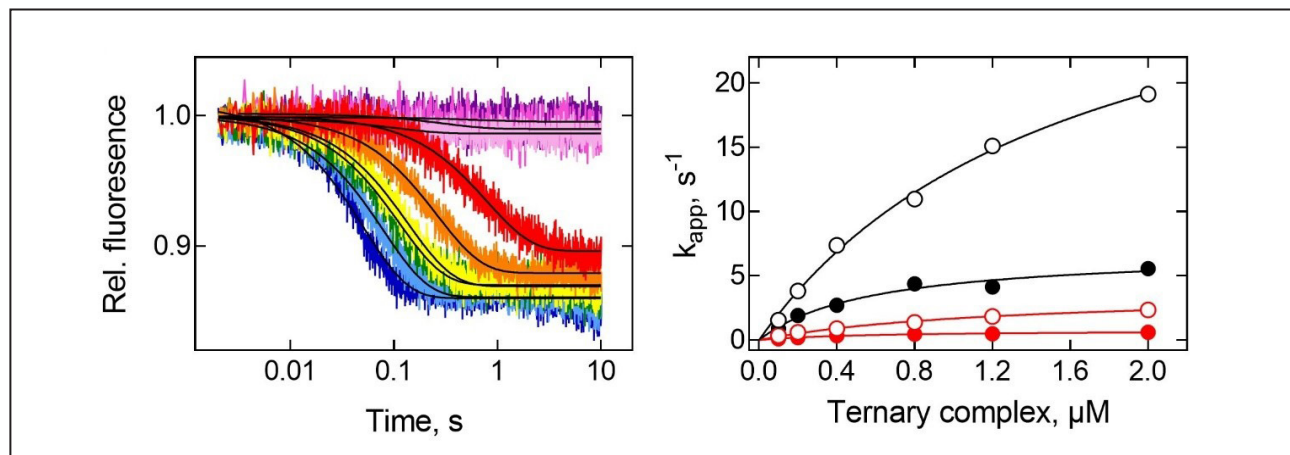
Differential contribution of protein factors and 70S ribosome to elongation

A.V. Paleskava, E.M. Maksimova, D.S. Vinogradova, P.S. Kasatsky, S.V. Kirillov, A.L. Konevega
Molecular and Radiation Biophysics Division of NRC “Kurchatov Institute” – PNPI

The growth of the polypeptide chain occurs due to fast and coordinated work of the ribosome and protein elongation factors EF-Tu and EF-G. However, the exact contribution of each of these components in overall balance of translation velocity remains not fully understood.

In our work, we created an *in vitro* translation system consisting of the elements of *Escherichia coli* with a single replacement of either of elongation factors with heterologous protein from thermophilic microorganism *Thermus thermophilus*. The rates of the A-site binding and decoding reactions decreased by an order of magnitude in the presence

of thermophilic EF-Tu, indicating that the kinetics of aminoacyl-tRNA delivery is determined by the properties of the elongation factor (Fig). At the same time, thermophilic EF-G had neither influenced the kinetic parameters of factor-dependent translocation, nor changed the effects of translocation inhibitors (spectinomycin, hygromycin B, viomycin and streptomycin) thus suggesting that the process of translocation to a large extent is determined by the interaction of the tRNAs and the ribosome and can be efficiently catalyzed by thermophilic EF-G even at suboptimal temperatures.



A-site binding kinetics. On the left – fluorescence time courses of ribosomal complex (0.05 μM) interaction with increasing amount of ternary complex (0.1 μM, red; 0.2 μM, orange; 0.4 μM, yellow; 0.8 μM, green; 1.2 μM, blue; 2 μM, dark blue), containing EF-Tu from *E. coli* at 37 °C. The reaction in the presence of inhibitors of A-site binding kirromycin (150 μM, light pink), tetracycline (30 μM, pink) or with buffer (violet). On the right – concentration dependences of apparent rate constants (k_{app}) on ternary complex (0.1–2 μM). k_{app} values were estimated by the single-exponential fitting of time courses as in left panel for A-site reactions rates with EF-Tu from *E. coli* at 20 °C (black circles), at 37 °C (black open circles), EF-Tu from *T. thermophilus* at 20 °C (filled red circles) or at 37 °C (red open circles)

Targeting evolution of antibiotic resistance by SOS response inhibition

A.P. Yakimov, I.V. Bakhlanova, D.M. Baitin

Molecular and Radiation Biophysics Division of NRC “Kurchatov Institute” – PNPI

The evolution of bacterial resistance is driven by genetic variation with the subsequent selection of resistant variants. Bacteria have developed a complex regulating evolutionary adaptation by acquiring resistance genes through horizontal gene transfer. In the absence of the above-mentioned defense mechanisms, bacterial cells can develop antibiotic resistance by activating the mechanisms of the cellular SOS response and related induced mutagenesis.

The strategy might be expanded to the search for more universal targets into other critical proteins from bacterial metabolism. For examples, the small molecules inhibiting the SSB, RecBCD, LexA, PolV, RecA proteins that regulate replication and recombination have been discovered recently. However, in our opinion, the approach to inhibiting most proteins is not optimal by itself for a number of reasons. Depending on the strain, the significance of modulatory effects of such proteins can vary, and therefore the extent of usefulness of such multitarget inhibitors always remains rather uncertain.

The RecA protein is involved in chromosomal transformation, conjugation, and is also known

as an inducer of the bacterial SOS response, and therefore RecA is an ideal target in the search for compounds able to block these processes. The structure and functions of the RecA protein are highly conservative among bacteria, including pathogenic ones.

Recently, many attempts have been made to search for RecA protein inhibitors. Within the first category, natural or synthetically synthesized compounds are searched or screened for the desired inhibition activity of the RecA protein. Unfortunately, all of these compounds have lower specificity and may have potentially high toxicity with a wide range of side effects. The second group of strategies implies generating peptides that represent functional fragments of the intermolecular interface. Due to their higher specificity combined with lower toxicity and fewer side effects, small peptides or proteins appear to be better candidates than low-molecular-weight organic compounds.

The implementation of the second strategy, according to the authors, holds the greatest promise.

Antibacterial properties of fucoidans from the brown algae *Fucus vesiculosus* of the Barents Sea

O.N. Ayrapetyan¹, E.V. Zhurishkina¹, D.V. Lebedev¹, A.A. Kulminskaya¹, I.M. Lapina¹, E.D. Obluchinskaya², Yu.A. Skorik³

¹ Molecular and Radiation Biophysics Division of NRC "Kurchatov Institute" – PNPI

² Murmansk Marine Biological Institute of RAS

³ Institute of Macromolecular Compounds of RAS

Fucoidans, sulfated polysaccharides from the cell walls of brown algae, which have a wide spectrum of biological activity, are seen as a promising antimicrobial component that could, where possible, replace the use of the strong chemical antiseptics and antibiotics. Natural fucoidans are polydisperse compounds, the composition of which can vary greatly depending on the species, habitat of algae, as well as methods for isolating and purifying polysaccharides.

The purpose of the work was to investigate the antibacterial properties of two fractions of sulfated polysaccharides of various degrees of purification from the brown algae *Fucus vesiculosus* against *Escherichia coli*, *Bacillus licheniformis*, *Staphylococcus epidermidis*, *Staphylococcus aureus*.

Fucoidans appear to have a bacteriostatic effect on the growth of all tested microorganisms, the minimum inhibitory concentration (MIC) varied from 4 to 6 mg/ml, while *E. coli* showed the highest sensitivity to both fractions of polysaccharides, while in general, the coarse fraction of fucoidans showed a greater inhibitory microbial activity compared to the purified one (Fig. 1).

Analysis of morphological changes in bacteria after treatment with fucoidans at MIC values for 24 h using atomic force microscopy (AFM) showed that the integrity of all bacterial cells was preserved, which correlates with the identified bacteriostatic rather than bactericidal properties of the studied polysaccharides. In gram-positive bacteria, a significant decrease in size was observed, accompanied by some increase in surface roughness (Fig. 2), which could indicate a change in the properties of the cell wall due to the influence of fucoidans on bacterial metabolism or the binding of fucoidan to the cell surface. However, despite the pronounced

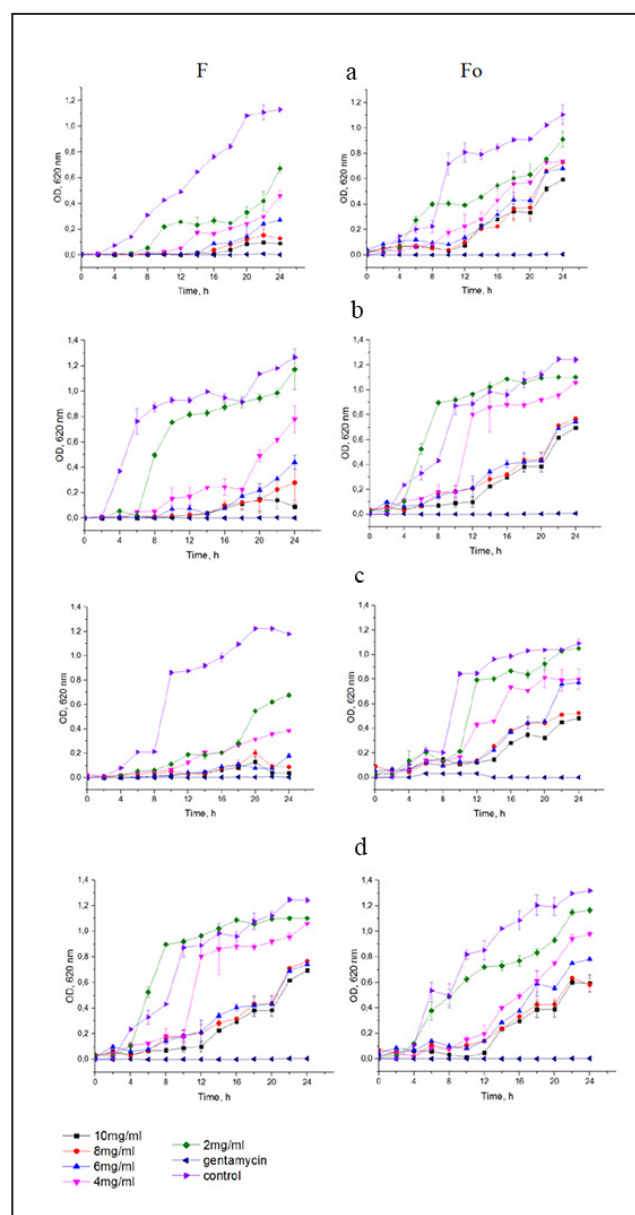


Fig. 1. Growth curves of bacteria treated with fucoidans F and Fo for 24 h (F – coarse fraction, Fo – purified fraction): a – *E. coli*; b – *B. licheniformis*; c – *S. aureus*; d – *S. epidermidis*. Each value is the mean \pm SD of three replicates

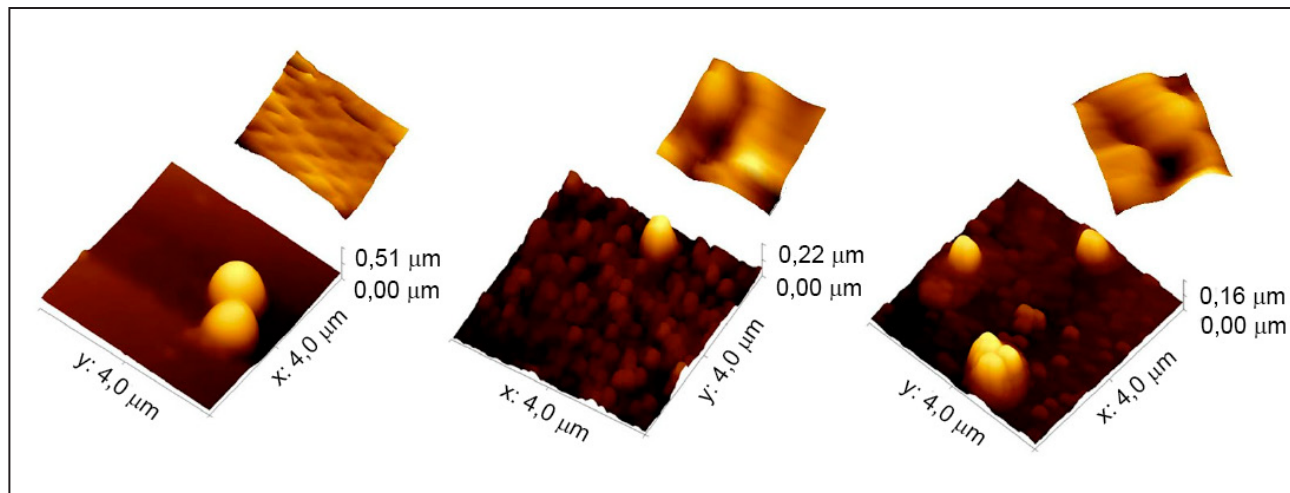


Fig. 2. AFM images of *S. epidermidis* treated with fucoidan F and Fo for 24 h: *left* – control; *middle* – treated with fucoidan F; *right* – treated with fucoidan Fo. Inserts show the surface topograms in $0.5 \times 0.5 \mu\text{m}$ field

bacteriostatic effect of fucoidans against *E. coli*, no morphological changes were observed in these bacteria, possibly due to the presence of an outer membrane. Therefore, it appears that the changes in cell morphology observed in gram-positive bacteria are a consequence of bacterial adaptation

rather than a mechanism of growth inhibition by fucoidans. We observed a significant decrease in the size of *S. aureus* and *S. epidermidis* when treated with sulfated polysaccharides. For rod-shaped bacteria, none of the fucoidans had a significant effect on cell size.

Long-term monitoring of the development and extinction of IgA and IgG responses to SARS-CoV-2 infection

A.V. Ivanov¹, E.V. Semenova²

¹ Saint Petersburg University's Pirogov Clinic of High Medical Technologies

² Molecular and Radiation Biophysics Division of NRC "Kurchatov Institute" – PNPI

Humoral immunity plays a key protective role against pathogens. It limits infection and prevents future reinfection. Studying the humoral link of COVID-19 immunology, which forms a protective pool of specific antibodies, determining the severity and duration of such immune protection after contact with SARS-CoV-2 and when evaluating the effectiveness of antiviral vaccines, epidemiological monitoring and tracking the population immunity formation stages are the most important areas in the fight against the pandemic.

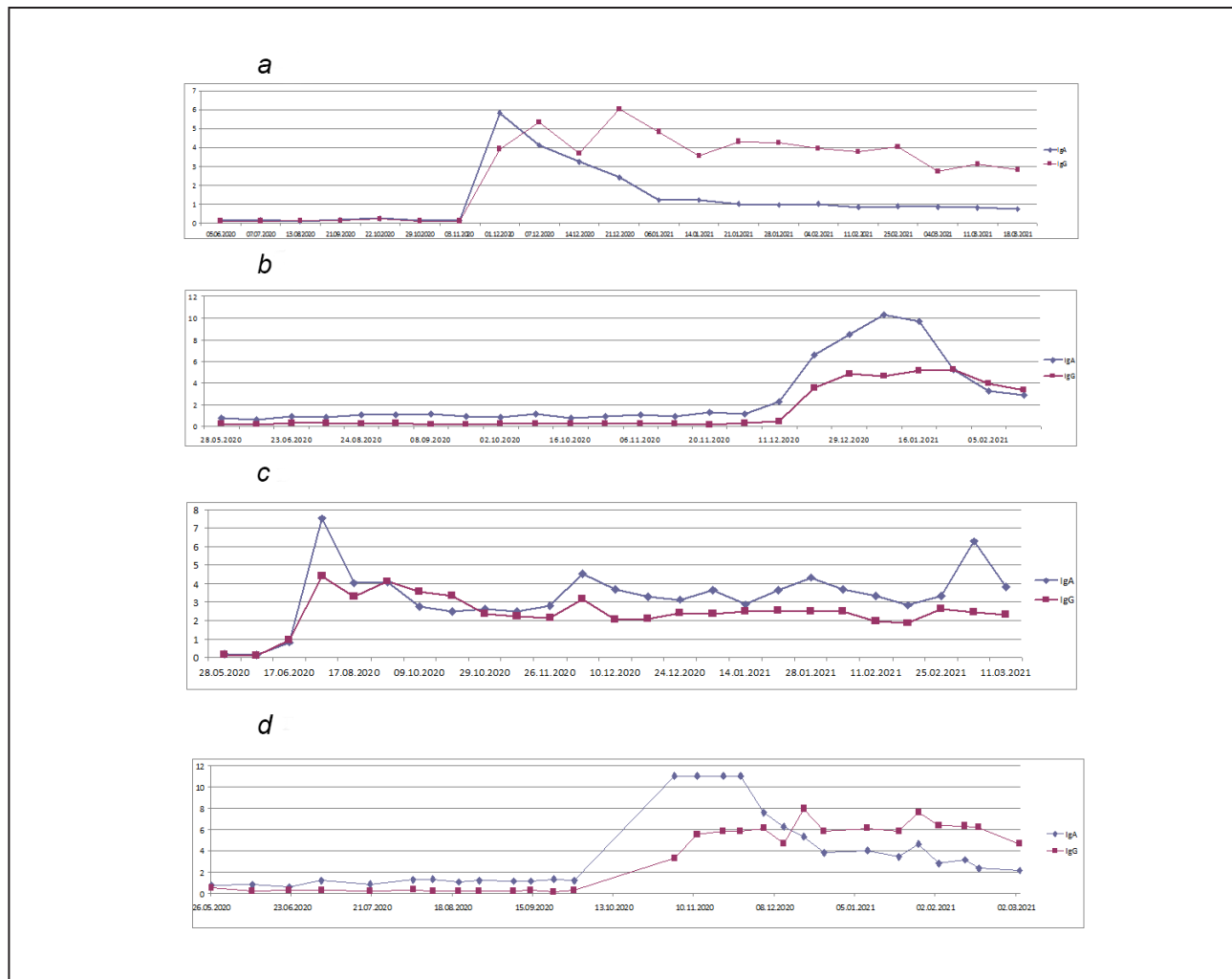
The aim of the project was a 9-month monitoring of the development and decline of the humoral immune response to SARS-CoV-2 infection with a quantitative assessment of anti-SARS-CoV-2 immunoglobulin levels in the blood of healthy donors living during a coronavirus pandemic and patients who have had COVID-19. The studies were carried out in the Saint Petersburg University's Pirogov Clinic of High Medical Technologies. The project involved 180 people: 84 men and 96 women. At intervals of 10–14 days the test data for SARS-CoV-2 infection by RT-PCR were recorded and the levels of specific IgA and IgG were determined using the enzyme-linked immunosorbent assay (ELISA). The recombinant S1 domain of the SARS-CoV-2 spike glycoprotein was used as an antigen. During the observation period the total number of tests (PCR + ELISA) per person reached 27–30.

COVID-19 was diagnosed in 51 people (26 men and 25 women). All these people have developed a stable humoral immune response against SARS-CoV-2 which lasts at least six months, *i.e.* naturally infected patients have the ability to fight reinfection for quite a long time.

The individual immune status had a number of features. Figure shows the most typical examples of changes in the plasma levels of anti-SARS-CoV-2 IgA and IgG in some project participants who were diagnosed (RT-PCR) with COVID-19 at different times. In a significant cohort of project participants with COVID-19 (39%) IgA appeared first and increased at an earlier stage reaching significant levels as early as two weeks after the disease onset. In this group IgA response was stronger and more stable than in the case of IgG. IgA concentrations peak were observed approximately one month after the COVID-19 diagnosis. Subsequently, plasma IgA remained at a fairly high level for a long time (ratio ~ 3). In a third of patients who recovered from COVID-19 the IgA level exceeded the IgG level. Thus, the behavior of IgA differs significantly from that of coronaviruses of previous generations. The dynamics of anti-SARS-CoV-2 IgG corresponds to the concept of "classical" humoral immunity for viral infection.

A rather large group of people (more than 15%) attracts more attention. In this cohort elevated levels of plasma anti-SARS-CoV-2 IgA (ratio from 0.8 to 2.4) were recorded throughout the entire observation period. In addition, the mean anti-SARS-CoV-2 IgA level gradually increased (ratio 0.8–1.2) in this group over time. It is possible that SARS-CoV-2-specific IgA play an independent role in providing protective immunity at low viral loads. However, an elevated IgA level is not an absolute protection against COVID-19 disease. One of this group patient was diagnosed with COVID-19 after four months of observation.

Further studies are needed on the function of virus-specific anti-SARS-CoV-2 antibodies and their protective efficacy over time.



Characteristic examples of changes over time in anti-SARS-CoV-2 IgA and IgG levels in plasma of project participants diagnosed with COVID-19: a – relatively “classical” variant of humoral immune response to a viral disease (IgA dropped to normal values; IgG gradually decreased); b – characteristic example of dynamics of IgA and IgG levels (after disease the concentration of immunoglobulins A and G in plasma decreased, but remained at rather high levels (ratio ~ 3)); c – example of long-term preservation of relatively high antibody levels after the disease; d – example of disease on the background of elevated IgA (changes in IgA and IgG levels in the only representative of the group of people with initially elevated IgA levels, who was diagnosed with COVID-19 in October 2020 was diagnosed with COVID-19). Abscissa axis – dates of analyses; ordinate axis – immunoglobulins ratio. Blue symbols are IgA; red symbols are IgG

1. Ivanov A.V., Semenova E.V. // J. Med. Virol. 2021. V. 93. P. 5953.

2. Fedorova N.D., Ivanov A.V., Semenova E.V. et al. // Russ. J. Biol. Phys. Chem. 2021. V. 6. P. 115.

3. Ivanov A.V., Semenova E.V. // Proc. X Int. Scientific-Practice Conf. “Molecular Diagnostics”. 2021. V. 2. P. 384.

Delivery of functional exogenous proteins by plant vesicles into human cells *in vitro*

L.A. Garaeva¹, R.A. Kamyshinsky², Yu.V. Kil¹, E.Yu. Varfolomeeva¹, N.A. Verlov¹, E.S. Komarova³, Yu.S. Garmay¹, S.B. Landa¹, V.S. Burdakov¹, A.G. Myasnikov¹, I.A. Vinnikov⁴, B.A. Margulis³, I.V. Guzhova³, A.M. Kagansky⁵, A.L. Konevega¹, T.A. Shtam¹

¹ Molecular and Radiation Biophysics Division of NRC “Kurchatov Institute” – PNPI

² NRC “Kurchatov Institute”

³ Institute of Cytology of RAS

⁴ Shanghai Jiao Tong University, China

⁵ Far Eastern Federal University

Extracellular vesicles (EVs), in particular exosomes, are nanovesicles surrounded by a lipid bilayer and secreted by many cells. Today, since EVs are natural particles capable of carrying large amounts of nucleic acids and proteins while maintaining their stability, the development of therapeutic biomolecule delivery systems based on EVs is of great interest to the scientific community.

Nevertheless, a number of ethical and production limitations stand in the way of using EVs derived from biological fluids as therapeutic agent delivery systems. Therefore, plant-derived EVs (PEVs) are more promising for such tasks. PEVs are believed to be biocompatible, biodegradable, and can be produced in significant quantities.

The aim of this study was to evaluate the efficiency of delivery of exogenous functional proteins by plant vesicles to human cells *in vitro*.

In the present work, PEVs from grapefruit juice were isolated by ultracentrifugation and then characterized for size, concentration and morphology using nanoparticle trajectory analysis, dynamic light scattering, atomic force microscopy and cryo-electron microscopy, which provided high-quality images of grapefruit membrane vesicles.

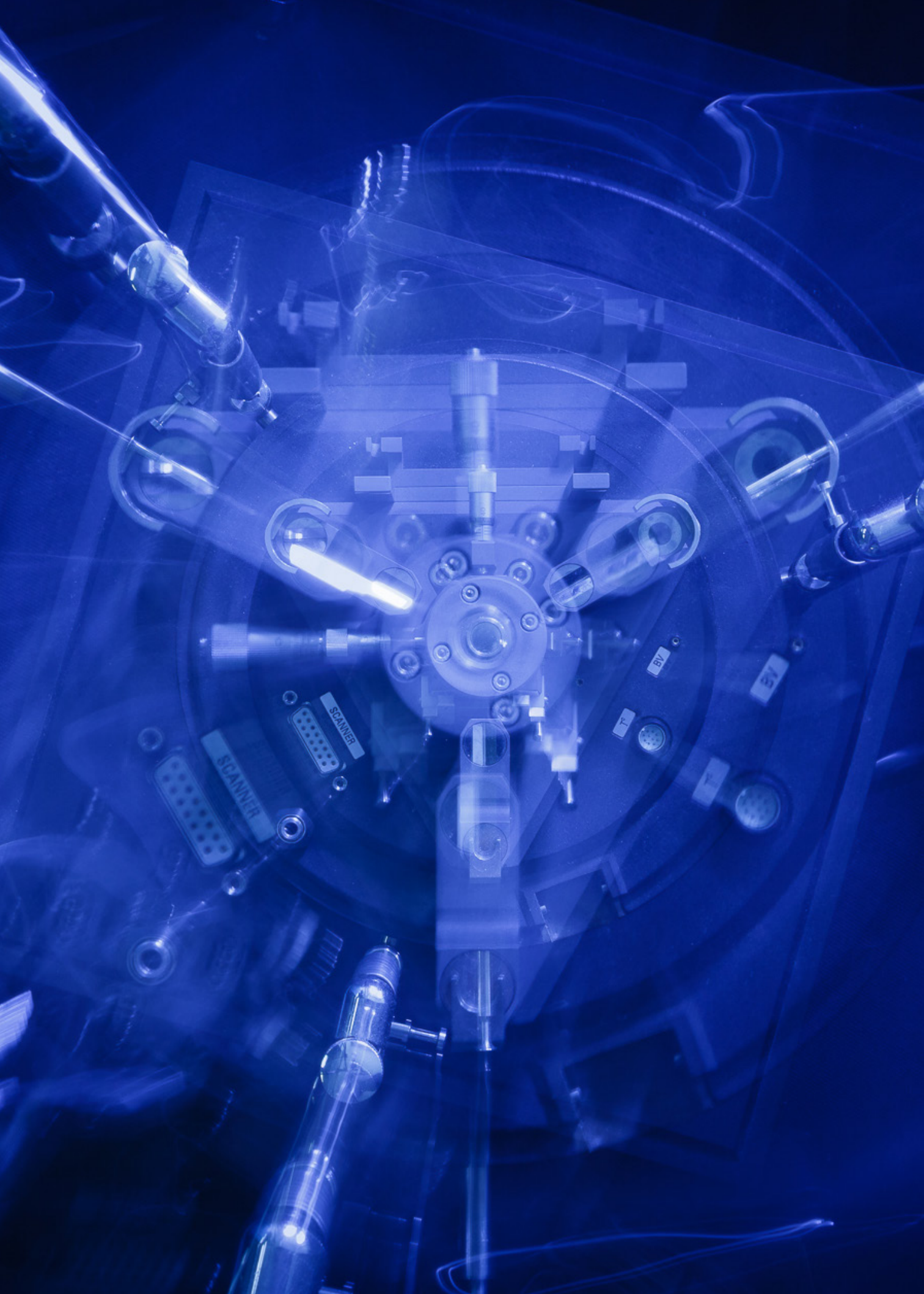
Most of the vesicles had a spherical shape formed by a lipid bilayer.

Using *in vitro* cell culture models, it was shown that grapefruit extracellular vesicles (GF-EVs) are highly efficient for delivery of exogenous bovine serum albumin (BSA) and heat shock protein (HSP70) labeled Alexa flour 647 into human colorectal adenocarcinoma cells HCT-116 and DLD1. In addition, the functional activity of the proteins delivered into human cell lines using plant vesicles *in vitro* was confirmed.

The work also assessed the distribution in tissues of GF-EVs loaded with BSA labeled with radioactive ¹²⁵I (¹²⁵I-BSA) *in vivo*. Biodistribution was quantified using *ex vivo* γ -counting. Radioactivity was observed in the lung, bladder, uterus and ovaries, liver, spleen, kidney, heart, and brain samples. It was demonstrated that ¹²⁵I-BSA loaded in GF-EVs is more efficiently distributed through the bloodstream and accumulates in various body tissues.

The results of this study prove the possibility of using native PEVs in therapeutic agent delivery systems.

The study was supported financially by the RSF within the framework of grant No. 19-74-20146.



Nuclear Medicine (Isotope Production, Beam Therapy, Bio- and Nanotechnologies for Medical Purposes)

- 88** Development and optimization calculation of proton beam paths in the nuclear medicine project of NRC “Kurchatov Institute” – PNPI

Development and optimization calculation of proton beam paths in the nuclear medicine project of NRC “Kurchatov Institute” – PNPI

D.A. Amerkanov, S.A. Artamonov, E.M. Ivanov, V.I. Maximov, G.A. Riabov, V.A. Tonkikh
Advanced Development Division of NRC “Kurchatov Institute” – PNPI

NRC “Kurchatov Institute” – PNPI is developing a project for a nuclear medicine facility based on the C-80 isochronous cyclotron, which accelerates negative hydrogen ions. It is envisaged that a new building will be designed, where the C-80 will be relocated and stations for the development of new methods for radionuclide and radiopharmaceutical production will be created (stage “Isotope” – “A” to the right of the cyclotron in Fig. 1). It is also proposed to create a proton therapy facility for the treatment of ocular diseases (stage “Oko” – “B” on the left in Fig. 1). For these purposes, the extraction system of the C-80 cyclotron needs to be modernized in order to develop and implement the simultaneous extraction of two beams. One beam with an intensity of $\sim 100 \mu\text{A}$ and an energy of 40–80 MeV will be used for the production of isotopes, the second – for ophthalmology with an energy of $\sim 70 \text{ MeV}$ and an intensity of up to $10 \mu\text{A}$.

Figure 2 shows the calculated optimized beam transport line and its envelopes to the “Isotope”

target stations. Similar data are shown in Figure 3 for “Oko”.

The optimization of particle transport lines was carried out using the Proton_MC program created at the NRC “Kurchatov Institute” – PNPI, which performs the calculation and optimization by the Monte Carlo method. The optimal parameters of the magnetic elements of the beam for the “Isotope” stage were found under conditions of minimal particle losses in the transport path, and that the beam size on the target was at least 20 mm (for the beam to have a maximum intensity). In Figure 4, in order to illustrate the quality of the “Isotope” beam, its cross-section is shown for the most distant direction T4.

The “Oko” proton beam line satisfies special requirements: beam energy 60–70 MeV; beam diameter at the entrance to the treatment room $\sim 60 \text{ mm}$; beam homogeneity in this region is not less than 90%; beam divergence angle $\sim 1 \text{ mrad}$.

To form a beam that satisfies the requirements of the “Oko” stage, a beam line was constructed

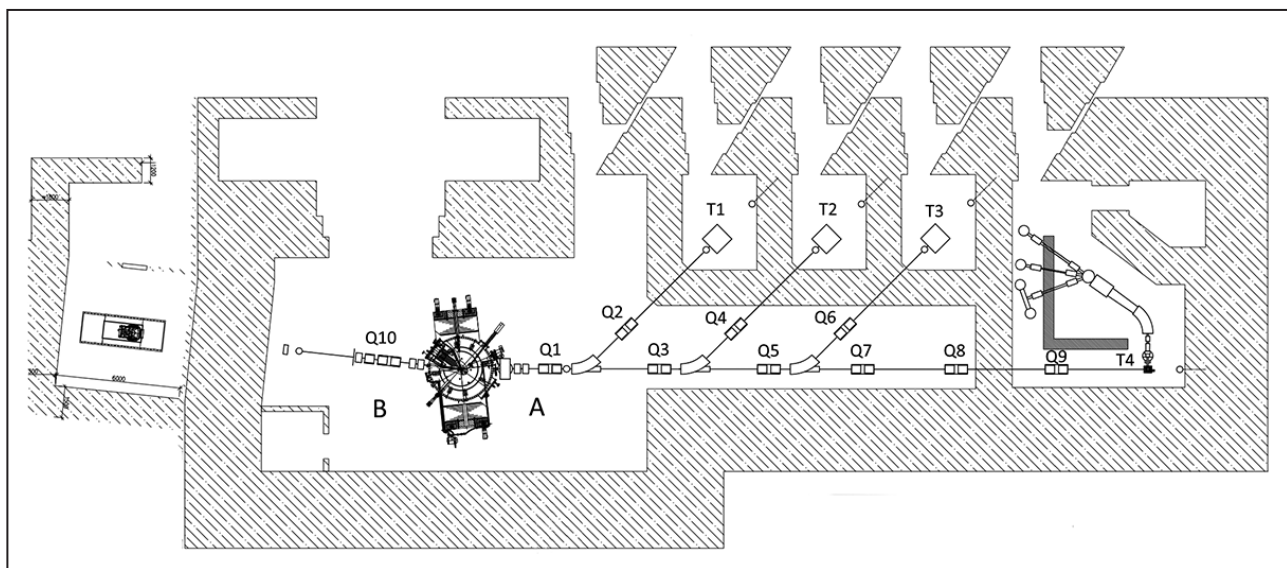


Fig. 1. Nuclear medicine project: A – “Isotope” lines; B – “Oko” line; Q1–Q9 – doublets of magnetic lenses; Q10 – triplet of magnetic lenses; T1–T4 – target stations

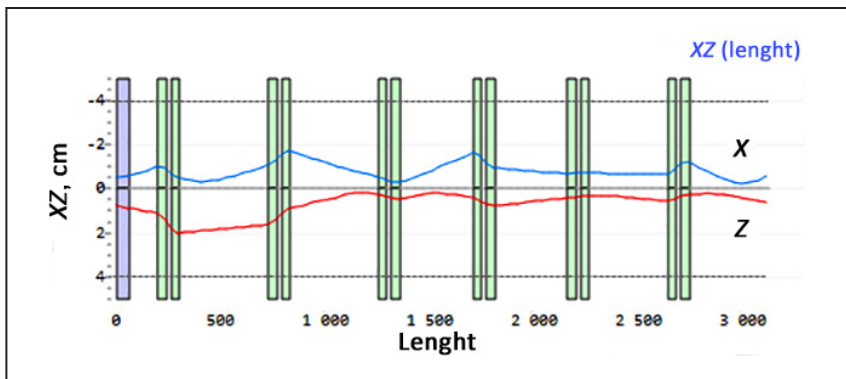


Fig. 2. Beam envelopes for T4 station (as an example): X – horizontal plane; Z – vertical plane

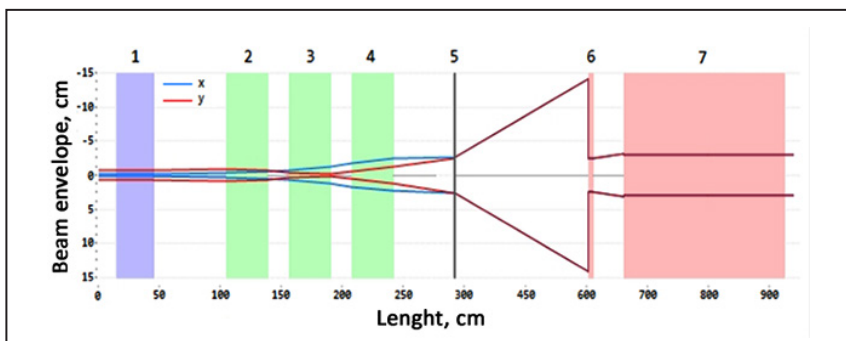


Fig. 3. Scheme of the line for ophthalmology and beam envelopes for the “Oko” line: 1 – corrector magnet; 2–4 – triplet lenses; 5 – beam diffuser (tantalum foil); 6 – collimator; 7 – protective wall in front of the treatment room

with a passive scatterer made of tantalum (Ta) foil 300 μm thick.

The proton beam $E = 70$ MeV extracted from the accelerator is transported to Ta foil, on which a triplet of lenses forms a beam size with a diameter ~ 30 mm. Optimization of the proton beam transport line in this section was also performed using the Proton_MC program. The results of the passage of protons through a Ta foil 300 μm thick ob-

tained using the GEANT4 program were the initial conditions of the Proton_MC program for further transport of a diverging proton beam in free space ~ 3.7 m.

A collimator with an optimal beam length of 100 mm and a diameter of 50 mm installed in front of the protective wall finally forms the beam with the given conditions.

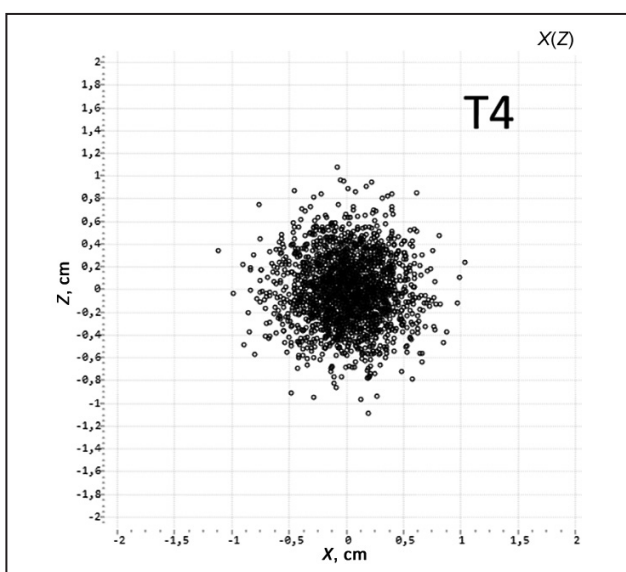


Fig. 4. Beam size on a T4 target



Nuclear Reactor and Accelerator Physics

- 92 Algorithm for calculation and optimization of high energy proton beam lines by Monte Carlo method
- 93 Focusing properties of the magnetic structure of isochronous cyclotrons with high spiraling angle of pole tips
- 95 Experimental facility for the study of isotope exchange on the hydrophobic platinum catalyst

Algorithm for calculation and optimization of high energy proton beam lines by Monte Carlo method

D.A. Amerkanov, E.M. Ivanov, G.A. Riabov, V.A. Tonkikh
 Advanced Development Division of NRC "Kurchatov Institute" – PNPI

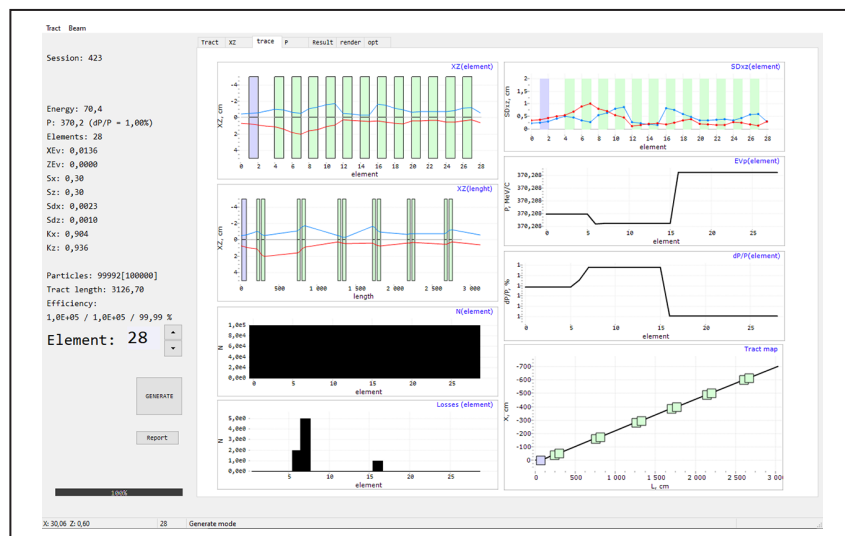
The calculation of the beam paths consists of calculating proton beam trajectories along the transport channel from the source to the target in order to determine the beam output parameters. The Proton_MC algorithm was developed to perform such calculations using the Monte Carlo method.

The proton beam is introduced as a multidimensional Gaussian distribution in the phase space x , x' , z , z' , $\Delta p/p$, which determines the set of initial conditions for the particle at the channel entrance. The transport channel consists of separate elements: quadrupole lenses, various magnets, free gaps. In a linear approximation, the relationship between the input and output coordinates and velocities in the channel element can be obtained using the transition matrix, and for each element the matrix has an individual structure. The particle trajectory along the channel is calculated by successive application of the transition matrices through its individual sections. At the output of each element, the x and z coordinates are compared with

apertures. If the particle goes beyond the aperture, then it stops its motion along the channel and leaves the beam. As a result of repeated repetition of such a procedure, a set of particles is obtained at the output of each element, which makes it possible to track all the main parameters of the beam.

If the absorber is installed in the transport channel, the beam parameters after the absorber are calculated using GEANT4. The GEANT4 output file can be used as input for Proton_MC. The algorithm makes it possible to calculate any beam parameters: intensity, spatial or phase density, energy distribution, etc. Proton_MC includes a beam parameter optimization block, which is a random search method with corrections based on the analysis of intermediate results to obtain the global maximum of a function of many variables.

The algorithm was tested in calculations of the beam transport paths for the C-80 cyclotron. The interface of the Proton_MC program is shown in the Figure.



Proton_MC program interface

Focusing properties of the magnetic structure of isochronous cyclotrons with high spiraling angle of pole tips

D.A. Amerkanov, S.A. Artamonov, E.M. Ivanov, G.A. Riabov, V.A. Tonkikh
 Advanced Development Division of NRC “Kurchatov Institute” – PNPI

Magnetic structures with a large spirality angle of the pole tips are typically used in superconducting isochronous cyclotrons as well as in “warm” cyclotrons accelerating H⁻-ions. The features of such structures were studied in a number of works, both before and after the appearance of reliable programs that allow sufficiently accurate calculation of three-dimensional magnetic fields. In connection with the creation of an isochronous H⁻-cyclotron with a proton energy of 40–80 MeV at NRC “Kurchatov Institute” – PNPI, such studies were continued both in the extended 2D approximation and in the framework of modern 3D calculations.

It is well known that the frequencies of vertical oscillations, which determine the focusing along the vertical axis for each radius r of the working area, can be expressed in a cylindrical coordinate system using the approximate formula:

$$\nu_z^2 \approx -k + F \cdot S(r, \gamma); \quad S(r, \gamma) = 1 + 2\tan^2\gamma, \quad (1)$$

where k is the rate index of average magnetic field growth along the radius $\langle B(r) \rangle$,

$$k = \frac{r}{\langle B \rangle} \frac{d \langle B \rangle}{dr} \approx \frac{2W}{E_0}.$$

Here W is the kinetic energy; $E_0 = 938.28$ MeV is the rest mass of the proton; γ is geometric spirality (GS) of the magnetic field (the angle between the radius vector and the tangent to the sector for a given value of r).

In this case, the azimuthal variation of the magnetic field is determined by the flutter $F(r)$:

$$F(r) = \langle (B - \langle B \rangle)^2 \rangle / \langle B \rangle^2, \quad \langle \dots \rangle = (2\pi)^{-1} \int_0^{2\pi} \dots d\theta.$$

Thus, based on expression (1), when designing new magnetic structures, it is necessary to strive for an increase in both the flutter F and the factor $S(r, \gamma)$ in the working region of the cyclotron, so that their product is greater than k .

It is known that for straight sectors, the flutter F is maximum, and $S(r, \gamma) = 1$, i.e., $\gamma = 0$. However, often, based on the available possibilities and other considerations (for example, the parameters of an existing magnet have already been determined and cannot be changed without alteration), one has to look for some compromise version of the magnetic structure. In particular, if it is not possible to achieve the necessary vertical focusing of particles in the designed accelerator with some parameters of the system already given, only due to the magnetic field flutter (field drop from the valley to the sector), then to increase it, edge focusing is also involved, which occurs in such structures due to the introduction of curved side surfaces of the sectors (large geometric spirality angle γ).

This situation, first, is typical for superconducting cyclotrons, since in a strong magnetic field of superconducting windings, the ferromagnetic sectors reach saturation and cannot provide the necessary focusing only due to the field drop from hill to valley. Second, a similar situation arises for isochronous cyclotrons accelerating negative hydrogen ions. Here, the maximum field in the accelerator hill is often deliberately limited (i.e., the flutter is reduced) in order to reduce the loss of H⁻-ions due to their electric dissociation. Thus, the introduction of large spirality with $S(r, \gamma) = 1$ into the structure makes it possible to provide the necessary focusing.

In this work, we have proposed an approach for the analysis of any projected magnetic structure with a large spirality angle of the cyclotron pole tips, based on approximate 2D and precise 3D calculations.

Part of the results of the work was obtained in the 2D approximation. For this purpose, the method of filling factors was developed, which makes it possible to select the gaps in the hill and valley of any designed magnetic structure. The introduction

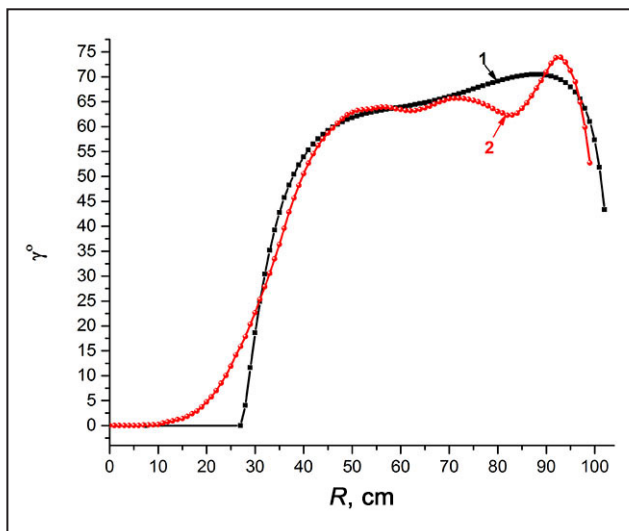
of a dimensionless parameter $x = r/N/g_h$ (r – current radius; N – number periodicity elements; g_h – gap in the hill) within the framework of the proposed approach makes it possible to investigate the possible flutter behavior with respect to the cyclotron radius and to reasonably agree on a reasonable choice of the geometric spirality γ with other cyclotron parameters. Here it is appropriate to note that the calculation of flutter in the form of an analytical dependence is a complex problem in both 2D and 3D approximations, and therefore approximate methods were used everywhere.

3D calculations made it possible to refine, modify, and find the optimal parameters of the magnetic structure chosen in the framework of the 2D approximation. It was found that an important role in such structures is played by the so called magnetic spirality γ_{MS} (MS), which is defined as $\text{tg}\gamma_{MS} = r \cdot d\Phi_N/dr$, where Φ_N is the phase of the fundamental harmonic in the expansion of the cyclotron magnetic field in the Fourier series.

It should be emphasized that in the 3D approach for the C-80, two new important effects were found

concerning the MS and GS that were previously unknown: the “penetration” effect and the “lag” effect. Their essence is reflected in Figure. It can be seen that MS leads to an undesirable change in the vertical focusing at radii less than 35 cm. Here, this is called the effect of MS “penetration” into the region of the direct sectors of the cyclotron. Therefore, it is expedient to use a structure with a large spirality angle at radii greater than 35 cm. Such a structure works well at radii exceeding the gap in the valley. Thus, the discovered effect of “penetration” easily explains the widespread use in practice in various cyclotrons of direct sectors in the central region.

On the other hand, Figure shows that at radii $\sim 75 \leq r \leq 88$ cm, there is a “lag” of the MS field from GS. Their maximum difference from each other can reach $\sim 7^\circ$, which, at a spirality of $\sim 65^\circ$, leads to a $\sim 30\%$ undesirable reduction in focusing, so the “lag” effect should be considered when designing magnetic structures for new cyclotrons, when relying, as a rule, only on the GS.



Spirality angles (in degrees) depending on the radius of the C-80 cyclotron: 1 – geometric spirality γ ; 2 – magnetic spirality γ_{MS} – derivative of the fundamental harmonic of the magnetic field, obtained in 3D calculations and measurements of the magnetic field

Experimental facility for the study of isotope exchange on the hydrophobic platinum catalyst

D.A. Kuzmin, O.A. Fedorchenko, A.A. Bryk, I.A. Alekseev

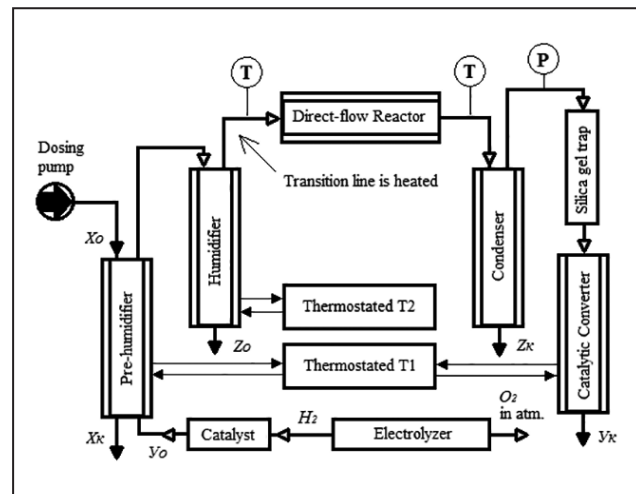
Department of Reactor Physics and Technology of NRC "Kurchatov Institute" – PNPI

Currently NRC "Kurchatov Institute" – PNPI continues the work on commissioning the tritium removal facility (TRF). It is based on the chemical isotope exchange (CIE) process, which requires the use of hydrophobic catalyst for the molecular activation of hydrogen RCTU-3SM.

The RCTU-3SM catalyst is represented by spherical granules of SDVB (styrene-divinylbenzene copolymer) with a diameter of 0.8–1 mm, on which platinum is deposited. The amount of metal in the catalyst is 0.8–1.2 wt. %.

To optimize the technological process due to the contribution of the catalytic exchange stage, an experimental setup was assembled in the laboratory for the separation of hydrogen isotopes to study the catalytic activity of catalyst samples (Fig.).

Hydrogen of natural composition from the electrolyzer enters the prehumidifier, where it is saturated with water vapor with a known concentration of deuterium and tritium at 90°C. Next, the vapor-gas mixture enters the humidifier, where the temperature is set by another thermostat in the range of 50–85°C. Thus, after the hydrogen leaves the humidifier, it is extremely saturated with water vapor at a given temperature. To prevent condensation, the path to the direct-flow reactor is heated. Further, hydrogen with water vapor enters the direct-flow reactor, heated to a temperature of 50–100°C by an electric heater, where catalytic isotope exchange takes place on the catalyst bed. Two thermocouples are installed before and after it for a more accurate temperature determination. The vapor-hydrogen mixture leaving the reactor enters a condenser cooled with tap water. Residual vapors are captured by a silica gel trap, and dry gas enters the catalytic converter, where it is oxidized in excess oxygen to water.



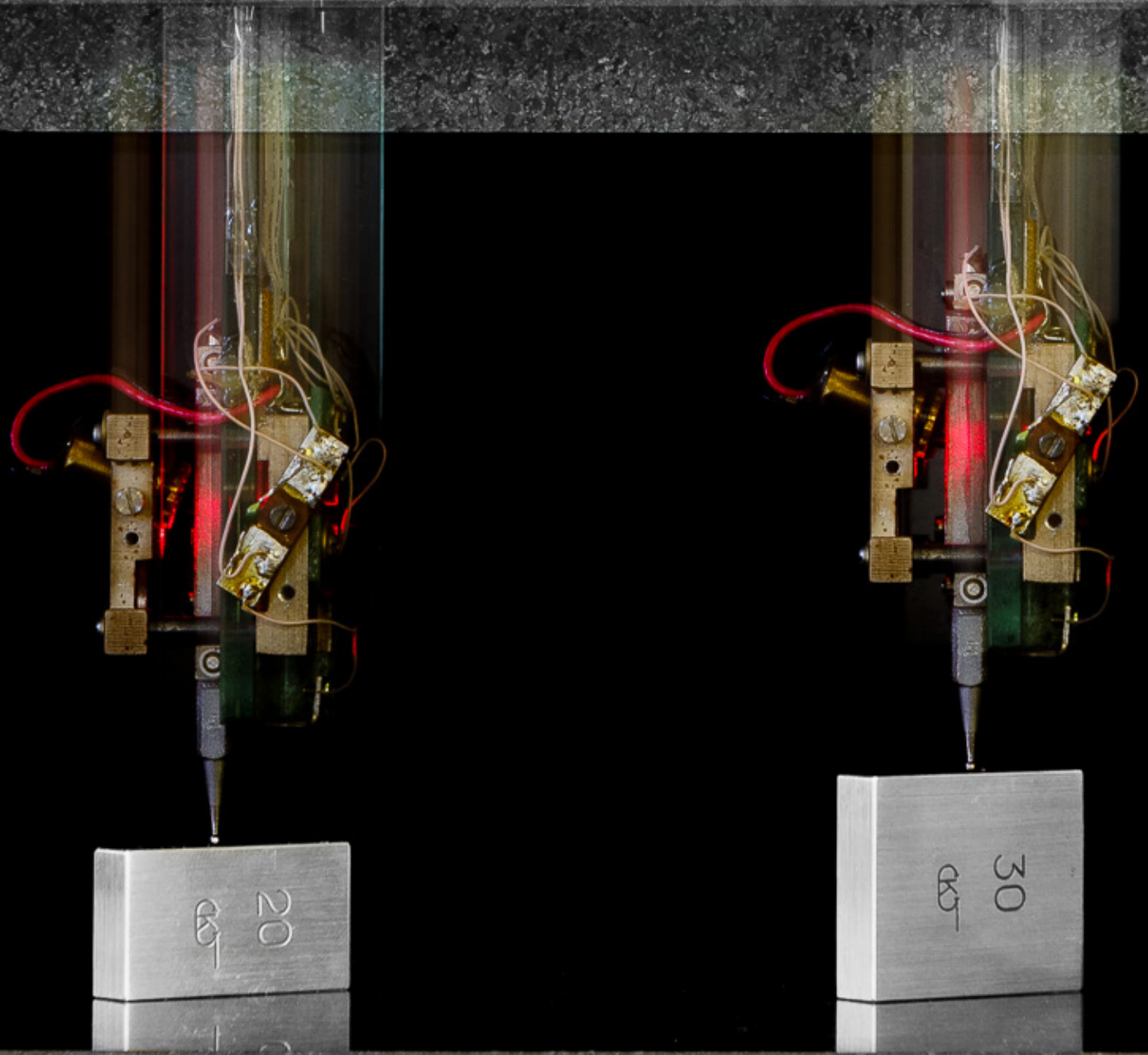
Scheme of the experimental setup for the study catalytic activity of catalyst samples

There are three sample points: humidifier, condenser, catalytic converter. Water analysis for the amount of deuterium is performed on a Nicolet iS50R FT-IR IR spectrophotometer, and tritium – on a Hidex 300 SL device.

Features of the facility are the following.

- Saturation of the gas occurs on a layer of spiral-prismatic packing, which is located in a thermostatically controlled glass tube, and not with the help of a bubbler.
- Independent regulation of temperatures in the humidifier and the direct-flow reactor.
- Variation of hydrogen consumption by adjusting the current strength in the electrolyzer.

At the moment, a large number of experiments have been carried out under different operating conditions of the catalyst. Data are being developed for mathematical modeling of the process of isotope exchange occurring in the direct-flow reactor.



Applied Research and Developments

- 98** Processing of metal-containing galvanic slurries into mixed water-soluble metal-carbon structures
- 99** Estimation of biodistribution of mesenchymal stem cells in preclinical renal tuberculosis model from non-linear magnetic response measurements
- 100** A new method of chemical enrichment of uranium with light isotopes
- 101** Structure of proton-conducting membranes according to neutron and X-ray scattering data
- 102** Investigation of radiation hardness of silicon detectors under irradiation with α -particles and fission fragments
- 103** Study of radiation erosion of multiwire proportional chambers in experiments at the Large Hadron Collider
- 104** Application of modified perlite to solve problems of technological and chemical safety of the Arctic region
- 105** Portable nanomeasurement holographic plane meter
- 106** High resolution digital holographic microscope for reflective objects
- 107** Computing infrastructure of a modern physics laboratory

Processing of metal-containing galvanic slurries into mixed water-soluble metal-carbon structures

V.P. Sedov¹, A.A. Borisenkova^{1,2}, S.V. Fomin¹, M.V. Suyasova^{1,3}, D.N. Orlova¹

¹ Advanced Development Division of NRC "Kurchatov Institute" – PNPI

² Saint Petersburg State Institute of Technology

³ Saint Petersburg University of State Fire Service of Emercom of Russia

The currently developed technologies of metal-containing galvanic sludge processing require multistage processes with the use of a great variety of reagents, including toxic ones (chemical methods), or high energy consumption (electrochemical methods). These technologies are designed for processing of the fixed-composition sludge of a certain production and cannot be applied if the chemical composition of the sludge fluctuates drastically.

In this paper, we propose a technological scheme for obtaining high yields of mixed water-soluble metal-carbon nanostructures from galvanic waste. The developed scheme of galvanic sludge processing includes consecutive operations of synthesis of mixed metal phthalocyanine pigment, pyrolysis of metal phthalocyanines, synthesis of fullerene-containing carbon black by electric-arc evaporation of composite electrodes containing pyrolyzed metal phthalocyanine, extraction of fullerenes and metalfullerenes from carbon black and synthesis of their water-soluble derivatives. This scheme implies the use of undehydrated galvanic sludge with the humidity of 80–85% without special preparation. Processing of galvanic sludge according to

the proposed scheme will make it possible to receive already at the first stage a commercial product – metal phthalocyanine pigment, suitable for dyeing polymers, paper, construction materials (fillers, cements, etc.).

It has been established that all metals in iron- and copper-containing galvanic sludge are capable of forming stable complexes with phthalocyanine and metalfullerenes. The metals contained in galvanic sludge contribute to the increased yield of fullerenes. When using pyrolyzed metal phthalocyanines synthesized from galvanic sludge, it is possible to use electrodes made of low-grade graphite in electric arc synthesis of fullerenes, which is economically advantageous. When processing galvanic sludge according to the proposed scheme, it is possible to obtain water-soluble mixed metal-containing fullerenes with a quantitative yield, which includes all the metals of the initial galvanic sludge.

The results of the work are of practical significance, because the developed integrated technology solves the problem of waste neutralization and reduction by processing toxic compounds of heavy nonferrous metals into commercial products.

Estimation of biodistribution of mesenchymal stem cells in preclinical renal tuberculosis model from non-linear magnetic response measurements

V.V. Deriglazov¹, Ya.Yu. Marchenko², V.A. Ryzhov², M.A. Shevtsov³, N.M. Yudintceva³

¹ Neutron Research Division of NRC “Kurchatov Institute” – PNPI

² Molecular and Radiation Biophysics Division of NRC “Kurchatov Institute” – PNPI

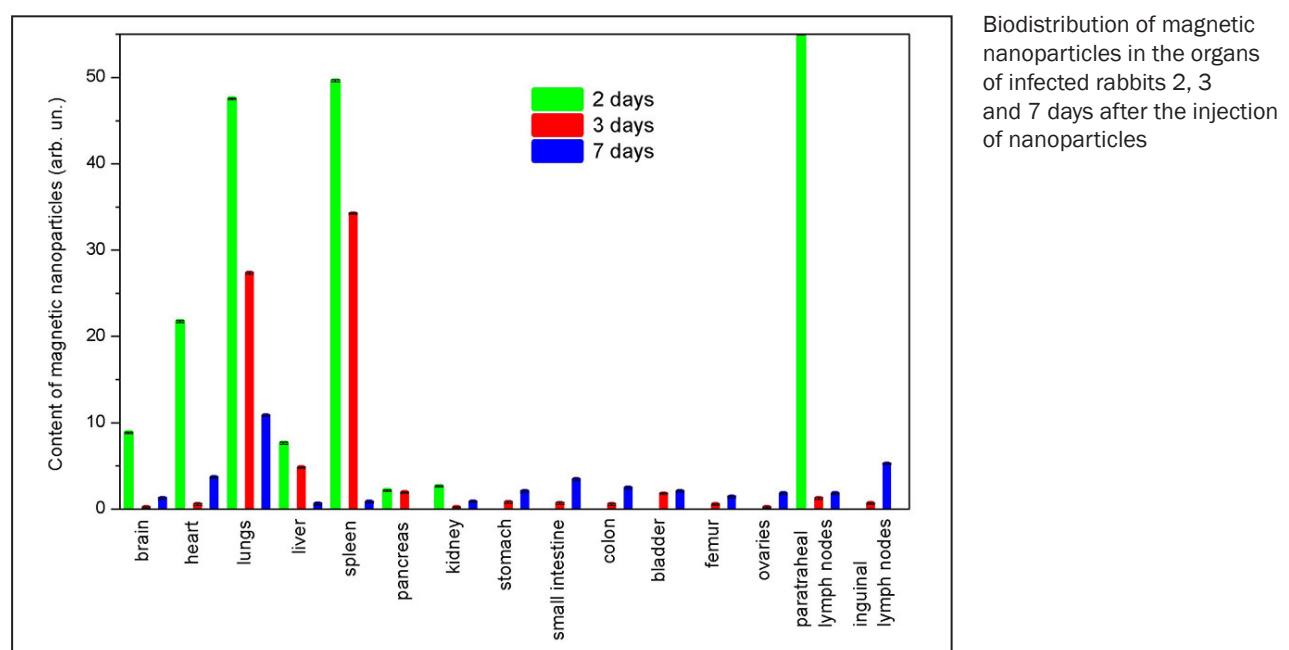
³ Institute of Cytology of RAS

Preliminary studies have shown real promise for the use of mesenchymal stem cells (MSCs) in the treatment of a socially significant disease, tuberculosis, in particular, for targeted drug delivery. The kinetics of biodistribution and accumulation of stem cells in organs and tissues during their intravenous administration to experimental rabbits was studied. Magnetite nanoparticles 10 nm in size in a dextran shell with superparamagnetic properties, previously introduced into stem cells during a 24-hour coincubation, were used as a model and markers of therapeutic agents.

Dissected tissue samples of various organs of experimental animals were studied by nonlinear response on the second harmonic of magnetization, M_2 . Approximation of the M_2 dependences on

a static magnetic field by numerical solutions of the Fokker–Planck kinetic equation made it possible to determine the saturation magnetizations and the magnetic parameters of the magnetic centers located in them, which were used to determine the biodistribution of nanoparticles and, consequently, stem cells in various organs.

The kinetics of accumulation of nanoparticles in the heart, lungs, liver, spleen, brain, stomach, and other organs of tuberculosis rabbits (points 2, 3 and 7 days after MSC injection were used) is shown in Figure. The data obtained made it possible to determine the parameters of the model that describes the kinetics of accumulation and excretion of stem cells by the studied organs.



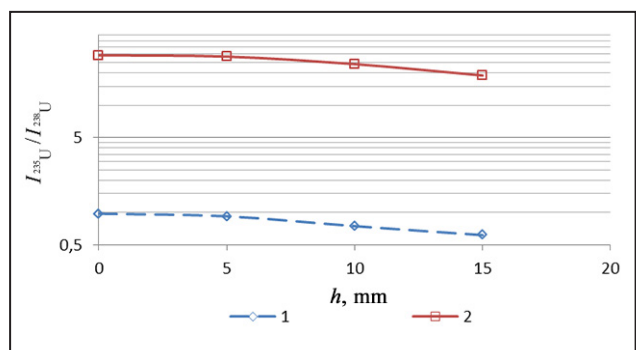
A new method of chemical enrichment of uranium with light isotopes

V.G. Zinoviev, D.A. Rumyantseva, I.A. Mitropolsky, A.P. Serebrov,
 P.A. Sushkov, T.M. Tyukavina, G.I. Shulyak, I.S. Okunev
Neutron Research Division of NRC "Kurchatov Institute" – PNPI

To increase the sensitivity of the γ -spectrometric method for determining the elemental and isotopic composition of samples, the adsorption of the $\text{UO}_2(\text{NO}_3)_2 \cdot 2\text{TBF}$ complex on the surface of polypropylene ($\text{C}_3\text{H}_6)_n$ was used in an extraction system based on a solution of nitric acid and the tributyl phosphate (TBF) extractant. The TBP molecule is a polar and surface active molecule. Such diphilic molecules, interacting simultaneously with polar and nonpolar media, spontaneously accumulate at their interface. A container made of polypropylene was a nonpolar component. In a boundary film of oriented molecules of the $\text{UO}_2(\text{NO}_3)_2 \cdot 2\text{TBF}$ complex uranium isotopes are distributed in height according to their atomic weight. As a result, the upper part of the film contains uranium enriched with light isotopes of uranium ^{234}U and ^{235}U .

The isotopic distribution is determined by the ratio of the intensities of γ -ray lines with energies of 185.739 and 92.7 keV (I_{185}/I_{92}) and with energies of 185.739 and 1 000.997 keV (I_{185}/I_{1001}). Figure shows the dependences of the measured intensity ratios of the analytical lines I_{185}/I_{92} and I_{185}/I_{1001} , which are proportional to the enrichment of uranium by isotopes ^{234}U and ^{235}U at different depths from the solution surface.

Thus, polypropylene (a nonpolar component) has been experimentally shown to firmly hold the



The ratio of the intensities of the analytical lines I_{185}/I_{92} (line 1) and I_{185}/I_{1001} (line 2) depending on the depth h of sampling

$\text{UO}_2(\text{NO}_3)_2 \cdot 2\text{TBF}$ complex in the upper part at the interface of the polar and nonpolar phases. At the same time, lighter isotopes of uranium are collected in the upper layers of a film consisting of molecules of the $\text{UO}_2(\text{NO}_3)_2 \cdot 2\text{TBF}$ complex. The concentration of light isotopes has increased:

- According to ^{234}U from 0.0016 ± 0.0003 at. % in the initial solution to 0.017 ± 0.002 at. %,
- According to ^{235}U from 0.471 ± 0.007 at. % in the initial solution to 1.49 ± 0.02 at. %.

These results were confirmed by X-ray fluorescence analysis of the distribution of uranium concentration along the axis of symmetry of the glass in the direction from the surface of the solution to the bottom of the glass.

Structure of proton-conducting membranes according to neutron and X-ray scattering data

Yu.V. Kulvelis¹, V.T. Lebedev¹, O.N. Primachenko²

¹ Neutron Research Division of NRC “Kurchatov Institute” – PNPI

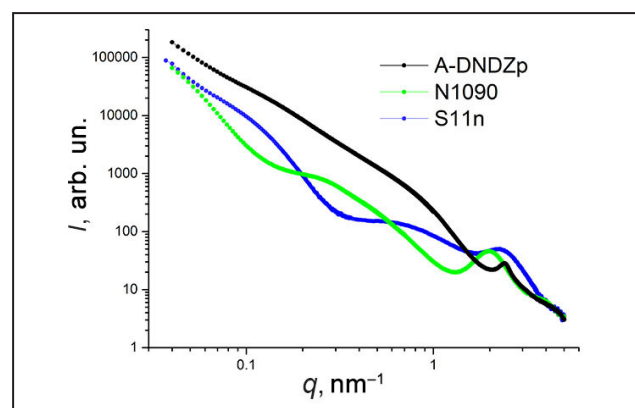
² Institute of Macromolecular Compounds of RAS

In order to create more efficient and economical hydrogen fuel cells, new proton-conducting membranes based on Nafion® and Aquivion® matrices (perfluorinated copolymers with different side chain lengths) modified with detonation nanodiamonds have been developed. The method to prepare membranes with enhanced conducting properties has been improved by introducing into the polymer solution small amounts (≤ 1 wt. %) of detonation nanodiamonds 4–5 nm in size with grafted to the surface groups (H, OH, COOH, SO₃H), removing the solvent and precipitating the mixture on a solid substrate.

The combined conductivity mechanism for Aquivion® type membranes is most successfully implemented in the presence of protonated diamonds (positively charged Z+ type) or diamonds with sulfonic acid groups. In the structure of membranes, according to small-angle neutron scattering data, with the introducing of diamonds an ionomer peak remains at the scattering vector value of $q \sim 2 \text{ nm}^{-1}$, meaning that the main structural elements in the polymer matrix – hydrophilic conducting channels and their mutual arrangement are preserved.

Similar structural data were obtained for a series of Nafion® type membranes with Z+ nanodiamonds. However, the proton conductivity of these membranes is significantly reduced in the presence of

2–3 wt. % of diamonds. For a deeper integration of diamond particles into the polymer matrix, an experiment was carried out to prepare a copolymer (emulsion copolymerization) of the Nafion® type in a mixture with Z+ nanodiamonds. The obtained composite membrane demonstrates a narrowed ionomer peak on the X-ray scattering curves, shifted to larger q (Fig.). Such changes demonstrate an increase in channels ordering with a decrease in the cross distance between them under conditions of high diamond filling (4.1 wt. %) due to a more uniform distribution in the membrane material, which showed good conducting properties.



Small-angle X-ray scattering on an A-DNDZp composite membrane, obtained by copolymerization in the presence of diamonds in comparison with other membranes of Nafion® type (N1090) and Aquivion® type (S11n) without diamonds

1. Primachenko O.N., ..., Kulvelis Yu.V. et al. // J. Fluor. Chem. 2021. V. 244. P. 109736.
2. Kulvelis Yu.V., Primachenko O.N., ..., Lebedev V.T. et al. // Russ. Chem. Bull. 2021. V. 70. No. 9. P. 1713.
3. Lebedev V.T., Kulvelis Yu.V., ..., Primachenko O.N. et al. // J. Surf. Inv. 2021. V. 15. No. 5. P. 939.
4. Primachenko O.N., ..., Kulvelis Yu.V., Lebedev V.T. // Polym. Adv. Technol. 2021. V. 32. No. 4. P. 1386.

Investigation of radiation hardness of silicon detectors under irradiation with α -particles and fission fragments

N.V. Bazlov, A.V. Derbin, I.S. Drachnev, I.M. Kotina, O.I. Konkov,

M.S. Mikulich, V.N. Muratova, M.V. Trushin, E.V. Unzhakov

Neutron Research Division of NRC "Kurchatov Institute" – PNPI

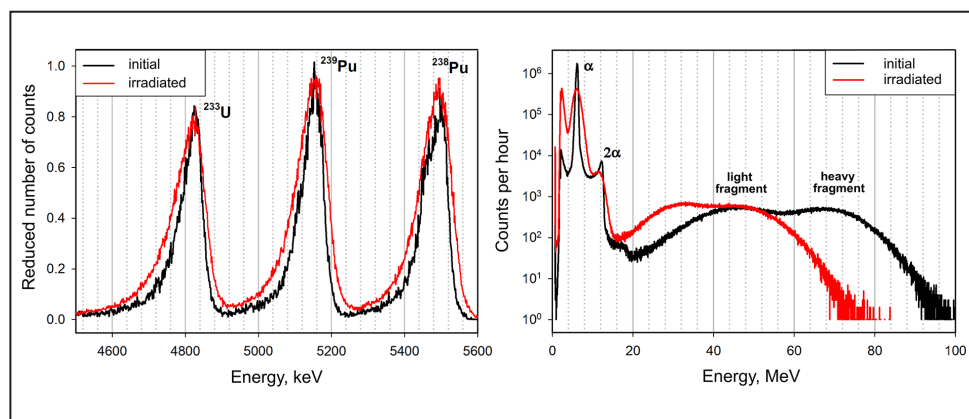
In a number of the nuclear physics experiments, silicon semiconductor detectors are forced to operate under intense levels of α -particles and fission fragments irradiation. High fluxes lead to the formation of a large number of radiation defects in the detector material, which seriously degrades the performance of the device.

To study the radiation hardness of the semiconductor detectors, we used a specially designed experimental setup intended for registration of fission fragments and α -particles spectra and determination of the operational signs of the detector degradation, such as deterioration of the energy resolution and signal-to-noise ratio, an increase of the reverse current, etc. Two types of Si-detectors manufactured in NRC "Kurchatov Institute" – PNPI were under investigation – silicon-lithium Si(Li)- p - i - n -detectors and silicon surface-barrier detectors.

The investigations performed have shown that long-term irradiation with α -particles results in a de-

terioration of the detector's resolution due to an increase of the reverse current (Fig.). At the same time, irradiation by fission fragments of the ^{252}Cf radionuclide leads to a gradual shift of the fission fragment peaks positions towards the lower energies (see Fig.). The established linear dependence of the revealed transformations on the irradiation dose makes it possible to predict the critical dose above which the detector will no longer be suitable for solving specific research tasks. As for example, it could be shown that the overlap of the signals due to fission fragments and α -particles (see Fig.) in case of ^{252}Cf fission products detection would occur upon exposure of about 10^9 of fission fragments and afterwards the detector will be unsuitable for detecting fission fragments. Additional experiments were devoted to the determination of the type and concentration of radiation-related defects formed in the irradiated detectors.

The work was supported by RFBR grant No. 20-02-00571.



The spectra of α -particles of ^{233}U , ^{239}Pu and ^{238}Pu nuclei (left) and the spectra of ^{252}Cf fission fragments (right) measured by the Si(Li)-detector at the beginning and at the end of the long-term irradiation period with α -particles and fission products of ^{252}Cf , respectively

1. Baklanov S.V., Bazlov N.V., ..., Derbin A.V., Drachnev I.S., Kotina I.M., Konkov O.I., ..., Mikulich M.S., Muratova V.N., Trushin M.V., Unzhakov E.V. // Phys. Stat. Sol. A. 2021. V. 218. P. 2100212.

2. Baklanov S.V., Derbin A.V., Drachnev I.S., Konkov O.I., Kotina I.M., ..., Mikulich M.S., Muratova V.N., ..., Trushin M.V., Unzhakov E.V. // J. Phys. Conf. Ser. 2021. V. 2103. P. 012138.

Study of radiation erosion of multiwire proportional chambers in experiments at the Large Hadron Collider

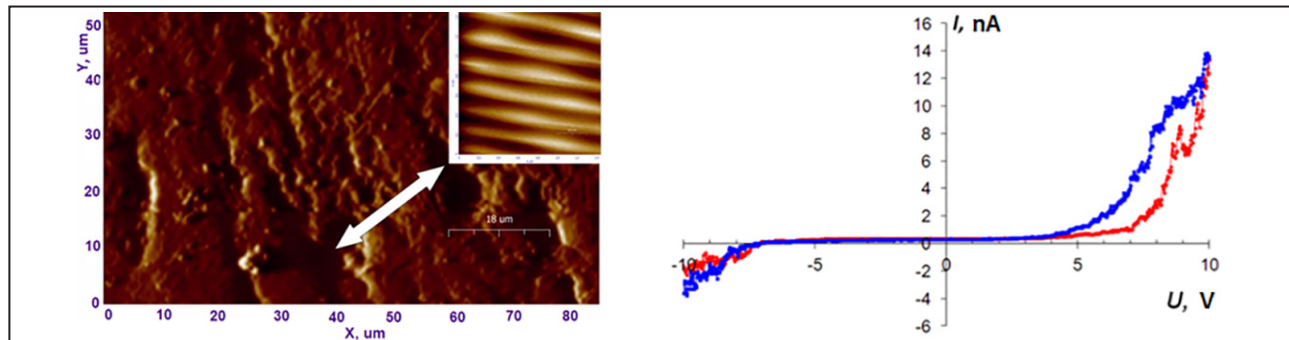
G.E. Gavrilov, A.A. Dzyuba, O.E. Maev

High Energy Physics Division of NRC "Kurchatov Institute" – PNP

Comprehensive resource studies have been performed for multiwire proportional chambers (MWPC) from experiments at the Large Hadron Collider (LHC). It was shown for the first time that the cause of the emergence of spontaneous self-sustaining currents in MWPC is a low-threshold emission of electrons from nanocarbon structures on cathode planes.

Cathode samples of MWPC prototypes from the muon system of the CMS experiment were studied after long irradiation of $2 \cdot 10^6$ s with a ${}^{90}\text{Sr}$ β -source (fluence 10^{13} cm^{-2}) in laboratory conditions to investigate the nature of the sources of spontaneous currents. By methods of atomic force microscopy (AFM) the changes of surface morphology in the cathode copper foil caused by the radiation defects were detected. A quantitative assessment of the evolution of these damages depending on the radiation dose was performed. However, laboratory tests failed to observe spontaneous currents in the prototypes of the MWPC for the CMS experiment. This is due to the small area of the prototypes and short exposure time with respect to LHC conditions.

The developed AFM methods were also applied for a comparative study of the cathode from a full-scale MWPC dismantled from the LHCb experimental setup. The construction materials of MWPCs at the LHCb and CMS are almost identical, and similar MWPC gas mixtures of Ar/ CO_2 / CF_4 were used in these experiments. The similar radiation defects were observed for samples of CMS prototype cathodes and for MWPC from LHCb. The comparison showed that heights of the so-called micro-peaks on the copper foil for the cathode samples taken from the spontaneous current emission zone are three times less with respect to the samples, which were obtained outside of this zone. Thus, the zones of spontaneous emission of electrons are caused by the plasma-chemical formation of point zones with low conductivity at the cathode, but not due to the amplification of the field at the micro-peaks. A comprehensive study of the elemental composition and current characteristics in the detected emission zones at the samples led to the discovery of nanocarbon structures, which are well known as low-threshold sources of electron emission.



AFM-scan image of nanocarbon structure in the cathode (left), icon size $1.5 \times 1.5 \mu\text{m}$. Current-voltage dependence in the area of the nanocarbon structure (right): red dots – current-voltage dependence with voltage increase from -10 up to $+10$ V (U); blue dots – with voltage decrease from $+10$ up to -10 V (U)

1. Buzoverya M.E., Gavrilov G.E., Maev O.E. // Zh. Tekhn. Fiz. 2021. V. 91. Iss. 2. P. 365–375.
2. Buzoverya M.E., Gavrilov G.E., Maev O.E. // Tech. Phys. 2021. V. 66. Iss. 2. P. 356–366.
3. Dzyuba A., Gavrilov G., Maev O. et al. // Book of Abstr. LXXI Int. Conf. "Nucleus-2021". 2021. P. 165.

Application of modified perlite to solve problems of technological and chemical safety of the Arctic region

A.V. Basharichev¹, I.S. Okunev², V.Ya. Sirotyuk¹

¹ Scientific Center for Integrated Security of NRC "Kurchatov Institute" – PNPI

² Neutron Research Division of NRC "Kurchatov Institute" – PNPI

When developing the Arctic zone, taking into account negative factors (thawing of permafrost, low temperature, remoteness from well-developed infrastructure, the threat of oil pollution, etc.), a simple and affordable solution is to use the foamy perlite to solve a number of problems regarding the technological and fire safety of the Arctic zone in the areas of production of:

- Expanded modified perlite (Fig. a) as a sorbent in the management of emergencies of various types (leakage of oil products, acids, etc.) and fire-resistant coatings;
- Light perlite concrete (Fig. b) in combination with shungesite and pumice with exceptionally low thermal conductivity for construction in permafrost and weak soils conditions;
- Composite panels (perlite foam; Fig. c), superior to concrete walls in terms of thermal insulation properties and lightness of structures. Modified perlite has a number of advantages, including:
- The structure is lighter by more than 40–70%;

- Higher thermal insulation properties in comparison with plastic foam by 18–27%;
- High degree of noise insulation;
- Undecomposable and rot-proof (pH neutral);
- Non-combustible (application temperature from –200 to 1 000 °C), non-toxic;
- Ease of regeneration of the used perlite sorbent with the possibility of application in construction and agriculture;
- Unique environmental safety of the material (can be used in agriculture in the form of agroperlite);
- It is lighter than water (can be used to eliminate the pollution on the surface of reservoirs).

Thus, the use of perlite makes it possible to significantly expand the range of effective, inexpensive, but high-tech products for fire protection, construction, etc. in extreme environmental conditions. The presence of significant reserves of pumice, perlite in Kamchatka, shungisite in Karelia helps to reduce the cost of production of materials for the Arctic region.



Expanded perlite (a); perlite concrete (b); foam perlite (c)

Portable nanomeasurement holographic plane meter

B.G. Turukhano, N. Turukhano, S.N. Khanov, Yu.M. Lavrov, V.V. Dobyrn,
 O.G. Ermolenko, L.A. Konstantinov, E.A. Vilkov, I.V. Ladatko
Advanced Development Division of NRC "Kurchatov Institute" – PNPI

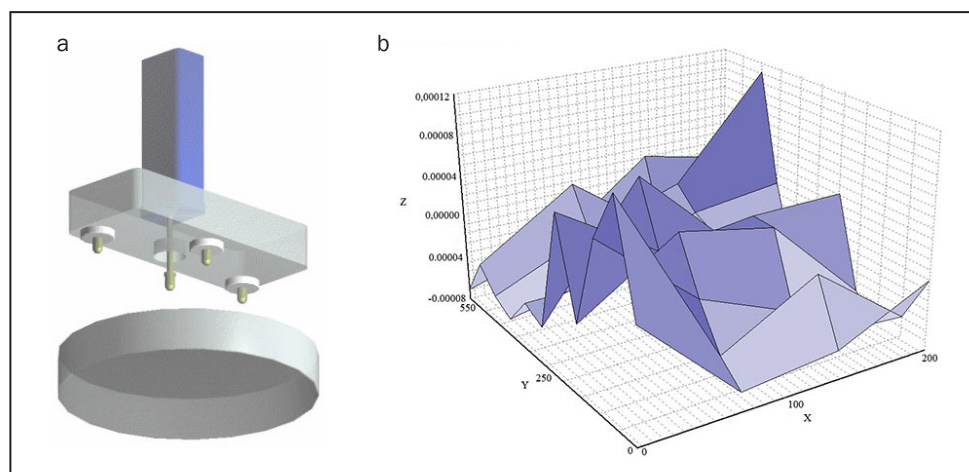
Portable nanomeasurement holographic plane meter – PNHPm (Fig. a) refers to measuring technology, more precisely to the field of measurement and quality control of optical surfaces, their deviation from a given surface shape, determination of surface roughness, including ultrasMOOTH surfaces, such as flat mirrors, polished substrates, etc. PNHPm leads to increased measuring accuracy, elimination of limitations on the size of the measured surface, acceleration of the measurement process and an increase in the operating temperature range.

Holographic length meters are small-sized linear transducers with a holographic measuring element that are designed for precision measurements of length and linear motion in real time, processing and saving the measurement results when working both in stand-alone mode and with automated

linear measurement systems. Information about the measured value is displayed digitally on the screen of the autonomous unit and/or the display screen of a personal computer in the form of tables and graphs.

The main measuring element of PNHPm, ensuring its high performance, is a holographic length meter – HLM. Figure b shows the deviation of the surface from the flatness.

The program plots the surface flatness deviation in three coordinates – X, Y, Z from the measured values. The design of the device is such that there is no limit to the number of measuring points and, therefore, to the size of the measured surface. Surface flatness deviation must be determined when designing many products and high-precision optical devices used in the instrument industry.



Plane meter (a); surface deviation from flatness (b)

High resolution digital holographic microscope for reflective objects

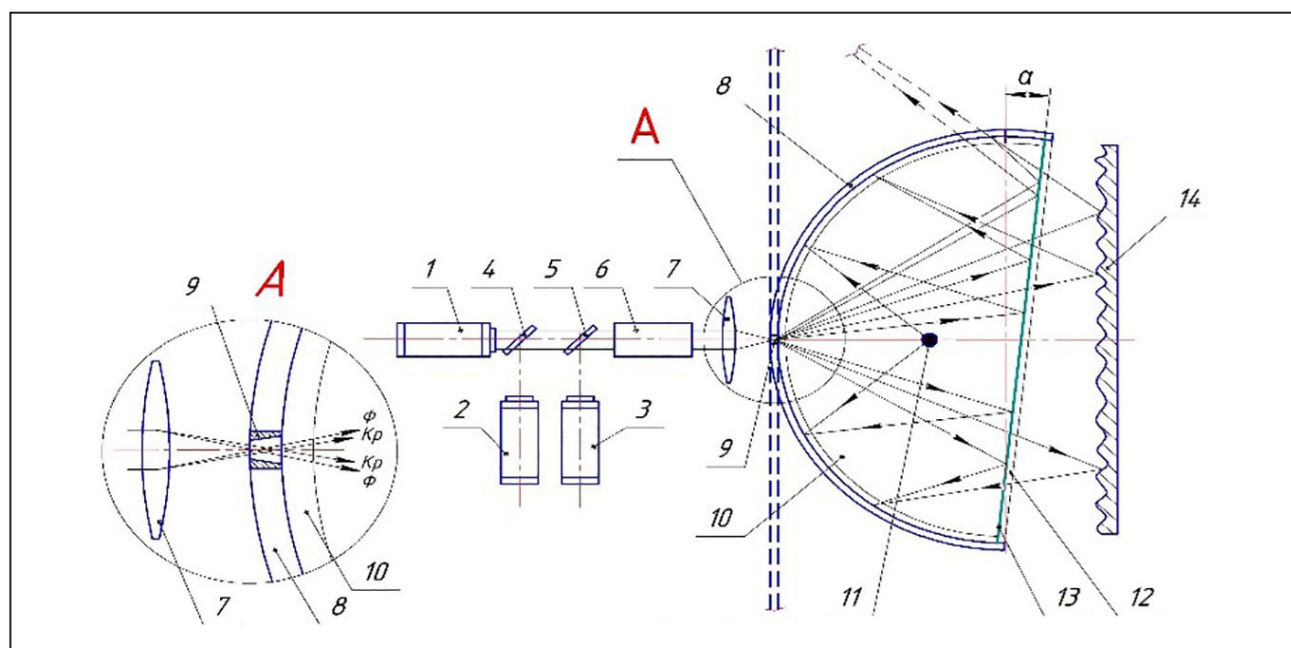
B.G. Turukhano, I.A. Turukhano, N. Turukhano
Advanced Development Division of NRC "Kurchatov Institute" – PNPI

High-resolution digital holographic microscope with hemispherical matrix (DHHM) is designed for recording hologram of reflecting and transparent objects. It has several advantages over an optical microscope, as well as over a classical digital holographic microscope (DHM) with a flat array.

The DHHM allows one to record a hologram on which the high-frequency component of the interference pattern created by the object and auxiliary waves is recorded. Its connection to a personal computer makes it possible to save the obtained

data, edit them, and also use them for further research, including incorporation into various automatic data processing and control systems. Recording the high-frequency component of the object allows to maximize the DHM's resolving power.

This is an attempt to create imaging technology for micro- and nanostructures based on optical holography, digital processing and computer technology to create the next generation of intelligent global systems (Fig.).



Comparison of hologram recording using a digital holographic microscope with a flat array and a digital holographic microscope with a hemispherical array. A – enlarged node; radiation sources – lasers: 1 – blue; 2 – green; 3 – red; 4, 5 – semitransparent mirrors; 6 – filter; 7 – focusing lens; 8 – spherical array; 9 – diaphragm; 10 – cell; 11 – phase object; 12 – transparent flat cell window; 13 – translucent coating of the cell window; 14 – reflective object

Computing infrastructure of a modern physics laboratory

A.V. Naikov, N.Yu. Samokhin, A.Ye. Shevel
High Energy Physics Division of NRC “Kurchatov Institute” – PNPI

HEPD is involved in a significant number of physical experiments in Russia and abroad. Preparation, testing of experimental equipment requires storage and processing of a large amount of distributed data, both experimental and textual. Organization of data processing tools and access to them, regardless of location, *i. e.* cloud infrastructure is an obvious approach. In the period 2020–2021, a specific version of the local cloud infrastructure of HEPD (or just “the cloud”) was implemented.

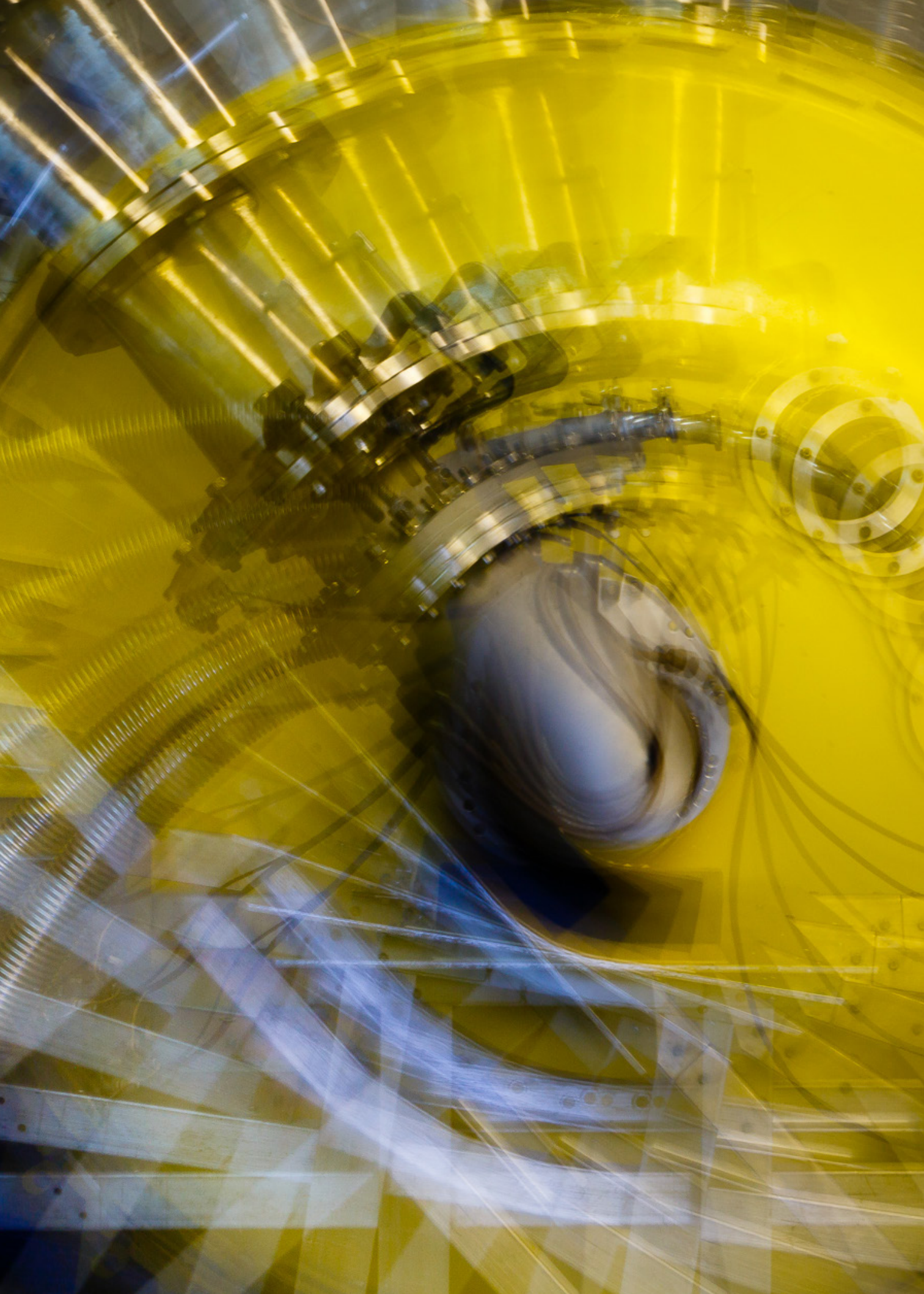
The hardware basis of the HEPD cloud infrastructure is a local network and centralized servers of the Division. DNS services, proxy, virtual computing microcluster, monitoring tools (Zabbix) including informing the manager by mail and Telegram about unusual events in the cloud, distributed storage (Nextcloud), software development platform (JupyterHub), inventory tools (GLPI), backup copying (BackupPC) and others are presented in the form of software agents running in operating isolated environments, in our case – in the form of virtual machines (VMs).

The interaction of VMs with each other is implemented using elements of NFV virtualization. The measures taken to ensure the necessary redundancy to improve the architecture reliability and prevent unauthorized network access provide

a high level of availability, eliminating the need for immediate manual intervention in most incidents.

Since VMs can be moved in a relatively short time from one server to another or to another computing cluster, users interact only with virtual components of the computer infrastructure. Together, such an organization of the computer infrastructure makes it possible to plan the development of a set of services for scientific research, to a large extent, regardless of the geographical location of hardware components.

Considering the useful features of the local cloud architecture described above, the question arises of using corporation and public clouds, for example, opendata.cern.ch, zenodo.org, SberCloud. Advanced, mail.ru, yandex.ru, amazon.com/ec2, google.com, azure.microsoft.com and many hundreds of others. In modern conditions, given the total cost of ownership of computing facilities, the use of public cloud resources should be considered as a serious alternative or addition to local resources. Of particular interest in a public cloud system may be the presence of advanced hardware capabilities, such as special high-performance processors, and/or complex software systems, such as artificial neural networks and others.



Basic Installations

- 110** Progress report of the PIK reactor power start-up program in 2021
- 111** Status of the Accelerator Department in 2021
- 113** Upgrade of the ATLAS muon spectrometer

Progress report of the PIK reactor power start-up program in 2021

A.S. Zakharov¹, A.S. Poltavskii², S.R. Friedmann¹

¹ Department of Reactor Physics and Technology of NRC "Kurchatov Institute" – PNPI

² Department of Nuclear and Radiation Safety of NRC "Kurchatov Institute" – PNPI

In 2021, as part of implementing the test program for the ramp up of the reactor's power up to 10 MW, the main volume of tests confirming the design characteristics of the PIK reactor was carried out.

The calculation maintenance of experiments was provided by a set of PC programs: MCNP (certification passport No. 259 of 14.12.2020), MCU-5 (certification passport No. 536 of 13.11.2021), RC (certification passport No. 520 of 09.07.2021) and other programs used by NRC "Kurchatov Institute" – PNPI (owner), NRC "Kurchatov Institute" (head scientific organization) – and JSC "Dollezhal Research and Development Institute of Power Engineering" (JSC "NIKIET", main design agency).

In 2021, a sequential reactor power ascension for power levels of 200, 400 and 800 kW was performed alongside the operational tests of the reactor systems and experimental equipment of research stations on neutron beams.

In order to justify the safe operation of the reactor under conditions of the reactivity hydrodynamic effect, the working program of investigations of reactor operating modes "Experiments on Measuring the Reactivity Hydrodynamic Effect" has been developed and performed. The operational safety

of the research nuclear reactor PIK in the presence of a positive hydrodynamic reactivity effect associated with the shutdown of the main circulation pumps of the reactor's primary circuit was ensured by the design solutions developed.

In 2021, works on reactor's safety justification when using PIK-2 fuel assemblies were carried out. Possible design and beyond-the-design basis accidents were considered subject to the requirements of regulatory documents. The analysis of the results obtained showed the safety of reactor operation when PIK-2 fuel assemblies are used. The radiation effect on the population and environment under normal operation, under abnormal operation, including design and beyond-the-design basis accidents does not lead to exceeding the established population radiation doses, standards for emissions/discharges and the content of radioactive substances in the environment.

Corresponding changes have been made to the new edition of the Report on the Safety Justification of the facility with the PIK research nuclear reactor.

The experimental and calculated results obtained in 2021 are the basis for justification of the operating safety and reliability of the PIK reactor systems at the next stage of power start-up.

Status of the Accelerator Department in 2021

S.A. Artamonov, E.M. Ivanov, L.A. Sukhorukov
 Advanced Development Division of NRC "Kurchatov Institute" – PNPI

The SC-1000 synchrocyclotron with an extracted beam current of 1 μ A and an energy of 1 000 MeV is one of the basic installations of the Institute. It has been successfully operating since 1970. Its main tasks are:

- Research in elementary particle physics;
- Study of the structure of atomic nuclei and mechanisms of nuclear reactions, including nuclei far from the β -stability band;
- Fundamental developments in various fields of solid state physics;
- Biomedical research.

In addition, SC-1000 is widely used for a whole range of applications. The most important among them are works on radiation tests of the electronic component base, developments to obtain new radioisotopes, and research in nuclear medicine. The SC-1000 is the only reliable, steadily operating facility in Russia, on the targets of which it is possible to obtain a spectrum of protons of variable energies \sim 60–1 000 MeV with a step of 50 MeV.

From November 2020 to November 2021, the synchrocyclotron worked 1 657 h for experimental tasks. Figure 1 shows the distribution of the operating time of the SC-1000 by months, and Figure 2 – in various areas of research as a percentage.

The NRC "Kurchatov Institute" – PNPI is developing a conceptual design of the nuclear medicine complex "Oko" and "Isotope" based on the isochronous cyclotron C-80. In accordance with the terms of reference, the main problems of this project were solved and optimized by the staff of the Laboratory of Physics and Technology of Accelerators of the Accelerator Department. This includes participation in the design of a new building, and the issues of relocating the C-80 in it, and the creation of optimal transportation lines for

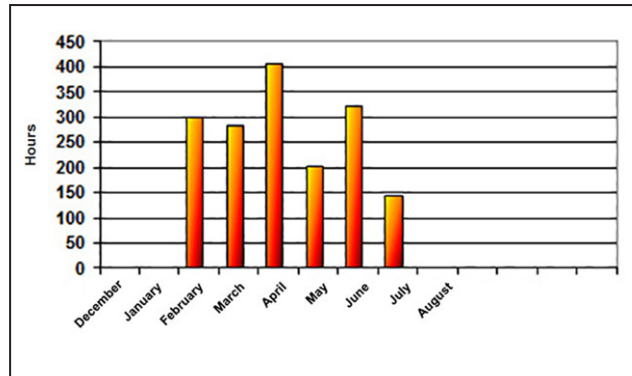


Fig. 1. Running time of SC-1000 in 2020–2021

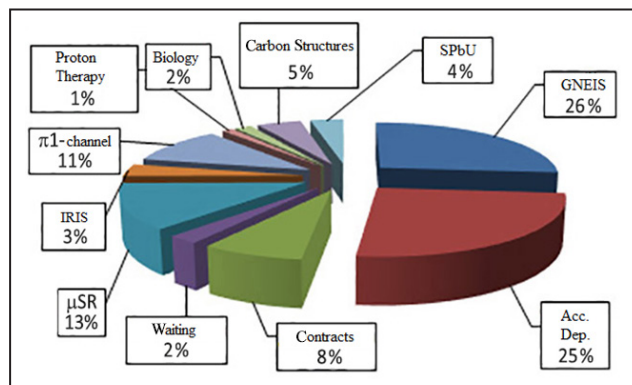


Fig. 2. The breakdown of operating time of SC-1000 by different lines of research

stations (4 pcs.) to develop new methods for obtaining radionuclides and radiopharmaceuticals (stage "Isotope", Fig. 3 "A", to the right of the cyclotron). The creation of a complex for proton therapy for eye diseases was also optimized (stage "Oko", Fig. 3 "B", to the left of the cyclotron).

It was revealed that this requires modernization of the extraction system of the C-80 cyclotron. Calculations and studies have been carried out, which make it possible to develop and implement

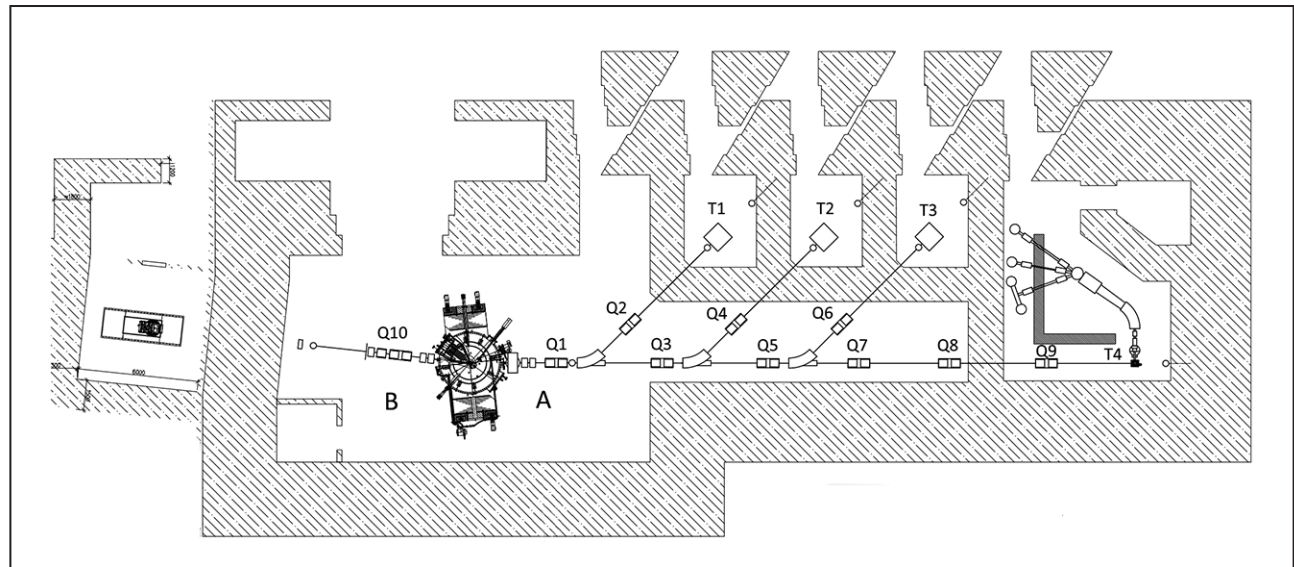


Fig. 3. Nuclear medicine project: A – “Isotope” lines; B – line “Oko”. Q1–Q9 are doublets of magnetic lenses; Q10 – triplet magnetic lenses; T1–T4 – target stations

the simultaneous extraction of two beams. One beam with an intensity of $\sim 100 \mu\text{A}$ and an energy of 40–80 MeV will be used for the production of isotopes, the second – for ophthalmology with

an energy of ~ 70 MeV and an intensity of up to $10 \mu\text{A}$, where an optimal tantalum moderator is used.

Upgrade of the ATLAS muon spectrometer

S.G. Barsov, A.E. Ezhilov, M.P. Levchenko, V.P. Maleev, Yu.G. Naryshkin,
 D. Pudzha, V.M. Solovyev, O.L. Fedin, V.A. Schegelsky
*High Energy Physics Division of NRC "Kurchatov Institute" – PNPI,
 ATLAS Collaboration*

The Large Hadron Collider (LHC) located at the European Organization for Nuclear Research (CERN) for a long time will remain the accelerator that provides the highest energy of proton-proton collisions and ensures the novelty and relevance of the experimental results obtained with its help. The LHC is now at the final stage of its upgrade and will be launched in 2022. The luminosity of the accelerator after the upgrade is expected to be $3 \cdot 10^{34} \text{ cm}^{-2} \cdot \text{s}^{-1}$. An increase in the luminosity of the accelerator will lead to a significant increase in the radiation background in the ATLAS detector, primarily in areas close to the interaction point of the LHC proton beams. This factor introduces serious restrictions on the efficiency of the ATLAS detector at a given accelerator luminosity. To solve these problems during the upgrade phase of the LHC, it is planned to replace the existing small muon wheels with new small muon wheels (NSW). The NSWs include detectors for precision measuring of coordinates and for generating a trigger signal, capable of operation in conditions of high radiation background, and having excellent spatial and time resolution in real time.

Micromegas will be used for precise measurement of coordinates and small-strip thin gap chambers (sTGC) will be used to generate a trigger signal in the NSW. sTGC are multiwire chambers that operate in the quasisaturated mode with a gas amplification factor of about 10^5 . The gas volume between the anode and cathode is 1.4 mm, and

the distance between the groups of wires is 1.8 mm. sTGC have two segmented cathodes on each side of the gas volume. The first cathode is segmented into strips 3.2 mm wide, and the opposite cathode into large pads. The wires are interconnected into groups of 20, which corresponds to a granularity of 3.6 cm.

Construction of sTGC took place at five construction sites: Russia, Israel, China, Canada and Chile. The production of the largest QL3 chambers was successfully completed at NRC "Kurchatov Institute" – PNPI in 2020. All produced quadruplets were sent to CERN and after quality control were installed in the NSW structures, which were delivered to cavern of the ATLAS experiment for commissioning before start of the Run 3 (Fig.).



NSW-A in the cavern of the ATLAS experiment



Scientific and Organizational Activities

- 116** Full-time personnel
- 118** Quantitative characteristics of scientific and educational activities
- 122** Awards. Prizes
- 126** Scientific events

Full-time personnel

Staff number

Professional qualification groups of positions	2019	2020	2021
Total not including part-time workers	1962	1987	1970
Researchers, total	473	473	462
<i>Of which holding the position of</i>			
head	68	66	60
chief researcher	9	9	9
leading researcher	42	44	44
senior researcher	151	146	140
researcher	86	83	83
junior researcher	58	59	53
other researchers	59	66	73
<i>With a science degree</i>			
Doctor of Sciences	66	62	59
Candidate of Sciences	218	215	203
<i>With an academic rank</i>			
Academician	-	-	-
Corresponding Member	2	2	1
Professor	9	8	6
Docent	87	80	74

Information on scientific experience of NRC “Kurchatov Institute” – PNPI researchers

Position	Total	Including with the experience		
		less than 5 years	more than 5 years	more than 10 years
Heads of laboratories and departments	46	2	3	41
Chief researchers	9	-	-	9
Leading researchers	44	2	-	42
Senior researchers	140	8	12	120
Researchers	83	9	24	50
Junior researchers	53	20	24	9

Information on age distribution of NRC “Kurchatov Institute” – PNPI researchers

Professional qualification groups of positions	Age, years old					
	20–29	30–39	40–49	50–59	60 and older	mean age
Researchers, total	78	88	51	62	183	52
<i>With a science degree</i>						
Doctor of Sciences	-	-	6	10	43	69
Candidate of Sciences	1	34	29	38	101	58
W/o science degree	77	54	16	14	39	41
<i>With an Academic rank</i>						
Academician	-	-	-	-	-	-
Corresponding Member	-	-	-	-	1	76
Professor	-	-	-	-	6	83
Docent	-	-	-	3	71	73

The number and average age of researchers of NRC “Kurchatov Institute” – PNPI by position

Position	2019		2020		2021	
	Number	Mean age	Number	Mean age	Number	Mean age
Chief researcher	9	82	9	83	9	80
Leading researcher	42	69	44	68	44	66
Senior researcher	151	62	146	62	140	61
Researcher	86	51	83	50	83	51
Junior researcher	58	32	59	32	53	32
Heads	68	63	66	62	60	63
Other researchers	59	27	66	27	73	30

Structure and staffing for 5 years

Category of staff	2017	2018	2019	2020	2021
Scientific workers	503.9	489.2	435.5	450.2	430.4
Scientific and engineering staff	241.8	251.8	290.7	296.05	299.4
Office and management personnel	1 121.9	1 181.4	1 253.1	1 290.15	1 318.2
Junior service staff	32.5	32.5	32.5	31.5	31.5
Total	1 900.1	1 954.9	2 011.8	2 067.9	2 079.5

Quantitative characteristics of scientific and educational activities

NRC “Kurchatov Institute” – PNPI has completed all events and achieved all target indicators intended for 2021, owing to, in particular, the state assignment implementation subsidies for 2021 and the planning period of 2022 and 2023.

In 2021, the employees of NRC “Kurchatov Institute” – PNPI were the authors and co-authors of 650 papers including 446 publications indexed in Web of Science database and associated with NRC “Kurchatov Institute” – PNPI, which constitutes 68.6% of the total number of published articles.

Dynamic pattern of the number of publications affiliated with NRC “Kurchatov Institute” – PNPI for 5 years

Year	Total number of publications / publications including those indexed in Web of Science database
2017	592/426
2018	689/507
2019	714/465
2020	674/473
2021	650/446

Dynamic of participation in scientific events for 5 years

Year	Number of facts of participation of employees in exhibition activities, conferences, forums and other similar events
2017	466
2018	420
2019	422
2020	387
2021	417

Number of international and Russian patents, whose holder is NRC “Kurchatov Institute” – PNPI obtained in 2021 depending on the title of protection type

Objects of patent law by title of protection type			
Patent for invention	Utility patent	Certificates of registration of computer software	Total
7	1	19	27

Dynamic pattern of titles of protections whose right holder is NRC “Kurchatov Institute” – PNPI for 5 years

Type of title of protection	2017	2018	2019	2020	2021
Patents for invention	4	7	10	5	7
Utility patents	5	4	2	8	1
Certificates of registration of computer software	6	25	12	13	19
Database certificates	1	1	-	-	-
Registered know-how	-	3	-	-	-
Total	16	40	24	26	27

In 2021, the scientific research of Institute's employees was financed by RFBR (24 grants) and RSF (13 grants). The Ministry of Education and Science of the Russian Federation also supported the Institute in the framework of Federal Special Purpose Program “Research and Development in Priority Development Fields of Russia's Science and Technology Sector for the Period of 2014–2020”.

In 2021, the employees of NRC “Kurchatov Institute” – PNPI defended 10 Candidate of Sciences dissertations and 2 Doctor of Science dissertations in line with the Program of Activities of NRC “Kurchatov Institute” – PNPI for 2018–2022.

Training of highly qualified personnel for 5 years

Year	Total number of dissertations / number of Doctor of Science dissertations
2017	11/1
2018	8/2
2019	7/-
2020	9/3
2021	12/2

NRC “Kurchatov Institute” – PNPI under the License to carry out educational activities of 02.06.2017 No. 2599 and the State Accreditation Certificate of 06.07.2020 No. 3414 performs training and education in accordance with higher education programs – programs of training of academic and teaching staff in post-graduate courses in compliance with the requirements of the Federal Educational Standards of the Higher Education within the following training programs:

- 03.06.01 “Physics and Astronomy”
 - subfields: 01.04.02 “Theoretical Physics”, 01.04.07 “Condensed Matter Physics”, 01.04.16 “Nuclear and Particle Physics”, 03.01.02 “Biophysics”;
 - 06.06.01 “Life Sciences”
 - subfields 03.02.07 “Genetics”.

In 2021, the first graduation from Institute's aspirantura (doctoral) program after the Institute had obtained its educational license. Seven graduation diplomas of aspirantura (doctoral) program were

issued, which certify the completion of the third level of higher education in four fields of science: "Genetics", "Nuclear and Particle Physics", "Condensed Matter Physics" and "Biophysics".

In 2021, 10 students entered the full-time doctoral course: 3 students for the training field 06.06.01 "Life Sciences" (subfield 03.02.07 "Genetics") and 7 students for the training field 03.06.01 "Physics and Astronomy" (subfields: 01.04.02 "Theoretical Physics", 01.04.07 "Condensed Matter Physics", 01.04.16 "Nuclear and Particle Physics", 03.01.02 "Biophysics").

The total number of postgraduate students by the end of 2021 is 48 people.

In 2021, NRC "Kurchatov Institute" – PNPI took part in an open competition of the Ministry of Education and Science of the Russian Federation on the distribution of admission quotas for post-graduate course training financed from Federal budget allocations for 2021–2022. The following admission quotas were obtained: 03.06.01 "Physics and Astronomy" – 8 places, 06.06.01 "Life Sciences" – 5 places.

In 2021, the proportion of young scientists (researchers without a degree, Candidates of Sciences under 35 years old and Doctors of Sciences under 40 years old) in the total number of employees involved in research and development amounted to 29%.

In 2021, more than 170 students of Russia's institutions of higher education conducted academic and research work, did practical training, prepared final qualification works for Bachelor's and Specialist's degree and master theses in the laboratories of the Institute.

The total number of students of field-oriented universities who did practical training in the Institute as part of implementing the Program of Activities of NRC "Kurchatov Institute" – PNPI for 5 years

Year	Number of students
2017	101
2018	122
2019	127
2020	154
2021	175

In an effort to popularize science and get young people interested in getting an education in physics and biology, NRC "Kurchatov Institute" – PNPI organizes and conducts excursions in the Institute and to the facilities of NRC "Kurchatov Institute" – PNPI (including excursions to the accelerator facility SC-1000 and C-80, PIK neutron facility, WWR-M reactor, the Molecular and Radiation Biophysics Division as well as other scientific divisions) and carries out occupational guidance for high-school children.

Under the Cooperation Agreement between the administration of the Gatchina Municipal District of the Leningrad region and the NRC "Kurchatov Institute" – PNPI and within the framework of existing cooperation agreements with educational institutions in Gatchina (Lyceum No. 3 named after the Hero of the Soviet Union A.I. Peregudov, Secondary School No. 9 with in-depth study of individual subjects, Secondary School "Apex", Center for Information Technologies, Secondary School No. 2, Secondary School No. 7, Gatchina Centralized Library System) employees of NRC "Kurchatov Institute" – PNPI are working with high school student which includes delivering popularscience lectures by employees of the Institute, selecting of promising students and conducting practical training in physics, mathematics and biology.

Research and Educational Center of NRC "Kurchatov Institute" – PNPI organizes lectures and extra-curricular classes for the in-depth study of some topics in physics and biology for the students of schools of Gatchina and Gatchina region. During these classes the students become acquainted with the advances of modern science and technology. There is occupational guidance for schoolchildren of major

schools of Saint Petersburg and Leningrad region as well as university students of the entire North-western District of Russia. We are conducting popular science lectures (including those when the scientists of the Institute visit schools), excursions to the primary Divisions of the Institute, where the advances of Russian science are discussed, thus increasing the interest in academic field and the activity of NRC “Kurchatov Institute” – PNPI among schoolchildren.

Under the Collaboration Agreement between Saint Petersburg University (SPbU) and NRC “Kurchatov Institute” – PNPI the employees of NRC “Kurchatov Institute” – PNPI conduct lectures and laboratory practicals in the frame of the academic program “Convergence and High-End Technologies” for students of 10th and 11th grade of D.K. Faddeev Academic Gymnasium of SPbU.

NRC “Kurchatov Institute” – PNPI carries out a unique project called “School Environmental Initiative” – “Young Talents”, whose goal is the environmental education of children and teenagers. In 2021, a lot of creative competitions, contests, environmental actions were held. Around five thousand young residents of Gatchina and Gatchina region took part in the project events.

Awards. Prizes

NRC “Kurchatov Institute” – PNPI is an actively functioning institution, which keeps pace with current world trends, as evidenced by numerous prizes and scholarships of its employees.

The active participation of the Institute’s employees in the competition for the **I.V. Kurchatov Prize** has already become a good tradition. It is particularly pleasant that not only leading and young scientists and engineers but also students are encouraged to participate in the competition.

In 2021, the list of Kurchatov Prize winners traditionally includes studies and teams of authors from NRC “Kurchatov Institute” – PNPI.

Among the works of young scientists and engineers the list of winners included a study conducted by E.A. Levlev “Non-Abelian strings in $N = 1$ and $N = 2$ supersymmetric QCD”, D.S. Vinogradova co-authored with E.M. Maksimova (Institute of Protein Research of RAS) titled “Novel translation initiation regulation mechanism by small molecules in *Escherichia coli*”, and a study by A.E. Kopytova, M.A. Nikolaev and A.A. Cheblokov “Ambroxol increases glucocerebrosidase (GCase) activity and restores GCase translocation in primary patient-derived macrophages in Gaucher disease and Parkinsonism”.

Among the works performed by students the study conducted by K.S. Basharova “Transcriptome analysis of primary macrophage culture from patients with Parkinson’s disease associated with mutations in the *GBA* gene” was recognized as one of the best science works.

Dynamics of receiving the I.V. Kurchatov Prize by the employees of the NRC “Kurchatov Institute” – PNPI in 2012–2021

Contest nomination	2012	2013	2014	2015	2016	2017	2018	2019	2020	2021
In the field of scientific research	1	1	1	1	3	-	2	1	1	-
In the field of engineering and technological developments	1	-	2	1	-	1	1	-	-	-
Among the works of young scientists and engineers	-	1	2	2	3	1	3	1	2	3
Among the works performed by students	-	-	3	4	5	2	1	3	1	1
Total	2	2	8	8	11	4	7	5	4	4

In 2021, the Institute’s employees did not take part in the annual competition of scientific papers for the **A.P. Aleksandrov Prize** at NRC “Kurchatov Institute”.

Dynamics of receiving the A.P. Aleksandrov Prize by the employees of the NRC “Kurchatov Institute” – PNPI in 2015–2021

Contest nomination	2015	2016	2017	2018	2019	2020	2021
Main section of the competition	1	-	1	1	-	1	-
Youth section of the competition	-	2	-	-	-	-	-
Total	1	2	1	1	-	1	-

In 2021, the Government of Leningrad region continued to support eight projects of employees of NRC "Kurchatov Institute" – PNPI who had been awarded **scientific scholarships of the Governor of Leningrad region**: 4 scientists were paid the Governor of the Leningrad region's scientific scholarship allowance in the "Young Scientists" category and 4 researchers – in the "Leading Scientists" category.

Holders of scientific scholarships of the Governor of Leningrad region in the "Leading Scientists" category:

- A.K. Emel'ianov, senior scientist of MRBD. "Epigenetic disorders in Parkinson's disease";
- N.S. Mosyagin, senior scientist of ADD. "Producing a new generation of relativistic effective core potentials for light elements of the periodic table, designed for high-precision predictions of the properties of their compounds";
- S.I. Vorobyov, acting head of a laboratory of HEPD. "Investigation of nanostructured magnetic systems using the μ SR-method at the synchrocyclotron of NRC "Kurchatov Institute" – PNPI";
- D.V. Fedorov, deputy head of a laboratory of HEPD. "Laser-spectroscopic studies of the evolution of the nuclear shapes on mass-separator complexes".

Holders of scientific scholarships of the Governor of Leningrad region in the "Young Scientists" category:

- K.A. Ivshin, researcher at HEPD. "Development and creation of a recoil proton detector for precision measurement of the proton radius (Proton experiment)";
- R.M. Samoilov, junior researcher at NRD. "The Neutrino instrument complex at the PIK research reactor";
- P.A. Melentev, post-graduate student, laboratory assistant at MRBD. "Study of the genetic basis of molecular and cellular mechanisms of aging";
- T.S. Usenko, researcher at MRBD. "Lysosomal dysfunction in synucleinopathies".

Names of the winners **of an award of the Governor of Leningrad region** were announced on the eve of the New Year. This is the award recognizing "the contributions to the development of science and technology in the Leningrad region" and "for the best research project".

A junior researcher at TPD Dr. E.A. levlev has become the laureate of the II degree of the award of the Governor of Leningrad region for the best research work among young scientists "Non-Abelian strings in $N = 1$ and $N = 2$ supersymmetric QCD".

For young scientists and specialists of NRC "Kurchatov Institute" – PNPI who demonstrate significant achievements in scientific research, **a scholarship program** was established in recognition of outstanding achievements and in memory of distinguished scientists S.E. Bresler, V.N. Gribov, G.M. Drabkin and V.M. Lobashev whose academic career is inextricably linked to the Institute. Scholarships are awarded annually in the following categories:

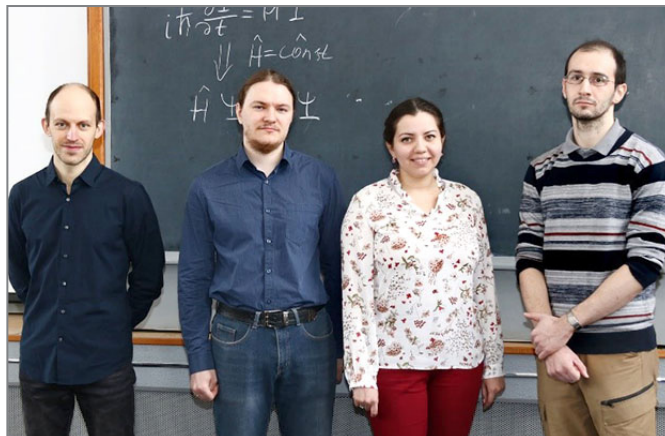
- Bresler scholarship for works in the field of biology,
- Gribov scholarship for works in the field of theoretical physics,
- Drabkin scholarship for works in the field of condensed matter physics,
- Lobashev scholarship in the field of nuclear physics.

In 2021, 5 young scientists of the Institute were the recipients of these scholarships.

Gribov scholarship for works in the field of theoretical physics was awarded to junior researcher of the High Energy Physics Sector of TPD E.A. levlev for his work "Non-Abelian strings in $N = 1$ and $N = 2$ supersymmetric QCD". **Bresler scholarship** for works in the field of biology was awarded to junior researcher of the Laboratory of Experimental and Applied Genetics of MRBD I.M. Golomidov ("The role of α -synuclein in the neuropathology development in the *Drosophila melanogaster* model of Parkinson's disease and the search for compounds capable of correcting this pathology"). **Lobashev scholarship** for works in the field of nuclear physics was



E.A. levlev



awarded to two young researchers: senior laboratory assistant at the Elementary Particle Physics Laboratory of HEPD D.E. Sosnov ("The first measurement of proton-nuclear diffraction processes at the Large Hadron Collider") and junior researcher at the Laboratory of Quantum Chemistry of ADD D.E. Maisan ("Search for CP-odd magnetic quadrupole moments of nuclei by spectroscopic methods of triatomic molecules"). **Drabkin scholarship** for works in the field of condensed matter physics was awarded to M.Kh. Iuzviuk, laboratory researcher

of the spectroscopy group of the Operation of Neutron Stations at the PIK Reactor Department of NRD ("In situ synchrotron study of anion exchange in layered double hydroxides and their structure").

The 2021, **Presidential Prize in Science and Innovation for Young Scientists** was awarded to L.V. Skripnikov, a senior researcher at the Quantum Chemistry Laboratory at ADD for "A series of papers on the development of the electronic structure theory of compounds of heavy elements to search for new physics and study the structure of the nucleus".

The scholarship of the President of the Russian Federation for young scientists and postgraduates engaged in promising research and development in priority areas of modernization of the Russian economy for 2021–2023



D.V. Chubukov

was awarded to D.V. Chubukov (SP-1213.2021.2 "Investigation of the properties of molecular systems and their application to search for P, T-odd interactions in nature").

P.A. Melentev received the scholarship of the Government of the Russian Federation for full-time undergraduate and post-graduate students for the academic year 2021/22.

O.I. Utesov was awarded the grant from the President of the Russian Federation for state support of young Russian scientists – candidates of sciences and doctors of sciences for scientific research MK-1366.2021.1.2 "Investigation of the properties of spiral magnets with the Dzyaloshinskii–Moriya interface interaction".



P.A. Melentev



L.V. Skripnikov

At the competition of scientific works of NRC "Kurchatov Institute" – PNPI 2021, the commission considered 26 works in 8 scientific areas of the Institute's activities.

Having performed an expert evaluation and comprehensive discussion of the works, the commission decided on the winners of the competition.

- The first prize ***in the field of high energy nuclear physics*** was awarded for the work “First observation of the production of three electrically weak bosons at $\sqrt{s} = 13$ TeV in the CMS experiment” (A.A. Vorobyov, G.E. Gavrilov, V.L. Golovtsov, Yu.M. Ivanov, V.T. Kim, E.V. Kuznetsova, P.M. Levchenko, V.A. Murzin, V.A. Oreshkin, I.B. Smirnov, D.E. Sosnov, V.V. Sulimov, L.N. Uvarov et al. (CMS Collaboration)).

- ***In the field of condensed matter physics***, the winner was the work “Magnetism of frustrated quasi-two-dimensional oxides with a trigonal superstructure of magnetic ions” (A.N. Korshunov, A.I. Kurbakov, M.D. Kuchugura, A.E. Susloparova, K.Yu. Bukhteev, A.N. Vasiliev, M.A. Evstigneeva, K. Zakharov, E.A. Zvereva, E. Komleva, V.B. Nalbandyan, Yu. Ovchenkov, G.V. Raganyan, S. Streletsov, Th. Mueller, V. Pomjakin, I.A. Safiulina, A. Senyshyn).

- ***In the field of low energy nuclear physics***, the first prize was awarded for the work “Detection of the phenomenon of high-energy long-lived atomic isomerism”(S.A. Eliseev, Yu.N. Novikov, P.E. Filyanin et al.).

Overall, 22 works were recognized the winners of the competition.



O.I. Utesov



Scientific events

Institute Seminars

- 19 January. Nuclear seminar of HEPD.** *E.L. Kryshen.* “Project of multipurpose detector ALICE 3 at LHC: physical program and design of experimental setup”.
- 26 January. Nuclear seminar of HEPD.** *A.D. Chubykin.* “Investigation of Xi_c baryons at LHCb”.
- 2 February. Nuclear seminar of HEPD.** *G.V. Fedotov.* “Current status of the PANDA FTOF wall detector”.
- 9 February. Nuclear seminar of HEPD.** *V.N. Panteleev.* “Radioisotope complex RIC-80 and new methods of radionuclide production for medicine”.
- 16 February. Nuclear seminar of HEPD.** *O.V. Miklukho.* “Observation of structure in polarization of scattered protons in inclusive (p, p') reaction with ^9Be and ^{12}C nuclei at 1 GeV”.
- 18 February. Joint seminar of HEPD and TPD.** *L.V. Skripnikov.* “Use of molecular systems to study nuclei properties”.
- 2 March. Nuclear seminar of HEPD.** *I.N. Solovyev.* “Experiment Polfusion for study of polarized deuteron fusion”.
- 4 March. Joint seminar of HEPD and TPD.** *M.G. Ryskin.* “QCD instanton. How it can manifest itself in the interaction processes at the Large Hadron Collider”.
- 9 March. Nuclear seminar of HEPD.** *N.Yu. Samokhin.* “An interactive platform for remote development and exchange of research data”.
- 11 March. Joint seminar of HEPD and TPD.** *E. Levin* (Tel Aviv University, Israel). “Deep inelastic scattering as a probe of entanglement”.
- 16 March. Nuclear seminar of HEPD.** *R.N. Chistov* (Lebedev Physical Institute of RAS). “ B -physics at CMS”.
- 23 March. Nuclear seminar of HEPD.** *M.P. Levchenko.* “Search for magnetic monopoles”.
- 25 March. Joint seminar of HEPD and TPD.** *M.V. Polyakov.* “Mechanical properties of hadrons”.
- 1 April. Joint seminar of HEPD and TPD.** *M.G. Ryskin.* “Comments on the odderon experimental discovery”.
- 6 April. Nuclear seminar of HEPD.** *V.A. Guzej.* “Vector meson photoproduction in ultraperipheral collisions of nuclei at LHC and nuclear screening”.
- 8 April. Joint seminar of HEPD and TPD.** *V.Yu. Petrov.* “Nonperturbative QCD phenomena (part 1)”.
- 13 April. Nuclear seminar of HEPD.** *P.I. Zarubin* (Veksler and Baldin Laboratory of High Energy Physics of the Joint Institute for Nuclear Research). “Correlation in creation of ^8Be and α -nuclei in relativistic nucleus fragmentation”.
- 15 April. Theoretical seminar on CSP.** *D.A. Parshin* (Saint Petersburg National Research Academic University of RAS). “The mysteries of flexural modes in graphene”.
- 15 April. Joint seminar of HEPD and TPD.** *V.Yu. Petrov.* “Nonperturbative QCD phenomena (part 2)”.
- 19 April. Seminar of CMRD.** *A.I. Kurbakov.* “Peculiarities of magnetic ordering in novel chiral magnet MnSnTeO_6 ”.

- 20 April. Nuclear seminar of HEPD.** V.N. Kovalenko (Saint Petersburg University). “Quark-gluon string junction and collective phenomena in relativistic collisions of protons and nuclei”.
- 22 April. Joint seminar of HEPD and TPD.** V.S. Vorobyov (Budker Institute of Nuclear Physics of SB RAS). “Status and the research program of the project of super charm-tau facility in RF”.
- 26 April. Seminar of CMRD.** E.K. Nigmatullina. “Phantom” atoms and thermal motion in fullerene C_{60} ”.
- 27 April. Nuclear seminar of HEPD.** K.V. Ershov. “Radiation accidents, Chernobyl disaster”.
- 29 April. Joint seminar of HEPD and TPD.** L.V. Grigorenko (Joint Institute for Nuclear Research). “Super-heavy hydrogen isotopes 6H and 7H in experiments at ACCULINNA-2”.
- 11 May. Nuclear seminar of HEPD.** T.A. Osviannikova (NRC “Kurchatov Institute” – ITEP). “Recent LHCb spectroscopy results”.
- 13 May. Joint seminar of HEPD and TPD.** V.Yu. Petrov. “Nonperturbative QCD phenomena (part 3)”.
- 18 May. Nuclear seminar of HEPD.** A.E. Barzakh. “Hyperfine anomaly. Status, problems and perspectives”.
- 20 May. Joint seminar of HEPD and TPD.** A.V. Yung. “Non-Abelian vortex strings: from classical solutions to critical superstrings”.
- 25 May. Nuclear seminar of HEPD.** A.V. Popov. “ ^{229}Th – in search of a bridge”.
- 27 May. Joint seminar of HEPD and TPD.** E. Epelbaum (Ruhr University, Germany). “Chiral effective field theory for low-energy nuclear physics (part 1)”.
- 3 June. Joint seminar of HEPD and TPD.** E. Epelbaum (Ruhr University, Germany). “Chiral effective field theory for low-energy nuclear physics (part 2)”.
- 8 June. Nuclear seminar of HEPD.** P.V. Neustroev. “Electronics of the Proton experiment”.
- 10 June. Joint seminar of HEPD and TPD.** Yu.N. Novikov. “The ion trap in fundamental research”.
- 17 June. Theoretical seminar on CSP.** K.V. Kavokin (Ioffe Institute). “Optical cooling of nuclear spins in semiconductor structures”.
- 17 June. Joint seminar of HEPD and TPD.** V.Yu. Petrov. “Nonperturbative QCD phenomena. Part 4. Instantons at high energies; confinement of quarks”.
- 24 June. Joint seminar of HEPD and TPD.** Yu.N. Novikov. “Ion traps. Part 2. Observation of high energy, high spin atomic isomerism”.
- 29 June. Nuclear seminar of HEPD.** A.A. Dzyuba. “Mixing of electrically neutral mesons. New LHC results”.
- 6 July. Nuclear seminar of HEPD.** S.A. Bulat. “Coronavirus SARS-CoV-2 science update June 2021”.
- 21 July. Seminar of MRBD.** E.M. Maksimova. “Translocation inhibition by the antibiotic amicoumacin A and mechanism of resistance to it due to changes in domain IV of EF-G”.
- 2 September. Theoretical seminar on CSP.** D.N. Aristov. “Spectrum of spin waves in skyrmion crystals and the stereographic projection method”.
- 14 September. Nuclear seminar of HEPD.** V.V. Lukashevich. “Linear beams of charged particles and optimization of mass separators”.
- 16 September. Joint seminar of HEPD and TPD.** A.P. Serebrov. “Possibility of experimental confirmation of the 3 + 1 neutrino model with one sterile neutrino”.
- 21 September. Nuclear seminar of HEPD.** I.M. Belyaev (NRC “Kurchatov Institute” – ITEP). “Observation of narrow exotic tetra quark with double charm”.

30 September. Theoretical seminar on CSP. F.D. Timkovskii. "Critical temperature and low-energy excitations in gapped spin systems with slit spectrum".

5 October. Nuclear seminar of HEPD. V.V. Abaev. " S_{31} pion-nucleon scattering length".

7 October. Joint seminar of HEPD and TPD. E. Epelbaum (Ruhr University, Germany). "Nucleon polarizabilities from chiral effective field theory".

12 October. Nuclear seminar of HEPD. O.L. Fedin. "Elementary particle physics and astrophysics in People's Republic of China".

13 October. Seminar of ADD. Yu.V. Barsukov (Princeton Plasma Physics Lab, USA). "Boron nitride nanotube precursor formation during high-temperature synthesis".

14 October. Joint seminar of HEPD and TPD. Yu.L. Dokshitzer. "Specific features of heavy quarks. "Dead cone" effect and around".

19 October. Nuclear seminar of HEPD. M.V. Malaev. "Recent status of the MPD experiment at NICA collider".

21 October. Theoretical seminar on CSP. A.G. Yashenkin. "Theory of Raman scattering in weakly disordered non-polar nanocrystals".

21 October. Joint seminar of HEPD and TPD. A.V. Sarantsev. "Scalar-isoscalar mesons and the scalar glueball from radiative J/ψ decays".

26 October. Nuclear seminar of HEPD. S.A. Fedotov (Institute for Nuclear Research of RAS). "Projection and developing of detector for charged particles for kaon and neutrino experiments".

28 October. Theoretical seminar on CSP. A.G. Yashenkin. "Theory of Raman scattering in weakly disordered non-polar nanocrystals. II. Phonon line broadening".

9 November. Nuclear seminar of HEPD. V.A. Zaitsev (Saint Petersburg University). "Modelling atoms and molecules using quantum computers".

10 November. Seminar of ADD. V.V. Panchuk (Institute of Chemistry of Saint Petersburg University; Institute for Analytical Instrumentation of RAS). "Development of nuclear γ -resonance and X-ray spectroscopy based on chemometric approaches".

11 November. Joint seminar of HEPD and TPD. N.N. Nikolaev (L.D. Landau Institute for Theoretical Physics of RAS). "Quantum mechanics of the coherent betatron oscillations of beam in the storage ring".

16 November. Nuclear seminar of HEPD. V.M. Soloviev. "Investigation of antimatter properties in the BASE experiment (CERN)".

18 November. Theoretical seminar on CSP. F.D. Timkovskii. "Critical temperature and low-energy excitations in gapped spin systems with slit spectrum".

18 November. Joint seminar of HEPD and TPD. D.E. Kharzeev (State University of New York at Stony Brook, USA). "Chiral magnetic effect: from quarks to quantum computers".

23 November. Nuclear seminar of HEPD. O.L. Fedin. "Elementary particle physics and astrophysics in People's Republic of China".

25 November. Theoretical seminar on CSP. O.I. Utesov. "Mean-field approach for skyrmion lattice description in centrosymmetric frustrated antiferromagnets".

30 November. Nuclear seminar of HEPD. A.V. Dobrovolsky. "Investigation of the structure of exotic nuclei at the facility with an active target IKAR by the method of elastic proton scattering in inverse kinematics".

- 1 December. Seminar of MRBD.** O.G. Shcherbakova. “Optogenetic reporters to study the differential release of neurotransmitters by sympathetic neurons innervating cardiomyocytes”.
- 2 December. Joint seminar of HEPD and TPD.** V.V. Baru (NRC “Kurchatov Institute” – ITEP; Ruhr University, Germany). “Hadronic molecules. Application to T_{cc} ”.
- 7 December. Nuclear seminar of HEPD.** T.A. Shtam. “Small players of a great game. Potential of using exosomes for diagnostics and therapy of some diseases”.
- 9 December. Theoretical seminar on CSP.** R.A. Niyazov. “Aharonov–Bohm interferometry based on helical edge states”.
- 14 December. Nuclear seminar of HEPD.** P.L. Molkanov. “Investigation of neutron-deficient Bi isotopes by in-source laser spectroscopy technique (IRIS, ISOLDE)”.
- 16 December. Theoretical seminar on CSP.** R.A. Niyazov. “Aharonov–Bohm interferometry based on helical edge states (continuation)”.
- 23 December. Theoretical seminar on CSP.** A.V. Syromyatnikov. “Cluster representation of spin 1/2 operators for studying exotic phases and spin dynamics in magnets. Part 1. Nematic phases in frustrated systems in the strong field”.
- 30 December. Theoretical seminar on CSP.** A.V. Syromyatnikov. “Cluster representation of spin 1/2 operators for studying exotic phases and spin dynamics in magnets. Part 2. Cluster representation of spins for quantum strongly correlated systems”.

Conferences

Within the context of a wide variety of areas of scientific research conducted in NRC “Kurchatov Institute” – PNPI we are convening our own conferences, lecture courses and workshops attended by scientists from leading research centers of Russia and abroad.

In 2021, the Institute organized 14 scientific events (meetings, conferences, schools).

The list of organized events

1. Series of lectures by Prof. I.A. Mitropolsky “Structure of the Atomic Nucleus” for young scientists, specialists and students doing an internship at NRC “Kurchatov Institute” – PNPI. **15 February – 30 April** (Gatchina).
 2. Environmental holiday “Ecoshow-2021”. **14 May** (Gatchina).
 3. Workshop “Neutron Diffraction – 2021”. **8–10 June** (Gatchina).
 4. VII International Conference and XIV International School for Young Scientists and Specialists Named after A.A. Kurdyumov “Interaction of Hydrogen Isotopes with Structural Materials”. **22–28 August** (Gatchina).
 5. First Summer School of the Council of Young Scientists and Specialists of NRC “Kurchatov Institute” – PNPI. **27–29 August** (Skamja, Slantsevsky district, Leningrad region).
 6. VI International Workshop Dzyaloshinskii-Moriya Interaction and Exotic Spin Structures (DMI-2021). **6–10 September** (Vyborg).
 7. V All-Russian Conference “Fundamental Glycobiology”. **21–24 September** (Gatchina).
 8. Open popular science lecture series “Science Is Our Life”. **22 October** (Gatchina).
 9. IV School “Neutron Research of the Condensed State” (NICONS-2021). **8–12 November** (Gatchina, Old Peterhof).
 10. VIII All-Russian Youth Science Forum with International Participation “Open Science 2021”. **17–19 November** (Gatchina).
 11. VI Youth School of the PIK Reactor “Professionalism. Intellect. Career. PIK-2021”. **15–26 November** (Gatchina).
 12. III Youth Conference “DARIA Project: Compact Neutron Sources in Russia”. **1–3 December** (Saint Petersburg).
 13. A final conference “Young Talents 2021” of the program “School Environmental Initiative”. **8 December** (Gatchina).
 14. X School on Polarized Neutron Physics “FPN-2021”. **16–17 December** (Gatchina).
- Also, in 2021 the researchers of the Institute participated in more than 150 international and Russian conferences and gave around 420 talks as speakers.

